

ABSTRACT

MCCOLLUM, MADILYNN. The Ultrasonic Polymerization of Isophorone Diisocyanate Based Polyurethane and Polyacrylamide with the in situ Sonication of Multi-Walled Carbon Nanotubes. (Under the direction of Dr. Richard Kotek).

Industrial polymerization techniques produce excellent polymers, but require long reaction times, high temperature, and high pressure to achieve these results. Polymerization through the use of an ultrasonic probe is a new method that could dramatically decrease the polymerization time when creating polymers for certain, specific applications. Although not able to be used yet for large scale projects, ultrasonic polymerization can provide insight into how to utilize such a unique technology to create high viscosity, high molecular weight polymers in shortened time frames for small-scale technical applications. This research aims to refine the ultrasonic polymerization for reproducible isophorone diisocyanate based polyurethane solutions along with expanding that research to ultrasonically polymerize polyacrylamide solutions. By creating both polyurethane and polyacrylamide solutions, ultrasonic polymerization has the potential to effectively work for both step growth and chain growth polymers.

Initial research focused on refining the methodology for the ultrasonic polymerization of polyurethane from monomers of isophorone diisocyanate and polyethylene glycol in a solvent of N,N-dimethylformamide and a catalyst of dibutyltin dilaurate. The components were combined in a plastic reactor bottle and sonicated for 15 minutes. After much experimentation with modifying factors such as nitrogen gas, probe tuning, power setting, and catalyst amount no reproducibility was found in polyurethane solutions and the focus of this research switched to acrylamide. During the polymerization of polyurethane, the substantial amount of side reactions that take place was found to interfere with the polymer formation and provide the

inconsistent results. Reproducibility was finally found in polyacrylamide samples after some altering of the monomer concentration, initiator concentration, and power setting. The sonication time remained constant at 15 minutes. During polyacrylamide polymerization the only reaction that can take place is the breaking of the double bond in the acrylamide monomer. Abundantly less side reactions are found during this chain-growth reaction as opposed to the polymerization of polyurethane. Polyacrylamide was made in a solvent of water along with potassium persulfate as the free radical initiator. All polymer solutions were characterized through viscosity measurements taken with a Brookfield DV-E digital viscometer. Molecular weights for select polyacrylamide samples was determined by gel permeation chromatography.

After the ultrasonic polymerization methodology was refined and reproducibility was achieved, the sonication of multi-walled carbon nanotubes (CNTs) in situ with the ultrasonic polymerization of polyacrylamide was investigated to create a CNT-polyacrylamide composite film. Films were created through solvent evaporation casting and characterized by a scanning electron microscope (SEM). To characterize the success of the in situ sonication and polymerization of CNTs and polyacrylamide, two features were looked at through the SEM images—the dispersion of CNT throughout the polyacrylamide polymer and the covalent grafting of polyacrylamide polymer onto the CNTs. Results showed that the in situ sonication and polymerization produces a decently dispersed CNTs as opposed to adding the CNTs to a previously made polymer. Grafting was not able to be seen with this particular SEM.

Overall ultrasonic polymerization does allow for certain polymers to polymerize faster and more rapidly than traditional methods, but this technique is limited for large scale manufacturing and the polyurethane made during this experiment. The combined one-step

polymerization/sonication method allows for better dispersed CNT/polymer composites to be made and used for technical small-scale applications.

© Copyright 2017 Madilynn McCollum

All Rights Reserved

The Ultrasonic Polymerization of Isophorone Diisocyanate Based Polyurethane and
Polyacrylamide with the in situ Sonication of Multi-Walled Carbon Nanotubes

by
Madilynn McCollum

A thesis submitted to the Graduate Faculty of
North Carolina State University
in partial fulfillment of the
requirements for the degree of
Master of Science

Textiles

Raleigh, North Carolina

2017

APPROVED BY:

Dr. Richard Kotek
Committee Chair

Dr. Philip D. Bradford

Dr. Karen K. Leonas

DEDICATION

My family for supporting me in this crazy dream to move to Raleigh, NC and get my masters. I had no idea this program even existed 4 months prior to applying to graduate school, but you all believed that I could and would succeed here. You all always had incredible faith in my ability to accomplish my dreams even when my faith in myself was faltering.

Garrett, Thank you for dealing with my mood swings and my tears and my need to wallow when nothing was working and I felt like a failure. You're reassurance and support was greatly needed and is so tremendously appreciated. I am so thankful I have you to take care of me when I'm too stressed to take care of myself. I couldn't make it without you.

My "best friend" and kindred spirit, Felicity Hightower. One day you're gonna realize your mom paid me to hang out with you because I'm your babysitter, but in the meantime, thank you for treating me as your equal and making sure that I never lost sight of my kid-at-heart spirit.

BIOGRAPHY

Madilynn McCollum was born in Nashville, TN in 1992 as the daughter of Chris and Jeanne McCollum and the sister of Christopher McCollum. She grew up in Franklin, TN as an active member in her school and community being captain of the dance team and a member of the student council. Always having a strong interest in the creative fields, she received a sewing machine in kindergarten and her love of textiles began. Science became a second interest to her in middle school during an introductory chemistry class. It had the ability to capture her interest as a way to connect the dots and explain the natural world around her. Her natural curiosity was able to be fostered in science class and her mind easily grasped the material.

Madilynn went on to major in chemistry at the University of Tennessee Knoxville with a minor in pre-medicine and secondary education through the VolsTeach program. After completing her degree in 2014 and having achieved licensure to teach chemistry in grades 7-12 in 2015 she decided she wasn't quite done being the student and that graduate school would be the next step for her.

Uprooting her life to Raleigh, North Carolina wasn't the easiest task, but she knew this was the place to study and work in the textile industry and that God had a plan for her here. She was selected to be a teaching assistant for a Textile Wet Processing lab (PCC 302) and her passion for teaching was able to grow while obtaining her graduate degree. After 4 semesters of teaching and learning and researching she is now able to graduate with her Master of Science and further the plan God has for her life.

ACKNOWLEDGMENTS

Dr. Richard Kotek, my advisor for his advice and willingness to help me every step of the way in my research. My committee members, Dr. Leonas and Dr. Bradford for their interest and help in my exploration of this topic. And specifically Dr. Bradford for allowing me to use his ultrasonic probe for the duration of this year. Professor Genzer and Dr. Efimenko for measuring molecular weight of my polyacrylamide samples. Judy Elson for allowing me access to the Brookfield Viscometer and analytical balance when I needed it. Charles Mooney in the Analytical Instrumentation Facility for helping capture high magnification images of films. Dr. Ericka Ford and the Ford Innovation Group for allowing me to use their thermocouple and particulate hood as well as providing me information about the sonication of CNTs in water. Joyce Cole for helping me order materials and ensuring that my glass jars got here eventually. The undergraduates assigned to assist in my research: Melisa Pasli, Jack Chen, and Patrick Snyder.

TABLE OF CONTENTS

LIST OF TABLES	viii
LIST OF FIGURES	ix
1.0 INTRODUCTION, LITERATURE REVIEW, AND MOTIVATION	1
1.1 Introduction	1
1.2 Polymer Classification	3
1.3 Polymerization Techniques	7
1.4 Ultrasound Waves and Acoustic Cavitation	11
1.5 Ultrasonic Induced Polymer Degradation	16
1.6 Disadvantages of Ultrasonic Polymerization	20
1.7 Previous Research with Ultrasonic Polymerization	20
1.7.1 Polymerization of Methyl Methacrylate Initiated by Ultrasound	20
1.7.2 Preparation of PVA Latex with Ultrasonic and Redox Initiation	21
1.7.3 Polymerization Resulting from Ultrasonic Cavitation	23
1.7.4 The Effect of High Intensity Ultrasound on Polyurethane Synthesis	25
1.8 Polyurethane Polymer Synthesis, Processing, and Characteristics	26
1.9 Polyacrylamide Properties and Synthesis	30
1.10 Previous Research on Polyacrylamide Hydrogel Composites	32
1.10.1 Application of cellulose nanocrystals in polyacrylamide hydrogels	32
1.10.2 Synthesis and Electrical Conductivity of a Polyacrylamide/Cu Hydrogel ...	33
1.11 Properties of Carbon Nanotubes	34
1.12 Previous Research with Carbon Nanotubes	39
1.12.1 Preparation of Biocompatible Multi-Walled Carbon Nanotubes	39
1.12.2 Novel Dispersion of MWCNTs in Polystyrene Polymer	40
1.12.3 Excellent Dispersion of MWCNTs in PEO Polymer	40
1.12.4 Effects of Polymer Wrapping and Functionalization on MWCNT Stability	42
1.13 Previous Studies on Ultrasonic Polymerization by R. Kotek and A. Leedy	43
1.13.1 Objectives	43
1.13.2 Results and Discussion	43
1.13.3 Conclusions	52
1.14 Research Motivation and Objectives	52

1.14.1 Research Motivation.....	52
1.14.2 Objectives.....	53
2.0 ULTRASONIC POLYMERIZATION OF ISOPHORONE DIISOCYANATE BASED POLYURETHANE	55
2.1 Introduction.....	55
2.2 Experimental Methods	55
2.2.1 Materials	55
2.2.2 Equipment	55
2.2.3 Polymerization Technique.....	56
2.2.4 Characterization Methods.....	59
2.3 Results and Discussion.....	60
2.4 Conclusions.....	77
3.0 ULTRASONIC POLYMERIZATION OF ACRYLAMIDE.....	79
3.1 Introduction.....	79
3.2 Experimental Methods	79
3.2.1 Materials	79
3.2.2 Equipment	80
3.2.3 Polymerization Technique.....	80
3.2.4 Characterization Methods.....	83
3.3 Results and Discussion.....	84
3.4 Conclusions.....	94
4.0 SONICATION OF CNTs IN SITU WITH POLYACRYLAMIDE POLYMERIZATION.....	96
4.1 Introduction.....	96
4.2 Experimental Methods	96
4.2.1 Materials	96
4.2.2 Equipment	97
4.2.3 Polymerization Technique.....	97
4.2.4 Characterization Methods.....	99
4.3 Results and Discussion.....	99
4.4 Conclusions.....	126
5.0 CONCLUSIONS	128

5.1 Final Conclusions	128
5.2 Future Work	128

LIST OF TABLES

Table 1. The Effect of Solvent Type and Molar Ratio of PEG to ID on Viscosity of IDPU Solutions (Kotek and Leedy 4)	44
Table 2. The Effect of Solvent Type and Molar Ratio of PEG to ID on Molecular Weight of IDPU Solutions (Kotek and Leedy 6).....	51
Table 3. The Effect of Nitrogen Gas on the Viscosity of IDPU Solutions over a 3 Day Period	61
Table 4. The Temperature Changes of IDPU Solutions due to Sonication.....	63
Table 5. The Temperature Changes after the Ultrasonic Probe was removed from the Reaction Bottle.....	65
Table 6. The Effect of Different Power Settings on the Midpoint Viscosity of IDPU Solutions over a 5 Day Period	67
Table 7. The Viscosity Measurements of IDPU Solutions with Varied Amounts of Catalyst	68
Table 8. The Effect of Catalyst on the Temperature Changes of IPDU Solutions during Sonication	70
Table 9. Viscosity Measurements of IDPU Solutions after 14 Days	71
Table 10. The Effect of Probe Tuning on the Viscosity of IDPU Solutions over a 2 Day Period	72
Table 11. Viscosity of IDPU Solutions over a 22 Day Period with Different Amounts of Catalyst	74
Table 12. Viscosity of IDPU Solutions with No Sonication.....	74
Table 13. The Effect of Power Setting on the Viscosity of IDPU Solutions over 18 Days...	76
Table 14. The Effect of Monomer Concentration on the Viscosity of IDPU Solutions	77
Table 15. Viscosity of PAM Solutions with Different Initiator Concentrations.....	85
Table 16. Viscosity of PAM Solutions over a 14 Day Period.....	86
Table 17. Viscosity of PAM Solutions over a 14 Day Period with No Sonication	88
Table 18. Viscosity of PAM Solutions over a 14 Day Period with No Initiator.....	89
Table 19. Viscosity of PAM Solutions Sonicated at a Power Setting 8 over a 14 Day Period	89
Table 20. The Temperatures Changes of PAM Solutions during Sonication	91
Table 21. The Temperature Changes after the Ultrasonic Probe was removed from the Reaction Bottle.....	92
Table 22. The Effect of C_m , C_i , and Power Setting on the Molecular Weight of PAM Solutions	94
Table 23. The wt % of MWCNTs in PAM Films casted through Solvent Evaporation.....	100

LIST OF FIGURES

Figure 1. Molecular weight for chain-growth kinetics as a function of reaction time beginning with only monomer (R; left) with reaction progressing toward the right	4
Figure 2. Depiction of stepwise chain growth for monomers R and R ₁ as the polymerization begins (left) progressing toward the right (Carraher 84).	5
Figure 3. Interfacial polymerization; removal of polymer film from the interface (O dian 91).	11
Figure 4. Schematic representation of the growth and collapse of cavitation bubbles (Paulesse and Sijbesma 5446).	13
Figure 5. Ultrasonic degradation of water and subsequent initiation of acrylonitrile (top) and acrylamide (bottom) radical polymerization (Paulesse and Sijbesma 5447).	15
Figure 6. Collapse of a cavitation bubble, producing a shear gradient (left), and the shear gradient, able to stretch and break polymers (right) (Paulesse and Sijbesma 5447).	18
Figure 7. Compounds used in the study and probable initial decomposition products: a – bromobenzene; b – isoprene (2-methyl 1,3-butadiene); c – methyl methacrylate (2-methyl propenoic acid, methyl ester); d – styrene (ethenylbenzene, vinylbenzene) (Kruus 201).	24
Figure 8. The formation of a urethane linkage by reacting an isocyanate with a hydroxyl compound (Saunders 359).	26
Figure 9. Isophorone diisocyanate is prepared by the phosgenation of isophorone diamine (Saunders 363).	28
Figure 10. The reactions of isocyanate with urethanes and ureas to form allophanate and biuret linkages (Saunders 366).	28
Figure 11. The trimerization of isocyanates (Saunders, 367).	29
Figure 12. Two different degradation reactions of polyurethanes (O dian 132).	29
Figure 13. Formation of polyacrylamide from acrylamide (Saunders 146).	31
Figure 14. The structures of eight allotropes of carbon: (A), (B) Graphite, (C) Lonsdaleite, (D) C ₆₀ (Buckminsterfullerene or buckyball), (E) C ₅₄₀ Fullerene, (F) c ₇₀ Fullerene, (G) Amorphous Carbon, (H) Single-walled carbon nanotube (Aqel et al. 3).	35
Figure 15. Structure of a multi-walled carbon nanotube made up of three shells of differing chirality (Balasubramanian and Burghard 181).	36
Figure 16. The temperature changes of DMF when sonicated (Kotek and Leedy 4).	46
Figure 17. The temperature changes of butanone when sonicated (Kotek and Leedy 5).	47
Figure 18. The temperature profiles during IDPU polymerization in DMF at various power settings (Kotek and Leedy 5).	48
Figure 19. Temperature profiles during IDPU polymerization in butanone at various power settings (Kotek and Leedy 6).	50
Figure 20. Reactor bottle before preparation.	56
Figure 21. Reactor bottle after preparation. The top is cut off and two small holes are visible to the left and the right of the enlarged opening for the gas syringe and the thermocouple... ..	57
Figure 22. The setup of the ultrasonic probe in the fume hood. The probe is clamped to a stand and held in place adjacent to the body of the sonicator. The syringe for N ₂ gas is inserted on the right and the thermocouple enters the bottle on the left.	59

Figure 23. Temperature changes of IDPU solutions due to sonication. $C_{ID}= 12.76\%$, $C_{PEG}= 28.63\%$, $V_{cat}= 20 \mu\text{L}$. IDPU-1a, 2a, and 4 were sonicated at power-7. IDPU-3 was sonicated at power = 6. IDPU-5 was sonicated at power = 8. IDPU-1a and 1b were sonicated with no N_2 gas. IDPU-2a, 2b, 3, 4, and 5 were sonicated with N_2 gas.....	64
Figure 24. The temperature changes after the ultrasonic probe was removed from the reaction bottle. $C_{ID}= 12.76\%$, $C_{PEG}= 28.63\%$, $V_{cat}= 20 \mu\text{L}$. IDPU-1a, 2a, and 4 were sonicated at power-7. IDPU-3 was sonicated at power = 6. IDPU-5 was sonicated at power = 8. IDPU-1a was sonicated with no N_2 gas. IDPU-2a, 3, 4, and 5 were sonicated with N_2 gas.	65
Figure 25. The effect of power on the viscosity of IDPU solutions over 5 days. $C_{ID}= 12.76\%$, $C_{PEG}= 28.63\%$, $V_{cat}= 20 \mu\text{L}$. IDPU-3 was sonicated at power = 6. IDPU-4 was sonicated at power = 7. IDPU-5 was sonicated at power = 8.	67
Figure 26. The effect of catalyst on the temperature of IDPU solutions during sonication. $20\mu\text{L}$ catalyst was used for IDPU-6a, b and c. No catalyst was used for IDPU-7a, b and c. $C_{ID}= 12.76\%$, $C_{PEG}= 28.63\%$, Power = 7.....	71
Figure 27. Reactor bottle before preparation	81
Figure 28. Reactor bottle after preparation. The top of the plastic reaction bottle is cut off allowing for a larger opening so the ultrasonic probe can be inserted into the vessel. One small hole is visible to the left of the mouth for the N_2 gas syringe. A second small hole is visible to the left for the thermocouple.	81
Figure 29. The setup of the ultrasonic probe in the fume hood. The probe is clamped to a stand and held in place adjacent to the body of the sonicator. Additional clamps are available for holding the reaction bottle in place. The syringe of N_2 gas is inserted in the hole to the right of the reaction bottle's mouth.....	82
Figure 30. Samples PAM-1a (left) and b (right) turned upside down. Some movement was seen from the polymer solutions after a several seconds, but the samples were too viscous for viscosity measurements to be taken.....	85
Figure 31. The Temperature Changes of PAM during Sonication. $C_m = 6.76\%$, $C_i = 0.113\%$, Power = 7.....	92
Figure 32. Film 1 - 0.355 wt% CNT/polyacrylamide film. CNTs were sonicated prior to polymerization of acrylamide.	100
Figure 33. Film 2 - 0.343 wt% CNT/polyacrylamide film. CNTs were sonicated prior to polymerization of acrylamide.	101
Figure 34. Film 3 - 0.00 wt% CNT/polyacrylamide film.	102
Figure 35. Film 4 - 0.00 wt% CNT/polyacrylamide film.	103
Figure 36. Film 5 - 0.355 wt% CNT/polyacrylamide film. Polyacrylamide was polymerized with ultrasound prior to sonication of CNTs	104
Figure 37. Cross-section of film 1. Area A. 1000x magnification.....	106
Figure 38. Cross-section of film 1. Area B. 1000x magnification.....	107
Figure 39. Cross-section of film 1. Area B. 3000x magnification.....	108
Figure 40. Cross-section of film 2. Area A. 1000x magnification.....	109
Figure 41. Cross-section of film 2. Area A. 3000x magnification.....	110
Figure 42. Cross-section of film 2. Area B. 330x magnification.....	111
Figure 43. Cross-section of film 3. Area A. 330x magnification.....	112

Figure 44. Cross-section of film 3. Area A. 1000x magnification.....	113
Figure 45. Cross-section of film 3. Area B. 1000x magnification.....	114
Figure 46. Cross-section of film 3. Area B. 3000x magnification.....	115
Figure 47. Cross-section of film 4. 1000x magnification	116
Figure 48. Cross-section of film 4. 3000x magnification	117
Figure 49. Cross-section of film 5. Area A. 1000x magnification.....	119
Figure 50. Cross-section of film 5. Area B. 1000x magnification.....	120
Figure 51. Cross-section of film 5. Area C. 1000x magnification.....	121
Figure 52. Cross-section of film 5. Area B. 3000x magnification.....	122
Figure 53. Cross-section of Film 1. 25000x magnification.	123
Figure 54. Cross-section of Film 1. 50000x magnification	124
Figure 55. Cross-section of Film 5. 10000x magnification	125
Figure 56. Cross-section of Film 5. 10000x magnification.	126

1.0 INTRODUCTION, LITERATURE REVIEW, AND MOTIVATION

1.1 Introduction

Polymers help build the world around us and are used abundantly in our day to day lives. Every time you put on a cotton t-shirt or reach for a plastic water bottle to take a drink-- you are grabbing for a polymer. Finding a technology to more effectively produce such a widely used material in a shorter time frame allows for reduced time and cost of production. Utilizing the power of ultrasound waves as a technique for polymerization allows for shorter reaction times while producing the same quality high or low molecular weight polymer.

Ultrasound waves harness high amounts of energy and transport it through sound waves. When traveling through an elastic medium, these sound waves exist as pressure waves of compression and expansion and through an acoustic cavitation process these waves produce free radicals and localized hot spots that reach extremely high temperature and pressure values. This unique technology is used in a variety of fields for numerous applications including biology, chemistry, and engineering. Research has been done on the degradation effects of ultrasound waves, but not much experimentation has been conducted in how to harness the energy of the waves to create a polymer.

Polyurethane polymers have a wide range of applications from workout pants to wood sealants and at first glance would make an optimal polymer for ultrasonic polymerization due to its abundant applications. Understanding and refining the ultrasonic polymerization of polyurethane will allow for such a diverse polymer to be made faster than with traditional methods. Polyurethane is a block copolymer that can be formed from the reaction of isocyanate with a glycol. Isophorone diisocyanate is a cyclic monomer containing two highly reactive

isocyanate groups. This can form a more rigid segment of the polyurethane, however, isophorone can also undergo numerous other side reactions and cause difficulties during the polymerization process. In between these isocyanate monomers lies the more flexible segment, the polyethylene glycol. The polyurethane formed from these specific monomers is an isophorone diisocyanate based polyurethane (IDPU).

Acrylamide is a hydrophilic monomer which undergoes a simple chain growth mechanism during polymerization. No known side reactions take place that can lead to variation in the final polymer product. Polyacrylamide is abundantly used for moisture absorption in hygiene products but also finds use as a hydrogel for contacts and technical applications. A conductive hydrogel polyacrylamide/CNT composite could open even more doors for this polymer allowing it to be used in more technological applications including dye-synthesized solar cells and lithium ion batteries. Incorporating multi-walled carbon nanotubes in and in situ continuous polymerization process would allow for a polyacrylamide hydrogel or film to be conductive as ultrasound is also used for dispersing CNTs throughout a solution. Previous research conducted at NC State has focused on the ultrasonic polymerization of a step-growth polyurethane, but the ultrasonic polymerization of a chain growth polymer like acrylamide during the sonication of CNTs has yet to be done to the best of my knowledge.

Thus, using ultrasonic technology for polymerization could lead to decreased polymerization reaction times for known polymers and the creation of new, novel conductive composites for advancements in nanotechnology.

1.2 Polymer Classification

Polymers are generally classified into two different categories based on the kinetics of the polymerization process. In 1929, Carothers coined the terms addition and condensation polymer to describe the two main types of polymers basing his distinction off of the repeating unit in the polymer chain (Saunders 22). If the polymer repeat unit had the same number of atoms as the monomer, Carothers called this an addition polymer. If the polymer repeat unit had a number of atoms less than the monomer, he called this a condensation polymer. During the formation of a condensation polymer small molecules like HCl and H₂O can be released (Carragher 83). An alternate way to classify polymers came years later after Carothers definitions and it distinguishes polymers based on their reaction mechanism. The terms chain growth and step growth describe these two mechanisms with chain growth typically referring to addition polymerization and step growth typically referring to condensation polymerization. Most polymerization reactions can be classified into one of these two categories with some exceptions (Carragher 83).

Chain growth polymerization occurs from the breaking of double bonds in a vinyl monomer. Monomers that proceed via a chain growth mechanism contain a minimum of one carbon-carbon double bond. These are vinyl monomers (O dian 4). To polymerize these monomers three steps are required: initiation, propagation, and termination (Saunders 8). The double bond in the monomer must first be broken by an initiator to create an active site that can continue the subsequent bond breaking. Initiators during this stage can be a free hydroxyl radical, heat, light or even an anionic or cationic molecule (Saunders 8-9).

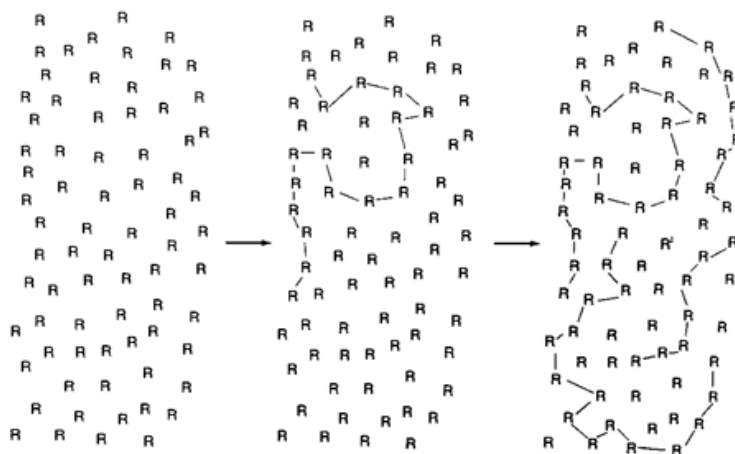


Figure 1. Molecular weight for chain-growth kinetics as a function of reaction time beginning with only monomer (R; left) with reaction progressing toward the right (Carragher 86).

Propagation is the following step where subsequent double bonds are broken and the polymer chain begins to grow one monomer at a time. The monomer is consumed steadily throughout the duration of the reaction, and the molecular weight of the growing polymer chains stays nearly constant (Carragher 87). Figure 1 models the chain growth kinetics of a growing polymer chain and the individual consumption of the monomers. The reaction proceeds from the left image to the right and the chain is extended by adding one monomer, R, at a time. Growing polymer chains cease growing during the termination step. Active polymer chain ends are deactivated by bonding with either another free radical initiator or another active site on a growing polymer chain. Common polymers formed through this process are polystyrene, polyethylene, polyvinyl chloride, and polyacrylamide (Saunders 8). In some circumstances, cyclic monomers like ethylene oxide or caprolactam can polymerize via ring-opening reactions and then proceed following a typical chain growth mechanism (Saunders 21)

Opposite to chain growth polymerization is step growth polymerization. In step growth polymerization two monomers, like or unlike, bond together via their functional groups and often release a small molecule byproduct. The monomer is consumed very early in the reaction as dimers form (Carraher 87). These dimers then bond with another monomer or dimer to form

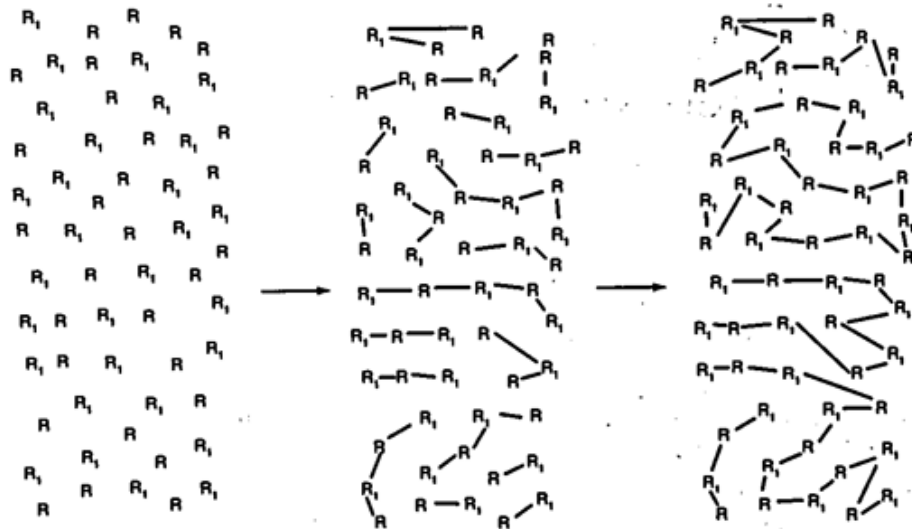


Figure 2. Depiction of stepwise chain growth for monomers R and R₁ as the polymerization begins (left) progressing toward the right (Carraher 84).

trimers or tetramers and these trimers and tetramers can further bond with each other or another polymer unit until all the monomer is consumed (Odián 6). Figure 2 demonstrates the step growth kinetics of two monomers, R and R₁, with the reaction proceeding from left to right (Carraher 84). The polymer chain length steadily increases throughout the duration of the reaction and the average molecular weight of the growing polymer chain increases as well (Saunders 23). Common polymers formed in this manner are polyesters, polyamides, and polyurethanes among many others (Carraher 87).

During polymerization, monomers can bond together in a few different geometries. Although linear polymers are the most simplistic, many other reactions can take place depending on the monomer, the number of active-species, and the number of functional groups present. Polymer chains can undergo back-biting, branching, crosslinking and chain transfer to form a different geometry. Back-biting produces branches in a polymer chain. The active species on the end of the chain can bond with a hydrogen atom in the middle of the chain and transfer a free radical to a carbon atom that the hydrogen was previously bound to. This creates a new active site (Saunders 97). This new active site, instead of being on the end of the chain, will be in the middle of the chain and the polymer chain will continue to grow from this new site exhibiting a branched geometry. Branches can be short or long depending on when and where the backbiting occurs and the amount of steric hindrance within the polymer chain. Polymers can exhibit high levels of branching or low levels of branching depending on the resonance stability of the free radical (Saunders 27). Another way branching can occur is by using multi-functional monomers (Carraher 96). In step growth polymerizations monomers bond together at their functional groups. By using a monomer with three functional groups other monomers can attach at both ends of the monomer and directly below the monomer. This entices the chain to grow in three directions. By using a monomer with four functional groups, monomers can attach in four directions leading to even more branching of the polymer chain. Crosslinking of polymer chains can also occur using multifunctional monomers (Saunders 28). When long polymers join at these sites a linked networked polymer structure begins to form. Crosslinked polymers will typically exhibit higher selected mechanical properties such as

strength because the polymer chains will be bonded together and less resistance to movement from an applied force.

1.3 Polymerization Techniques

Polymers can be made through several different methods with the major techniques for free radical polymerization being bulk polymerization, solution polymerization, suspension polymerization, and emulsion polymerization (Carragher 185). These processes require different monomer specifications and produce polymers in different ways for varying applications. However, all of these methods require extended time periods up to several hours and most require elevated temperatures and pressure for the polymerization reaction to proceed.

Bulk polymerization is a method primarily used for step growth polymerization reactions and is the simplest of the polymerization techniques. This technique involves the monomer or monomers and sometimes the addition of a catalyst or initiator to increase the reaction rate. No solvent or surfactant is required. The monomer(s) are gradually heated up in a reactor to a high temperature to induce polymerization. A gradual heating of the reactants is required in order to keep the viscosity of the polymer low and allow the mixture to keep moving as a liquid throughout the reactor (Saunders 24). To work most effectively in bulk polymerization, the monomers need to have a relatively low heat of polymerization to avoid scorching or burning the polymer. Heat removal is a disadvantage in this technique. (Saunders 24). One advantage of this technique is the high polymer yield upon completion of the reaction; however, removal of excess monomer from the reactor can cause difficulties (Carragher 186).

Poly(vinyl chloride) (PVC) can be made using the bulk polymerization technique in a two stage process that lasts 5-6 hours. The temperatures of these two stages ranges from 55-75°C at a pressure of 5-12 atm (Saunders 94). Once polymerized, the formed polymer can be extruded through, cooled and then cut for molding, injection, and other processing methods.

Solution polymerization is a more costly alternative to bulk polymerization because the final polymer is mixed into a solvent. The monomer, initiator, and resulting polymer must all be soluble in the same solvent. The solvent reduces the viscosity of the growing polymer chains so the solution can be stirred easily. Unlike with bulk polymerization, this technique can control the heat more effectively so a high heat of polymerization is acceptable (Carragher 186). High density polyethylene (HDPE) can be efficiently produced via this method as well as acrylic polymer solutions. Acrylic polymers solutions can be made with 0.2-1% of benzoyl peroxide initiator at temperatures of 90-110°C in an insulated and pressurized reactor. The solution is then stirred vigorously for one to four hours and a 40-60% polymer solution is obtained for use as an acrylic coating in the automotive industry along with others (Saunders 141). If a solid polymer is desired instead of a polymer solution, the polymer can be precipitated or solvent can be evaporated and then polymer is extruded and cut into pellets for processing. Polycarbonates can be formed and isolated in this way as well (Saunders 269).

Suspension polymerization is predominantly used for chain-growth polymers and produces small polymer beads or pearls (0.001-0.50cm in diameter) in solution (Saunders 26). For this technique the monomer and the initiator must be insoluble in the desired solvent. An advantage of this technique is the good heat control because water is the most popular solvent. Water acts as an effective heat transfer medium that maintains a low heat of reaction.

Due to the formation of solid, hard polymer beads the removal of the polymer from the solution can be easily performed through simple filtration techniques (Carraher 186). The polymer yield for this suspension polymerization is lower than the polymer yield in bulk polymerization, however this technique is very convenient for making resins and certain copolymers (Carraher 186). Poly(methyl methacrylate) (PMMA) can be formed via suspension polymerization for use in injection molding and extrusion. Methyl methacrylate along with benzoyl peroxide as an initiator, magnesium carbonate as a suspension agent, and water as a solvent will react in an insulated reactor with a mechanical stirrer (Saunders 139). During this exothermic reaction the temperature ranges from 80-120°C. The polymerization of PMMA is relatively quick and can reach completion in one hour after which time the polymer mixture can be cooled. The PMMA beads are then removed from the mixture, rinsed and dried and can be used for molding or other processing methods (Saunders 139).

Emulsion polymerization is another major polymerization technique and it is primarily used for chain growth polymerization polymers. The polymer forms inside micelles having diameters of 400-800 angstroms and yields a stable dispersion of the polymer particles in the solvent (Saunders 26). For emulsion polymerization to occur, a surfactant is needed to effectively disperse the monomer throughout the solvent. The free radical initiators in the solvent then enter the micelles containing the monomer and polymerization begins. The micelles are swollen with the newly formed polymer and are stabilized by the surfactant. The reaction continues until all the monomer is consumed (Saunders 26). Upon completion of polymerization, a latex forms that can be used for paints and adhesives. This stable dispersion of small polymer micelles can be broken with the addition of an acid (Saunders 27). In

emulsion polymerization, high molecular weight polymer is formed very quickly because the polymers are very stable in the micelles and this stability in turn, lowers the termination rate (Carragher 187). Poly(vinyl acetate) (PVA) is produced through emulsion polymerization in an insulated reactor equipped with a stirrer. The average reaction temperatures range from 75-80°C and lasts for 4-6 hours. PVA is typically used as a latex and kept in the dispersion (Saunders 115).

A fifth type of polymerization used in certain specific applications is interfacial polymerization. “Polymerization of two reactants is carried out at the interface between two liquid phases, each containing one of the reactants” (Odiان 90). The polymer forms as a film at the interface of these two immiscible solutions via a step growth mechanism. The polymer can be continuously drawn from the container until one, or both monomers is exhausted. Advantages of this technique are that interfacial polymerization can be done at temperatures ranging from 0-50°C and the polymer is formed very rapidly (Odiان 90). However, this technique has limitations when it comes to large-scale, commercial production because of the high cost of the solvents and the difficulty of solvent recovery (Odiان 92). Figure 3 shows the interfacial polymerization of a polyamide precipitating out at the interface of diamine and diacid chloride monomers (Odiان 90). Interfacial polymerization makes for a great educational demonstration and resource, but it is not feasible for industry. Nylon 6,6 can be easily made via interfacial polymerization as well as some polyesters, polyurethanes, and polycarbonates (Odiان 92).

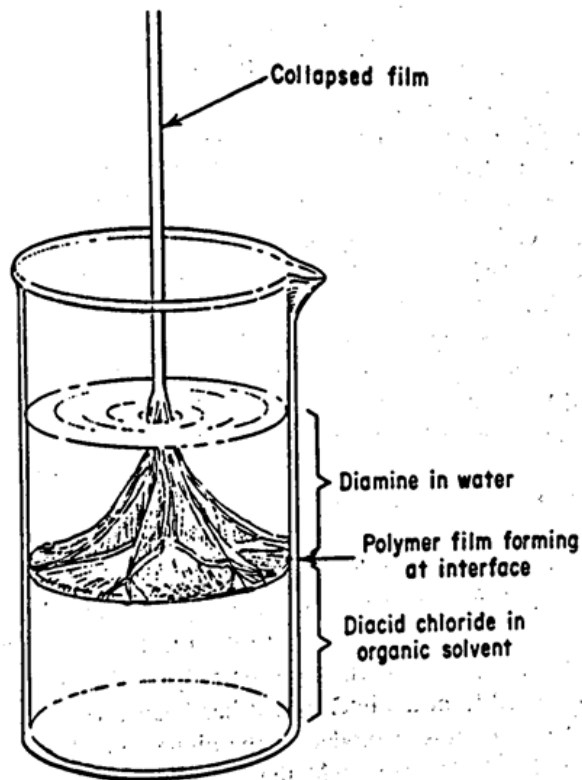


Figure 3. Interfacial polymerization; removal of polymer film from the interface (Odian 91).

1.4 Ultrasound Waves and Acoustic Cavitation

Ultrasound waves are characterized by having frequencies above that which the human ear can hear (Chen et al. 24). They can be classified by their frequencies and they fall into two categories: destructive or nondestructive. The frequency of destructive ultrasound waves starts at 16-18 kHz and can go up to 2 MHz whereas nondestructive, diagnostic ultrasonic waves range from 2-10 MHz (Paulesse and Sijbesma 5446). Ultrasound waves of 20-100 kHz are also used in other industrial applications including welding, cleaning, biology and chemical analysis (Mason and Lorimer, 3). For sonochemical purposes, destructive ultrasonic waves are needed because of their high energy levels. Medicinal ultrasounds are the lower frequency

ultrasounds used primarily for obstetrics (Mason and Lorimer 4). Ultrasound waves having frequencies even lower (20-50 kHz) are sometimes used in physiotherapy (Mason and Lorimer 4).

Ultrasonic polymerization is a technique that utilizes these high intensity, destructive sound waves to initiate and speed up a solution polymerization reaction. As these sound waves travel through water, or the selected solvent, several reactions take place leading to faster initial polymerization times. As traditional solution polymerization can take up to several hours, ultrasonic polymerization can reduce the reaction time substantially. Polymerization by ultrasound can be initiated in one of two ways or a combination of both — by high temperature and pressure created at hot spots in the solution and/or by the production of free radicals in the solution.

Sound is a form of kinetic energy with the energy being derived from the vibratory movement of the soundwave itself (Mason and Lorimer 23). The sound waves can travel through elastic mediums at an approximate velocity of 1,500 meters/second and induce a corresponding wave-like motion of molecules in the medium (Mason and Lorimer 25). As sound waves are transmitted through a medium of solid, liquid, or gas, they exist as pressure waves of compression and expansion (Chen et al. 24). The movement of the liquid aligns with the movement of the sound waves and the liquid is compressed and expanded accordingly. Figure 4 is a representation of how the sound waves induce corresponding pressure waves and how the bubble formation is in synchronization with these expanding and compressing pressure waves. As the sound waves move in this wave-like motion, the large space in between molecules allows cavities, or bubbles, to form during this process (Paulesse and Sijbesma

5446). As the ultrasound waves continue to travel through the liquid solution the small gas bubbles grow, and compress or collapse in an implosive process referred to as cavitation (Suslick 3). Cavitation can occur from several different actions including laser heating and boiling; however, cavitation from acoustic irradiation, which is the case with ultrasound waves, is referred to as acoustic cavitation (Suslick 2). This happens “when the pressure within the liquid drops sufficiently lower than the vapor pressure of the liquid” (Suslick 2). The cavitation process is dependent on many factors, as sound waves at different power or frequencies will induce waves and corresponding bubbles of different sizes.

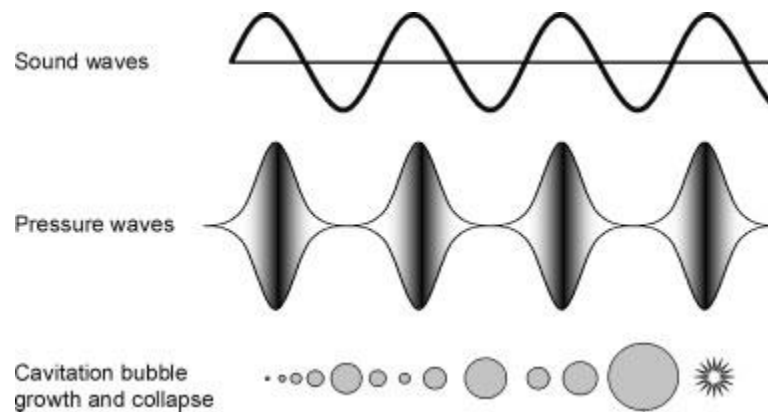


Figure 4. Schematic representation of the growth and collapse of cavitation bubbles (Paulesse and Sijbesma 5446).

Cavitation can produce two separate types of bubbles in a liquid. Bubbles that experience complete implosion are transient bubbles and those that oscillate in radius are stable bubbles (Mason and Lorimer 35). The classification of a transient or stable bubble depends on many factors and it is not permanent. Some stable bubbles can become transient as sonication continues and vice versa. Both of these bubbles grow through a nucleation process. According to theory, liquids contain “microscopic spaces, filled with gas or vapor, which act as cavitation

nuclei” for the bubbles (Chen et al. 24). As transient cavities in the liquid grow, pop, and implode, high-energy quantities are concentrated into the cavities and then released out into the solution (Suslick and Crum 271). “The high local temperatures and pressures, combined with extraordinarily rapid cooling, provide a unique means for driving chemical reactions under extreme conditions” (Suslick and Price 295). Exact temperatures are difficult to confirm during cavitation because a cavity lasts only for nanoseconds before implosion, and the diameter of some bubbles is only 1 mm (Suslick and Crum 272). Previous studies by Kruus et al., found that the bubble size is variable. And, although at the horn of the ultrasonic probe the measured intensity of the sound wave may be 20 kHz, the intensity of the sound waves outside of this localized area could be altered due to the “diffraction, reflection and absorption of the ultrasound” (Kruus et al. 354). The high temperature of the gas inside the bubble remains only for tens of nanoseconds until the bubble implodes and collapses sending shock waves throughout the solution (Suslick and Crum 279). “Bubble collapse induced by cavitation produces intense local heating, high pressures, and very short lifetimes. In clouds of cavitating bubbles, these hot spots have equivalent temperatures of roughly 5000 K, pressures of about 2000 atm, and heating and cooling rates above 10⁹ K/s” (Suslick and Crum 271). With these extreme temperatures inside the solution, the solution polymerization can be easily induced in shorter amounts of time than what is customary.

In sonochemical applications a commercial probe system is most often utilized. These probes have a pulse setting that allows the ultrasound to be delivered at programmed intervals (Mason and Lorimer 31). This allows for short cooling periods during the sonication process to aid the formation and collapse of the cavitation bubbles. “This is due to a time delay between

the application of the acoustic excitation (i.e. the sound wave) and the onset of cavitation” (Mason and Lorimer 31). Experiments by Mason and Lorimer, show that for ultrasound waves with a frequency of 5 MHz and 5.5 W/cm² a bubble can form and collapse in 160 nanoseconds (32).

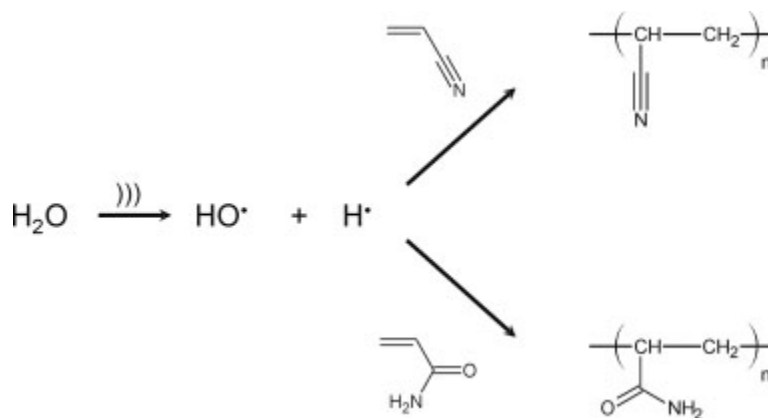


Figure 5. Ultrasonic degradation of water and subsequent initiation of acrylonitrile (top) and acrylamide (bottom) radical polymerization (Paulesse and Sijbesma 5447).

Along with cavitation producing extreme temperatures and pressure in the solution, bubble implosion can subsequently produce free radical species. Water molecules can break down into hydrogen and hydroxyl free radicals upon the pressure of the implosion. These radicals can then initiate chain growth polymerization reactions of vinyl monomers. “The primary products are H_2 and H_2O_2 ; other high-energy intermediates have been suggested, including HO_2 , H , OH , and perhaps e^- ” (Suslick and Crum 264). Figure 5 from Paulesse and Sijbesma displays a possible mechanism for the degradation of water into free radicals and how these free radicals are used to polymerize acrylonitrile and acrylamide. Their proposed mechanism suggests that water breaks down into both hydroxyl and hydrogen free radicals

which can then be used to break the double bonds in these vinyl acrylamide and acrylonitrile monomers to produce a polymer.

Ultrasonic polymerization of vinyl monomers through the formation of free radicals was first discovered by E. El'piner, a Russian scientist in the late 1950s (El'piner 1). El'piner writes,

it is generally accepted that the initiation of chemical reactions in an aqueous medium irradiated by ultrasonic waves is brought about by the breakdown products of the water molecules-atomic hydrogen and free hydroxyl radicals. The breakdown of water molecules to form the extremely reactive, $H\cdot$ and $HO\cdot$ radicals takes place in the cavity as a result of the ionisation of the molecules by the moving charges. (2)

During polymerization ultrasound can be used to completely replace free radical initiators or as a supplement to them (Paulesse and Sijbesma 5447). “A complication in ultrasound-induced polymerizations is the increase in the viscosity during the polymerization of a monomer. This slows down the production of cavitation bubbles and therefore the production of radical initiators” (Paulesse and Sijbesma 5447). The use of an ultrasonic probe to create free radicals can help streamline the polymerization process and allow for the minimized use of initiators in solution.

1.5 Ultrasonic Induced Polymer Degradation

Along with polymerization, ultrasounds have a wide variety of other uses in the scientific realm. Sonication can be used for everything ranging from sonar imaging to machine cleaning. Carbon nanotubes are sonicated before use to stop them from aggregating later on

(Kharissova et al. 24813). Biologists can use ultrasound waves to disrupt cells and rupture cell walls (Mason and Lorimer 4). And in the realm of chemistry, scientists were well aware of its ability to break bonds and induce scission of polymer chains long before ultrasound was discovered as a way to initiate polymerization. Degradation of polymer chains is possible by the formation of free radicals in the solution as well as the creation of shear gradients among the polymer chains (Paulesse and Sijbesma 5447). More research has been conducted on the degradation of polymers through ultrasound, then how to form them.

The depolymerization of macromolecules with ultrasound waves was first thought to be discovered by A. Szalay in 1933 (El'piner 2). Szalay exposed starch, arabic gum, and other macromolecules to ultrasound waves and noted a decrease in viscosity which directly correlated to a decrease in the molecular weight and polymer chain length (El'piner 2). "In certain cases, however, this viscosity decrease was temporary and reversible" (El'piner 2). Szalay's work proved that short term exposure of polymers to ultrasound waves may not be permanent because after sonication the viscosity of the polymer increased again as the monomers continue to react. But, "the prolonged exposure of solutions of macromolecules to ultrasonic waves leads to a permanent, irreversible decrease in viscosity, indicating a breakdown in the molecular structure as a result of the rupture of valency bonds" (El'piner 2). With increased sonication time polymers and other molecules are able to be permanently broken down by ultrasound waves.

A mechanical result of cavity implosion in the solution is the creation of a shear gradient acting on the polymer. As the cavity implodes the decrease in pressure causes a

shearing effect on the polymer chain. The chain is lengthened and stretched rapidly leading to a scission of the covalent bonds in the backbone of the polymer chain as seen in figure 6

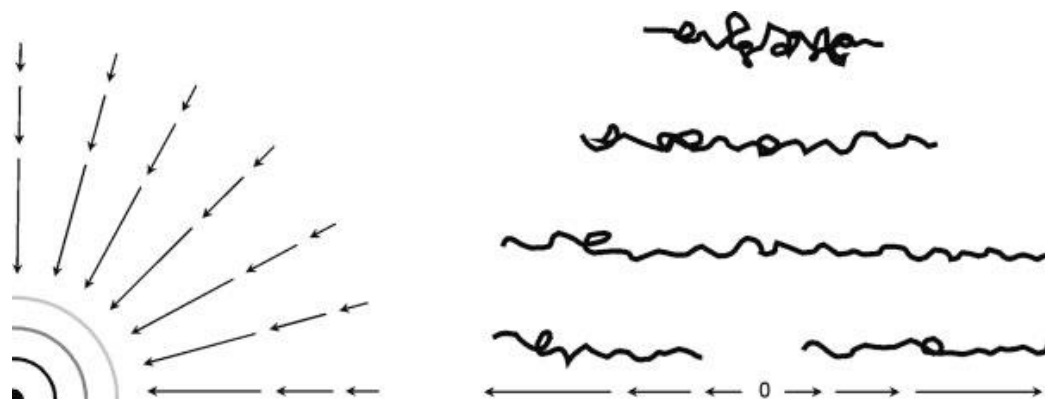


Figure 6. Collapse of a cavitation bubble, producing a shear gradient (left), and the shear gradient, able to stretch and break polymers (right) (Paulesse and Sijbesma 5447).

(Paulesse and Sijbesma 5447). In order for this mechanical action to have enough energy to break the polymer chain, the polymer chain being extended and experiencing the shear gradient needs to have a substantially high molecular weight. Therefore, polymer degradation by this mechanism primarily acts on the chains having the highest molecular weight (Paulesse and Sijbesma 5448). The scission of polymer chains via shear gradients produces two very reactive heterogeneous or homogenous species that will generate side reactions or intramolecular rearrangements with other molecules in the solution (Paulesse and Sijbesma 5448). Mason and Lorimer have concluded that “scission of polymer chains is either a random process or that it takes place at the midpoint of the polymer chains” with more evidence pointing to scission at the midpoint (123). They continue to say that bond cleavage may be due to the formation of unstable intermediates like ions or free radicals that can act on the weaker bonds in the polymer backbone (124). If scission does not occur at the midpoint of the polymer chains, small and

long chains will be produced during the polymerization leading to a larger PDI of the formed polymer. Side reactions due to bond cleavage may also lead to increased branching in the geometry of the forming polymer (El'piner 9). As ultrasonic polymerization of the monomers continues and higher molecular weight polymer forms, covalent bond cleavage in the chains is more apparent and a threshold exists for the maximum molecular weight achievable by this polymerization method. (Paulesse and Sijbesma 5447). A threshold also exists for cavitation intensity, and when this threshold is exceeded, degradation may also be induced (Mason and Lorimer 112). For ultrasonic polymerization to be as effective as possible, the reaction must be stopped before the polymer begins to undergo degradation (Suslick and Price 301).

Degradation during ultrasonic polymerization can also lead to increased production of free radicals in the solution. As bonds in the polymer chains are broken, simultaneous free radical formation is observed (Paulesse and Sijbesma 5452). Suslick and Price found that these radicals, whether they are free species or parts of a degrading polymer chains, can also lead to copolymerization in the presence of other monomers (308). Also with sonication time ranging up to 400 minutes, the degradation of polymer chains continues until the molecular weight approaches a lower limiting value (Suslick and Price 299). Suslick and Price concluded that ultrasonic degradation is jointly due the radical production and the shearing effect, but not a result of the high temperature and pressure values reached during cavitation (300).

Incorporating inert gas into the sonication process helps reduce the effect of oxygen interfering with the polymerization reaction. By degassing the solution or solvent before exposure to sonication, oxygen can be eliminated from the reaction and lead to an increase in polymerization rates because the free radical side reactions will be inhibited (Mason and

Lorimer 128). By eliminating excess free radicals in solution, less polymer degradation by the interference of free radicals will be observed. Higher monomer conversion rates are found when monomers are sonicated in the presence of nitrogen gas as opposed to oxygen (Mason and Lorimer 129).

1.6 Disadvantages of Ultrasonic Polymerization

Ultrasound waves have the power to quickly and effectively initiate a small-scale polymerization reaction because of the high kinetic energy of the waves. However, the implementation of ultrasound in a large-scale industrial or commercial application would lead to complications. The efficient creation of cavitation bubbles is difficult to achieve on an industrial scale (Paulesse and Sijbesma 5452). Due to the insertion of the probe into the reactor, the frequencies of the emitted waves are not homogeneous throughout the solution. There is a localization of high energy waves surrounding the probe and higher temperatures and pressures are reached at this area due to the increased vibrational compression and expansion of the sound waves. This results in higher molecular weight polymer being polymerized in one area and not others. The volume of the reaction is also limited by the use of the probe. Multiple probes could be used, however the reaction would still not produce a homogeneous polymer.

1.7 Previous Research with Ultrasonic Polymerization

1.7.1 Polymerization of Methyl Methacrylate Initiated by Ultrasound

Scientists Price, Norris and West researched the free-radical initiated polymerization of methyl methacrylate using high-intensity ultrasound. Since methyl methacrylate is a vinyl monomer, free radical initiation was chosen. Operating from the theory that hydrogen and

hydroxyl radicals are formed during sonication, Price et al. wanted to use the ultrasound to create polymers with a set “molecular weight, polydispersity and tacticity” (“Methyl Methacrylate” 6447).

Poly(methyl methacrylate) was polymerized using an ultrasonic probe operating at a frequency of 22 kHz in a specially made four-necked pear shaped flask. Deoxygenated methyl methacrylate was polymerized in the flask in a nitrogen-gas rich environment. In some samples an initiator of azobisisobutyronitrile (AIBN) was added to the solution and in some samples a bulk polymerization technique was followed. Price et al. found that with no added initiator conversion rates of 12% were reached after 6 hours of sonication (Price et al. “Methyl Methacrylate” 6448). When the AIBN was incorporated into the polymerization a conversion rate of 13% was reached after 4 hours showing that added initiator is crucial to reach higher monomer conversion rates (Price et al. “Methyl Methacrylate” 6453).

They discovered from their experiment that controllable ultrasonic polymerization of PMMA is possible however a limitation of their work was the low monomer conversion percentages achieved. High molecular weight polymers form early, but then there is a pronounced depreciation of the molecular weight at longer reaction times (Price et al. “Methyl Methacrylate” 6453). Traditional free radical polymerization doesn’t experience the same polymer degradation effects as polymerization via ultrasound waves.

1.7.2 Preparation of PVA Latex with Ultrasonic and Redox Initiation

M. Bahattab used ultrasonic polymerization in combination with a redox emulsion polymerization process to polymerize a poly(vinyl acetate) (PVA) latex. The goal of

Bahattab's experiment was to obtain a higher conversion rate of the monomer at ambient temperatures than is achieved with a redox initiator alone (812). Due to the solubility of the vinyl acetate monomer in water a very good initiator is needed to speed up the reaction and the addition of ultrasound will induce this.

For polymerization, a 20 kHz ultrasonic probe was used at a power level of 50W. Prior to polymerization the monomer, surfactant, solvent, and initiators were all combined in a beaker for ultrasonic polymerization and a three-necked flask for redox polymerization (Bahattab 813). Bahattab conducted polymerization experiments on poly(vinyl acetate) via ultrasonic polymerization and redox polymerization separately and together. The sonication time of the polymers varied, but the highest time reached was 30 minutes (815). For polymer classification the molecular weights were taken by gel permeation chromatography (GPC). The number average molecular weight (M_n) after five minutes using sonication alone reached 112,000 g/mol with the weight average molecular weight (M_w) reaching 607,000 g/mol and a polydispersity index (PDI) of 5.52. After 20 minutes of sonication the M_n and M_w were 93,600 g/mol and 342,000 g/mol respectively with the PDI of 3.65. After sonication for 30 minutes the M_n and M_w decreased even more to values of 76,100 g/mol and 284,000 g/mol; however the PDI increased to 3.73. (Bahattab, 816). These values indicate that ultrasonic polymerization is most successful at sonication times greater than five minutes, but less than 20 minutes. At sonication times of 30 minutes, noticeable decreases in the molecular weight is observed due to polymer scission via the ultrasonic waves. Another outcome of longer sonication times is a greater polydispersity index. Also of note is that a greater PDI is achieved

when redox and sonication are used in conjunction rather than just using redox polymerization alone (Bahattab 816).

1.7.3 Polymerization Resulting from Ultrasonic Cavitation

Kruus researched the effect of temperature on the ultrasonic solution polymerization of bromobenzene, isoprene, methyl methacrylate and styrene monomers (201). These monomers proceed through a chain growth polymerization mechanism and were all initiated by a different technique. All samples were made using a 20 kHz fixed frequency sonicator set at a power output of 50W. Each polymer was made in slightly different ways to test the effect of various conditions on the final polymer product and sonicated for times ranging from 25-240 minutes. Argon was bubbled through some solutions during sonication to remove impurities (Kruus 202). Several runs were completed under differing temperature conditions (-55, 3, 15, and 30 °C) to see the effect of temperature on the polymerization results. The polymerization of bromobenzene was investigated and produced a graphite-like polymer structure. This was “initiated by dissociation of the weakest bond (the C-Br)” as a result of the collapse of the cavities in the solution (Kruus 202). Three runs were conducted at 30°C and one run at 15°C. Argon was bubbled through two of the samples and oxygen was bubbled through the third. Isoprene was sonicated at -55°C with the hypothesis that a higher rate of “cavitation-induced polymerization would be even greater at lower temperatures” (Kruus 203). Through ultra-violet absorption spectra, results showed that polyisoprene samples made ranged from eight to ten carbon units long. Kruus suspects this is due to the ultrasound induced chain scission along the polymer backbone (203). Methyl methacrylate was sonicated at 3°C for 200

minutes. Viscosity measurements were taken and showed a viscosity decrease for the first 20 minutes, and then a dramatic increase for the remaining 180 minutes. Kruus supposed that the initiation of poly(methyl methacrylate) resulted from bond breaking within the monomer and that polymerization proceeded through free radical addition mechanism (203).

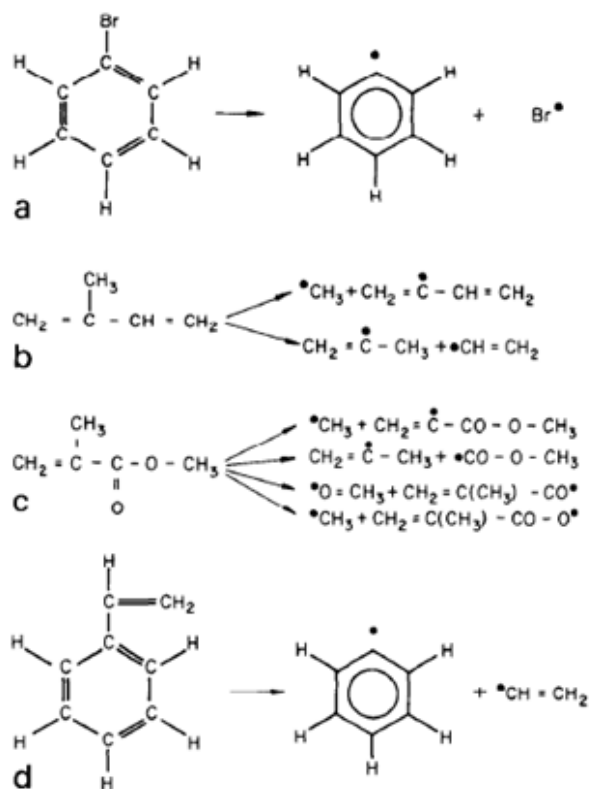


Figure 7. Compounds used in the study and probable initial decomposition products: a – bromobenzene; b – isoprene (2-methyl 1,3-butadiene); c – methyl methacrylate (2-methyl propenoic acid, methyl ester); d – styrene (ethenylbenzene, vinylbenzene) (Kruus 201).

Styrene was sonicated at 3°C for 4 hours; however, results showed that no viscosity change was observed during this time. The probable products formed throughout all of Kruus' experiments are seen in figure 7. These molecules were thought to be the first product of polymerization formed from the interaction of the ultrasound and the monomer and this

product was able to initiate the polymerization reactions. Kruus' overall conclusions state that additional research is needed to fully understand polymerization initiated by ultrasound, however it does seem advantageous for specific polymer applications (204).

1.7.4 The Effect of High Intensity Ultrasound on Polyurethane Synthesis

Price, Lenz, and Ansell created polyurethanes from several diols and diisocyanates with a sonicator bath, an oven, and a high intensity ultrasound probe operating at 23 kHz ("High Intensity Ultrasound" 1532). The sonication reactions were carried out in a three-necked flask in the presence of a nitrogen rich environment. A 1:1 molar ratio of the reactants was used and in some experiments 0.1% by weight of dibutyltin dilaurate was added as a catalyst (Price et al. "High Intensity Ultrasound" 1532). Polymerization times ranged from 1-360 minutes, with the shorter times used during ultrasonic polymerization and the larger times used when the reactants were stirred in an oven.

The polyurethanes polymerized by sonication reached a higher extent of reaction as seen by the presence of longer polyurethane chains. The researchers were able to conclude that in all cases "there is a clear acceleration of the reaction under ultrasound in both catalysed and uncatalysed reactions" and not just due to an increase in temperature (Price et al. "High Intensity Ultrasound" 1533). All molecular weights were measured through GPC and were relatively low, however the polyurethanes produced through sonication, generally had elevated values. Consequently however, the sonicated samples also had a higher PDI ranging from 2.5-4 whereas the PDI for polymers produced by the other methods ranged from 2.0-2.9 (Price et al. "High Intensity Ultrasound" 1534).

Final conclusions from Price, Lenz, and Ansell stated that ultrasound does increase the reaction rate of the polyurethane polymerization reaction, but this technique might be better used in applications where multicomponent systems are used to capitalize on the efficient mixing of sonication (1536). The researchers also concluded that increasing the intensity of the ultrasound had no major impact on the final molecular weight of the polymer (Price et al. “High Intensity Ultrasound” 1536).

1.8 Polyurethane Polymer Synthesis, Processing, and Characteristics

Polyurethane polymers are multi-use, block copolymers characterized by a urethane linkage in the main backbone. A urethane linkage is seen in figure 8 and is formed by the reaction of an isocyanate and an alcohol (Odian 130). Depending on the specific monomers chosen for polymerization many other groups can be present in the backbone as well (esters, amides, ethers, etc) (Saunders 358). The polymerization mechanism for polyurethane is generally a step growth reaction with no byproduct because an internal rearrangement of the hydrogen occurs during polymerization (Carraher 88). By changing the monomers and the monomer concentrations a wide range of polyurethanes can be made as both rigid and flexible segments exist in the polymer. Polyurethanes have uses ranging from bowling pins to swimsuits and fibers to wood sealants (Carraher 89).



Figure 8. The formation of a urethane linkage by reacting an isocyanate with a hydroxyl compound (Saunders 359).

The polymerization process is complex due to the large amount of side reactions that can occur during the process. Isocyanates are common monomers for polyurethane polymerization as they are an extremely reactive species (Saunders 166). Figure 9 shows the production of isophorone diisocyanate by phosgenation. Isophorone diisocyanate is a polyurethane monomer with two reactive isocyanate groups. They are quick to react with macroglycols to form polyurethane, but also quick to react with many other compounds that may be found during the reaction process. Diamines could react with isocyanates to introduce urea linkages in the polymer thus giving the polymer both urea and urethane linkages (Odián 130). These urethane and urea linkages can then form allophanate and biuret linkages which may or may not be wanted in the final product of the reaction (Odián 131). Allophanate linkages result from the reaction of an isocyanate and a urethane whereas biuret linkages result from the reaction of an isocyanate and a urea (Saunders 366). Figure 10 shows both the formation of an allophanate and a biuret linkage starting with an isocyanate. The amount of these linkages in the final product are a result of the amount of urea and urethane linkages which arise from the original monomers chosen for the polymerization process. Isocyanate groups also have the tendency to form an isocyanurate molecule as shown in figure 11 (Odián 131). Instead of forming polyurethanes, three isocyanate groups can form a ring together and halt future polyurethane formation. The catalyst choice for the polymer and the reaction temperature also influence the amount of these side reactions. For most polyurethanes, the reaction temperature ranges from 100-120°C because polyurethane degradation is known to happen at temperatures above 120°C. Two possible degradation mechanisms are shown in figure 12. Both reactions produce carbon dioxide as well as other products. In some cases,

polyurethanes can also degrade back to the original isocyanate and alcohol monomers (Odiان 132). The correct balance and molar ratios of the monomers and catalyst is crucial to obtain the suitable polyurethane for every application.

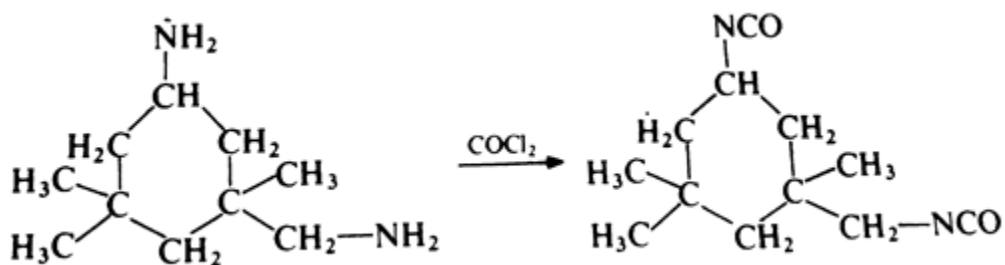
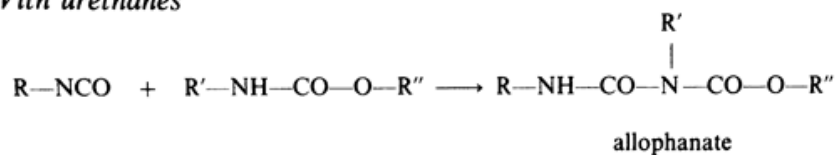


Figure 9. Isophorone diisocyanate is prepared by the phosgenation of isophorone diamine (Saunders 363).

(v) *With urethanes*



(vi) *With ureas*

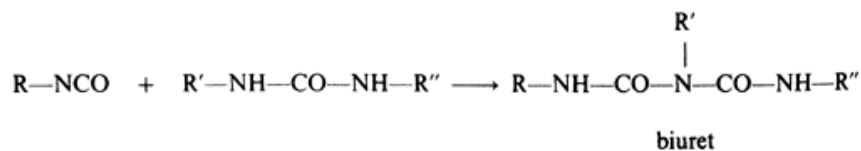


Figure 10. The reactions of isocyanate with urethanes and ureas to form allophanate and biuret linkages (Saunders 366)

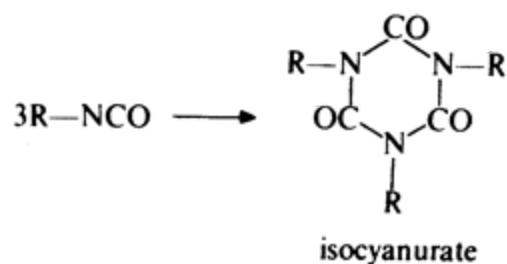


Figure 11. The trimerization of isocyanates (Saunders, 367).

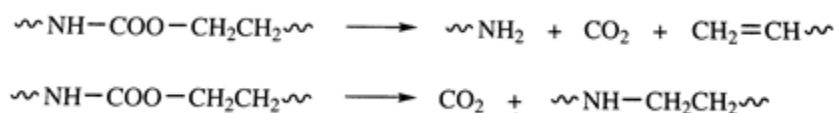


Figure 12. Two different degradation reactions of polyurethanes (O'dian 132).

Polyurethanes are generally divided into several major types and can have a range of properties depending on what the final polymer will be used for (Saunders 358). Polyurethane foams can be flexible, rigid, or integral, but they all generally have a good strength per weight ratio, good rebound, and a high impact strength (Carragher 89). Polyurethane elastomers have a good elasticity, good resistance to abrasion, good hardness, and a good resistance to grease (Carragher 89). Polyurethane can be made into a fiber commonly known as spandex (Saunders 382). It can also be used as a one-component or two-component surface coating (Saunders 3). One component systems cure with the help of air, moisture, or heat without the need of prior mixing (Saunders 383). Two component systems can be isocyanate-polyol mixtures or

prepolymer polyol mixtures. These systems are mixed immediately prior to use and curing takes place as these two components instantaneously react with each other (Saunders 385). These two component systems can be used as both flexible and hard polyurethanes for a range of applications (Saunders 386). Some isocyanate-polyol systems can also be used as adhesives for bonding wood, metal, glass, fibers, and plastics. Crosslinking occurs through the functionality of the isocyanate monomers and a strong and stable adhesive is formed relatively quickly (Saunders 387).

The polymerization of polyurethane is a difficult process as many unwanted side effects may occur during the reaction. Careful selection of monomers is crucial, along with correct molar ratios. Slight errors in any of the above variables can lead to a very sticky or a very brittle polyurethane. However, this does make polyurethane a very popular polymer with a vast array of applications.

1.9 Polyacrylamide Properties and Synthesis

Superabsorbent polymers like polyacrylamide were first introduced into the market for application in diapers and agriculture and have sensed grown in popularity in the thirty years since (Omidian 4). Depending on the specific polymer used, they can absorb hundreds to thousands of times their own weight in water and store it in a stable matrix (Lin et al. 489). Polyacrylamide is a networked and very hydrophilic, superabsorbent, polymer hydrogel (Tang et al. 215). It consists of long chain, inert and non-toxic polymer chains with mechanical and chemical properties that can be modified based on application (Zhou et al. 116). Acrylamide is a vinyl monomer as shown on the left side of figure 13 and polymerizes as the figure models.



Figure 13. Formation of polyacrylamide from acrylamide (Saunders 146).

Polyacrylamide can be easily produced through traditional free radical solution polymerization with an initiator of a potassium persulfate and a solvent of water (Lin, H. 1507). The polymer chains traditionally grow linearly, but can be crosslinked when multifunctional monomers like N,N-methylenebisacrylamide are incorporated into the free-radical polymerization process. Higher monomer conversions are reached when the monomer concentration is increased to 1.76 mol/L (Lin, H. 1508). Throughout Lin's experiment the initiator concentration was held constant at 2.25×10^{-3} mol/L (1508). For traditional solution polymerization according to Lin's work, polymerization continued for two hours at a constant temperature of 55°C and monomer conversions of 94% were reached (1509). Since the polymerization of polyacrylamide proceeds rather simply, extremely high molecular weights can be achieved. The molecular weight of polyacrylamide can range from several hundred thousand g/mol to one million g/mol with values even reaching 6 million g/mol in some cases (Fevola 563). After synthesis the product can be dehydrated and made into sheets, films, particles, spheres, or a variety of other shapes (Omidian 8). The dried polymer product is hard and brittle, but in the presence of water polyacrylamide begins to swell within seconds (Omidian 10). In the absence of crosslinking polyacrylamide is very brittle and falls apart easily when in a swollen state. To solve this mechanical issue, much research has turned to

ways to increase the mechanical properties of these hydrogels with the incorporation of nanoparticles being the most favored (Zhou and Wu 155).

1.10 Previous Research on Polyacrylamide Hydrogel Composites

1.10.1 Application of cellulose nanocrystals in polyacrylamide hydrogels

Zhou et al. incorporated rod-shaped cellulose nanocrystals (CNC) into polyacrylamide hydrogels through in situ free-radical polymerization to increase the mechanical properties of the gel by reinforcing the polymer structure with additional crosslinking (116). Polyacrylamide was formed from acrylamide and N,N-methylenebisacrylamide monomers with potassium persulfate and sodium bisulfate as free-radical initiators (Zhou et al. 117). All monomers and initiators were stirred in a nitrogen atmosphere for 5 minutes and then incubated at 25°C for 20 hours to fully complete the hydrogel gelation process (Zhou et al. 117). The gels were then dried in a vacuum for 12 hours at a constant temperature of 50°C before characterization and testing (Zhou et al. 117). The samples were characterized by FTIR, SEM, swelling ratios, and compression properties (Zhou et al. 117).

Results from Zhou et al. concluded that a CNC polyacrylamide hydrogel absorbs less water than polyacrylamide hydrogels alone. The incorporation of CNCs into polymerization accelerated the formation of the polyacrylamide hydrogel and increased the crosslinking between polymer chains as the polymer grafted onto the CNCs (Zhou et al. 122).

Zhou furthered this research with Wu to create a polyacrylamide/chitosan composite through in situ free radical acrylamide polymerization (155). The same acrylamide monomers and methods were used as described above and the characterization methods were kept the

same also. The natural chitosan nanofibers hydrogen bonded and covalently bonded to the polymer creating a mechanically stronger hydrogel by nearly seven times (Zhou and Wu 161).

1.10.2 Synthesis and Electrical Conductivity of a Polyacrylamide/Cu Hydrogel

Lin, Tang, and Wu synthesized a superabsorbent and conductive polyacrylamide/copper composite by solution polymerization with hopes that it has potential uses in lithium batteries, dye sensitized solar cells, supercapacitors, and fuel cells (489). The composite hydrogel was prepared in a two-step process. First, acrylamide, N-N'-dimethyleneacrylamide, and copper powder were combined in water and degassed for 30 minutes. Then the free-radical potassium persulfate initiator was added. The mixture was heated to 75°C and stirred in a water bath for 30 minutes. The final product was filtered, dried, milled, sifted and then ready for the next step. For step two, three grams of the powder was submerged into 500 mL of water and left for three hours to induce formation of the hydrogel (Lin et al. 490).

The researchers followed the above basic procedure and made modifications to investigate the effect of monomer concentration, initiator concentration, crosslinker concentration, and Cu content on the conductivity of the hydrogel. The hydrogel conductivity reached a maximum value at 42-50 wt% monomer, 0.9 wt% initiator, and 0.08 wt% crosslinker. The optimum polymerization temperature for maximum conductivity was found to be 83°C and the optimum Cu content was 12 wt% (Lin et al. 491-92). Lin et al. were able to successfully synthesize a polyacrylamide/Cu composite with a conductivity of 1.08mS m⁻¹ (489).

1.11 Properties of Carbon Nanotubes

Carbon can exist in many different forms because of its hybridized orbitals and relative stability achieved through valence bonding (Zhang 1). Diamond and graphite are both different forms of carbon differing only by the bonding structure of the carbon molecule. The molecular structures of diamond and graphite can both be seen in figure 1.14, A and B respectively. Six-membered, hexagonal carbon rings are able to bond together to form a one dimensional sheet known as graphene. Rolling these graphene sheets into hollow cylinders on the molecular level forms carbon nanotubes (CNTs) as seen in figure 14 (Haghi and Mottaghalab 5).

CNTs have been the topic of much research and experimentation since their discovery by S. Iijima in 1991 (Zhang 2). “There has been intensive research activity in the area of carbon nanotubes, not only because of their fascinating structural features and properties, but also because of their potential technological applications” (Rao et al. 79). Because of their advantageous conductive properties, high strength, and high modulus they have a wide variety of uses in nanotechnology as fillers in polymer matrices and sensors. They also can be used for fibers, hydrogen storage, medicine, aeronautics, tissue engineering and electronics (Tasis et al. 1105). CNTs are currently the stiffest and strongest materials measured according to their Young’s modulus and yield strength. “Their Young’s modulus is about 1 TPa, and the tensile strength is about 11– 63 GPa for individual multiwall CNTs (MWCNTs) and 13– 52 GPa for individual single-wall CNTs (SWCNTs)” (Zhang 502). They can exist as single-walled nanotubes (SWCNTs) or multiwall nanotubes (MWCNTs) and have the capacity to be further modified by functionalization and modification. SWCNTs are composed of one sheet of graphene rolled into a hollow cylindrical tube with capped ends, and MWCNTs as seen in

figure 15 consist of nested, graphene cylinders with capped ends (Zhang 2). MWCNTs have larger diameters ranging from 10-400 nm whereas SWCNTs typically have diameters of 0.8-2 nm (Haghi and Mottaghitlab, 5). Both SWCNTs and MWCNTs have lengths up to several micrometers long. The different geometries of CNTs affect their properties and allow them to be used for many different applications. For example, due to their single walled structure SWCNTs are more useful as conductors than MWCNTs (Aqel et al. 4).

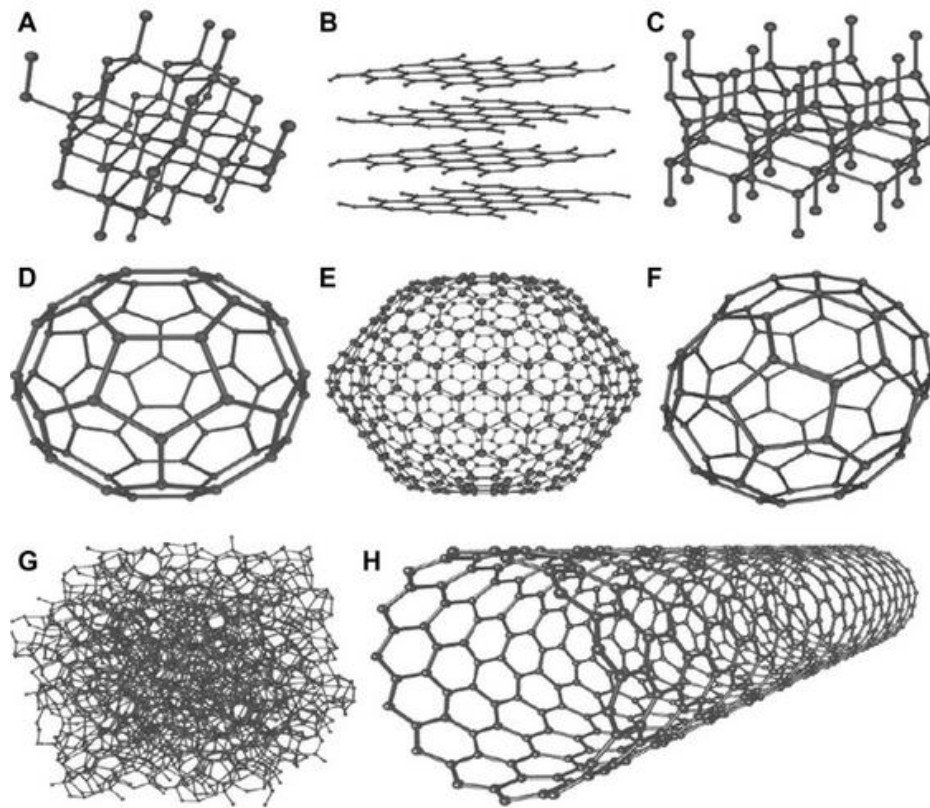


Figure 14. The structures of eight allotropes of carbon: (A), (B) Graphite, (C) Lonsdaleite, (D) C₆₀ (Buckminsterfullerene or buckyball), (E) C₅₄₀ Fullerene, (F) C₇₀ Fullerene, (G) Amorphous Carbon, (H) Single-walled carbon nanotube (Aqel et al. 3).

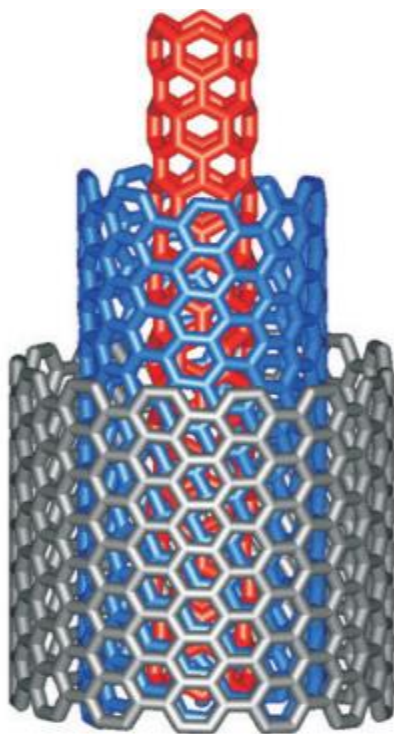


Figure 15. Structure of a multi-walled carbon nanotube made up of three shells of differing chirality (Balasubramanian and Burghard 181).

CNTs can be synthesized through three major techniques: discharge, laser ablation, and chemical vapor deposition (Aqel et al. 8). All three techniques are not cost effective so further research is needed before the large scale use of nanotubes. The growth mechanism of CNTs is not completely known, however several mechanisms exist with the two most popular growth mechanism theories being tip-growth and root-growth models (Aqel et al, 8). Depending on the axis at which the graphene sheets are rolled during synthesis, CNTs with different chirality are formed (Balasubramanian and Burghard 182). Achiral CNTs can be further classified into an armchair or zigzag conformation. (Rao et al. 84). “Chiral nanotubes show spiral symmetry

and their mirror images are not identical to the original ones” (Zhang, 1). The different chiralities of the tubes affect their optical, mechanical, and electrical properties (Aqel et al. 8).

Applications of CNTs present some limitations and difficulties due to their hydrophobic surface and tendency to aggregate. CNTs form bundles very easily to build a highly complex network of solid nanotubes (Tasis 1105). Prior to use, CNTs must be efficiently dispersed in solution to lessen the high amount of van der Waals forces between molecules. This also gives CNTs poor solubility in water and organic solvents (Kharissova et al. 24812). “They can be dispersed in some solvents by sonication, but precipitation immediately occurs when this process is interrupted” (Tasis et al, 1105) CNTs can also be dispersed throughout solution by plasma discharge, irradiation, and ozonolysis (Kharissova et al. 24813). MWCNTs can effectively be dispersed in water by ultrasonication along with a surfactant (Kharissova et al. 24814). During sonication, dispersion of CNTs in solution is governed by the mechanical forces created by transient cavitation of the bubbles, but stable cavitation from the ultrasound waves can also affect dispersion and induce surface damage on the CNTs. (Sesis et al. 15149). Most sonication procedures require surfactants for effective CNT dispersion although Sesis et al. concluded that surfactants can undergo degradation and create radical scavengers during the aqueous dispersion of CNTs (Sesis et al. 15149). The correct sonication procedure and surfactant choice are crucial during this process. SWCNTs are not as easily dispersed in water when compared to MWCNTs and require longer sonication times. CNTs can be sonicated by immersion of an ultrasonic probe, or by a sonicator bath. The probe is more powerful and allows for shorter sonication times, but using an ultrasonic probe presents more challenges as localization of the ultrasound waves is increased and can lead to

cavitation shielding effects in the solution. Sonication with an ultrasonic probe also presents difficulties when used with large volumes of solution. A sonicator bath is more applicable to industrial and commercial use due to increased cavitation uniformity (Sesis et al. 15149). Double sonication is also possible by immersing a probe into a sonicator bath for increased sonication (Kharissova et al. 24814). Proper dispersion of CNTs is necessary in order to maintain their excellent conductive and mechanical properties after processing (Kharissova et al. 24812).

Several modification techniques exist for increasing the dispersibility of CNTs in an aqueous solution. Functionalization of MWCNTs increases the solubility and dispersion stability in polar solvents like methanol and water (Kharissova et al. 24819). The functionalization of CNTs by the introduction of hydrophilic, carboxylate groups can be done through an acid oxidation process (Li et al. 169). The carboxylate groups are able to covalently bond to both the sidewalls and the end caps of the nanotubes. This dramatically increases the solubility of the CNTs, but it can consequently decompose CNTs during the long sonication process required to graft the carboxylate groups onto the nanotubes (Haghi and Mottaghitlab 6). Non-covalent modification of CNTs is not only more environmentally friendly, but also inflicts less side effects to the nanotubes. Non-covalent modification can be achieved by adding surfactants, wrapping the CNT with a polymer, or the endohedral method which involves inserting small molecules into the center of the nanotube (Haghi and Mottaghitlab 7). Research has shown that polymer assisted dispersion of CNTs leads to reinforced polymer which can be used in some drug delivery applications. (Kharissova et al. 24831). CNTs can

be modified through a variety of methods to allow for easier processing and manufacturing allowing for more applications and uses for such novel nanoparticles.

1.12 Previous Research with Carbon Nanotubes

1.12.1 Preparation of Biocompatible Multi-Walled Carbon Nanotubes

Li et al. prepared multi-walled carbon nanotubes in situ with the polymerization of acrylic acid and methyl methacrylate for use as lymph node tracers. MWCNTs were selected due to their increased solubility in water; however, CNTs with no additional polymer grafting have high tendencies to accumulate in cells, organs, and tissues when used for biological and medicinal applications. By grafting polymers onto the CNT structure, MWCNTs exhibit increased biocompatibility and have a good potential for in vivo applications.

The grafted poly(acrylic acid) CNTs (PAA-g-MWCNTs) were prepared by carefully adding 0.25g acrylic acid to a mixture of 100mL acetone and 0.1g MWCNTs. The mixture was then sonicated at a frequency of 59 kHz for 10 minutes and purged with nitrogen gas. Then 2,2-Azobisisobutyronitrile (AIBN) was added to the reactor to initiate the free radical polymerization of acrylic acid. A high heat of 55 °C was maintained for 4 hours after the addition of the initiator and then the PAA-g-MWCNTs were dried in a vacuum for 16 hours at 40 °C (Li et al. 170). PAA-g-MWCNTs were characterized by gel permeation chromatography, high resolution transmission electron microscopy, and ¹H NMR analysis.

Acetone was chosen for use in this experiment because it is a poor solvent for poly(acrylic acid) (PAA). Using a poor solvent forces the polymer chains to precipitate out of solution and graft onto the CNTs. The active free radical species on a growing polymer chain

is able to covalently bond to the MWCNTs. With poor solvents the grafting percentage of the polymer to the CNT increases. The maximum amount of PAA grafted onto the surface of the CNTs was 22% by weight and the CNTs were able to be easily dispersed in water and therefore suitable for lymph node identification during surgery (Li et al. 173)

1.12.2 Novel Dispersion of MWCNTs in Polystyrene Polymer

An experiment by Abdel-Rahem et al. dispersed MWCNTs in polystyrene and cast a film to investigate CNT dispersion in the polymer and the electrical conductivity of the polymer (747). The MWCNTs were sonicated with b-HNA in a THF solvent for two minutes. Then the polystyrene was added to the mixture and sonicated for an additional 15 minutes. The mixture was then poured into a 15cm, glass petri dish and set to dry for 24 hours at room temperature to produce a 0.08nm film (Abdel-Rahem et al. 748).

Electrical conductivity measurements were determined with AC and DC applied electrical fields and FTIR spectra were gathered. For effective electrical conductivity, the CNTs must be close enough for electrons to travel between them however, physical contact between nanotubes is not mandatory (Abdel-Rahem et al. 752). Results showed that through the solvent evaporation film casting technique, CNT dispersion does not change or alter and that the electrical conductivity results for homogenous films are reproducible (Abdel-Rahem et al. 753).

1.12.3 Excellent Dispersion of MWCNTs in PEO Polymer

A study conducted by Park et al. dispersed MWCNTs in a solution of polyethylene oxide to achieve an excellent dispersion of CNTs in a polymer composite. The goal of this

research was to create “a simple, reliable, and cost-effective evaporation method casting procedure to fabricate MWCNT-PEO composite films having microstructures of well dispersed MWCNTs within the polymer” (2). The absence of a cost effective film fabrication method is the primary limitation to the lack of CNT-polymer composites being used in commercial and industrial applications. The composite was made by sonicating MWCNTs (length 1–5 μm , diameter 15 ± 5 nm, purity 95%, and bulk density 1.8 g cm^{-3}) in a 1% sodium dodecyl sulfate solution and then adding them to PEO polymer. The solution was then sonicated for 30 more minutes at 20 kHz (Park et al. 3). The mixture was poured into a glass and silicone mold and dried in an oven at 85°C to evaporate the solvent. After all solvent was evaporated, the film was set to cool at room temperature conditions (Park et al. 3).

The film formation method was a solvent evaporation method from a dilute polymer solution. This is a relatively cheap and easy fabrication method that could work with MWCNTs or SWCNTs and does not require purification or filtration of the polymer-CNT solution. The dispersion of the CNTs throughout the polymer film was characterized by morphology, conductivity, percolation, and crystallinity through the use of field-emission scanning electron microscopy, small angle x-ray scattering, and direct current two-point electrical resistance measurements (Park et al. 3). The results showed that “the thickness of the fabricated composite film is uniform and the MWCNTs were well dispersed inside the PEO matrix” with no distinct aggregation of CNTs (Park et al. 4). The film casting method as outlined in this paper is sufficient to produce a composite with enhanced mechanical properties, however more research is necessary when using a polymer with a higher melting point than that of PEO.

1.12.4 Effects of Polymer Wrapping and Functionalization on MWCNT Stability

A study conducted by Ntim et al. discovered that the polymer wrapping of MWCNTs (OD 20–30 nm, purity 95%) with polyvinyl pyrrolidone (PVP) led to less aggregation and stability of the CNTs in solution (383). The grafting of the PVP polymer on the surface of the CNTs decreases their hydrophobic nature by decreasing the van der Waals interactions. PVP is very water soluble and covalently bonds or grafts itself on the CNT. One end of the PVP polymer floats freely in solution and the other end attaches to the CNTs. Functionalized CNTs also lead to increased hydrophilicity and better dispersion; however, “the water dispersibility of covalently functionalized CNTs originates from electrostatic repulsive forces between negative surface charges, whereas a polymer-wrapped CNT is stabilized sterically by the presence of the hydrophilic polymer on the surface” (Ntim et al. 383).

Purified MWCNTs were dispersed in a solvent of deionized water (50mg MWCNTs per 1 liter of water) along with 1% SDS surfactant and 1% by weight of PVP. The mixture was incubated at 50°C for 12 hours and then the CNTs were filtered, rinsed and then three times in deionized water to remove any excess surfactant. PVP wrapped MWCNTs were compared to carboxylated MWCNTs and the two types of CNTs were characterized by SEM images (Ntim et al. 384). Results found that polymer wrapped CNTs have lower stability than that of functionalized CNTs in water, with functionalized CNTs showing higher long term stability in the presence of electrolytes (Ntim et al. 388).

1.13 Previous Studies on Ultrasonic Polymerization by R. Kotek and A. Leedy

1.13.1 Objectives

A. Leedy and R. Kotek conducted studies on ultrasonic polymerization to gain a better understanding of how the ultrasonic polymerization of polyurethane works. The first objective included the examination of how different solvents, molar ratios of the monomers, and power settings of the ultrasonic probe affected the viscosity and molecular weight of the polymerized polyurethane. The second objective involved gathering temperature measurements in order to evaluate temperature profiles for the two solvents individually, as well as for polymer solutions at different power settings. The third objective was to characterize the polymer through viscosity measurements and gel permeation chromatography (GPC) results (Kotek and Leedy 2).

1.13.2 Results and Discussion

Experiments were first designed to investigate the effect of changing the molar ratio of the monomers on the viscosity of the isophorone diisocyanate based polyurethane (IDPU) solutions. Two different solvents, 2-butanone and N,N-Dimethylformamide (DMF), were used in these experiments and their effects on the viscosity were also noted. All experiments were sonicated for 15 minutes pulsing for 2 seconds on and 1 second off. Table 1 displays the effect of solvent type and molar ratio on the viscosity of the IDPU solutions. Samples with molar ratios of 1:1.2 show the highest viscosity values of all samples for both DMF and butanone solvents on both day 1 and day 30. Samples run with a 1:1 molar ratio have the lowest viscosity in both solvents on both day 1 and 30. Reactions run in a 20% molar excess of isophorone

diisocyanate produce higher viscosity polymer. Diisocyanates are a very reactive species so this excess allows for more isocyanate to participate in the polymerization reaction and less to participate in side reactions. For the duration of the experiments a molar ratio of 1:1.2 polyethylene glycol to isophorone diisocyanate was used.

Table 1. The Effect of Solvent Type and Molar Ratio of PEG to ID on Viscosity of IDPU Solutions (Kotek and Leedy 4)

Sample Code	Solvent	Molar Ratio of PEG to ID	C _{TOT} (%)	Power Setting	Solution Viscosity (cP)	
					Day 1	Day 30
AL-1	DMF	1:1.2	46.16	7	742	802
AL-2	DMF	1:1.1	41.40	7	342	284
AL-3	DMF	1:1	41.44	7	112	118
AL-4	Butanone	1:1.2	45.31	7	220	1964
AL-5	Butanone	1:1.1	45.34	7	166	1956
AL-6	Butanone	1:1	45.38	7	176	202
AL-10.1	Butanone	1:1.2	45.31	3		56
AL-10.2	Butanone	1:1.2	45.31	5		82

Note: V_{cat} = 20 μL

Samples run in a solvent of butanone generally had lower viscosity values than those run in DMF with sample AL-3 being the exception. However, this result could be primarily because of the 1:1 molar ratio used in this sample and the sample having the lowest C_{TOT} value. Samples AL-1, 2 and 3, exhibited a less drastic viscosity increase from day 1 to day 30 due to the use of DMF as solvent. Polymerizing IDPU polymer in DMF leads to a more consistent polymer overall and evidence infers that the reaction does not continue after sonication. Over the 30 days between viscosity measurements, butanone samples AL-4 and 5 increased by factors of 8.9 and 11.8 respectively with butanone sample AL-6 only increasing by 26 cP. When comparing only AL-1, 2 and 3, the samples seem to no longer polymerize after

sonication, but when comparing samples AL-4, 5 and 6, continuation of the reaction is seen because of the increase in viscosity. Based off of the day 30 measurements of AL-1, 2, 3, 4, 5 and 6 it is inconclusive to whether the polymerization reaction continues after sonication or not as some samples increased dramatically, some increased by only a few cP, and one sample experienced a decrease in viscosity.

No measurements were taken on day 1 of samples AL-10.1 and 10.2, however day 30 measurements were taken and indicate that a higher power setting on the probe produces a higher viscosity IDPU solution.

Temperature data was gathered from the sonication of both DMF and Butanone individually. Each solvent (26 mL) was put in the reaction bottle and sonicated for 15 minutes on a power setting of 3, 5 and 7. The temperature changes occurring in DMF during sonication are displayed in figure 16. All three samples of DMF showed the same general trend. The temperatures of the samples increased steadily to a point around minute 6 and then plateaued reaching the maximum temperature at minute 15. DMF sonicated at power 3 showed the smallest temperature increase during sonication only reaching a maximum temperature of 36.8 °C. Power 5 showed a greater temperature increase than power 3, but sonication at power 7 resulted in the greatest temperature increase with a maximum temperature of 114.9°C. DMF sonicated at power setting 5 reached a maximum temperature of 83.7 °C. A high power setting on the ultrasonic probe correlates with a higher temperature during sonication. In all three experiments, the temperature DMF stayed well below its boiling point of 153 °C.

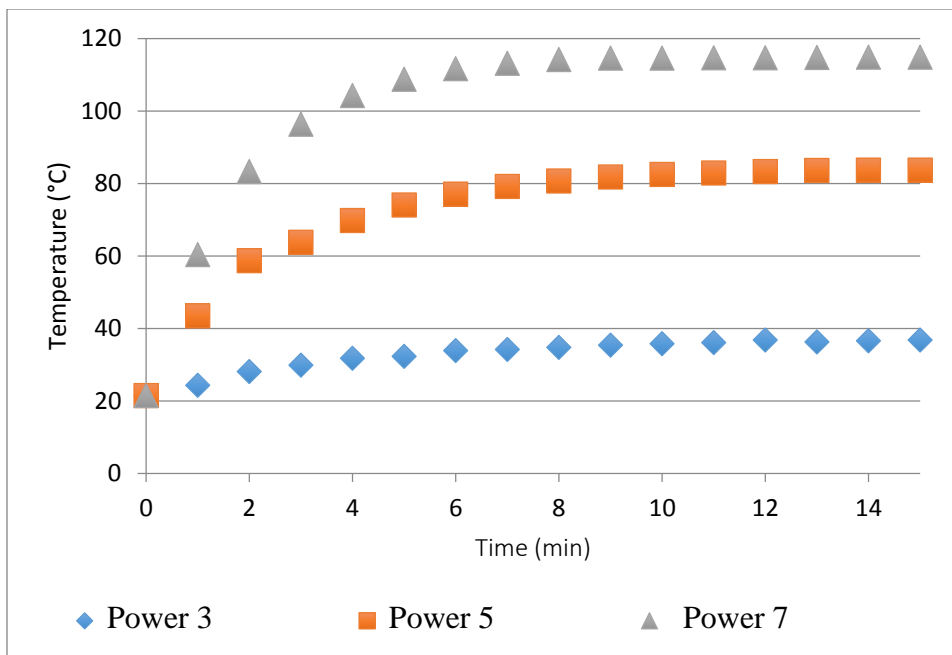


Figure 16. The temperature changes of DMF when sonicated (Kotek and Leedy 4).

When butanone was sonicated, two samples (power 3 and power 5) exhibited behavior similar to DMF, and one sample (power 7) showed a different profile. These results are seen in figure 17. Samples sonicated at power 3 and 5 had temperature increases up to minute 5 and then plateaued reaching maximum temperatures of 37.1 °C and 62.8 °C respectively. The sample sonicated at power 7 reached a maximum temperature of 59 °C by minute 4 and steadily

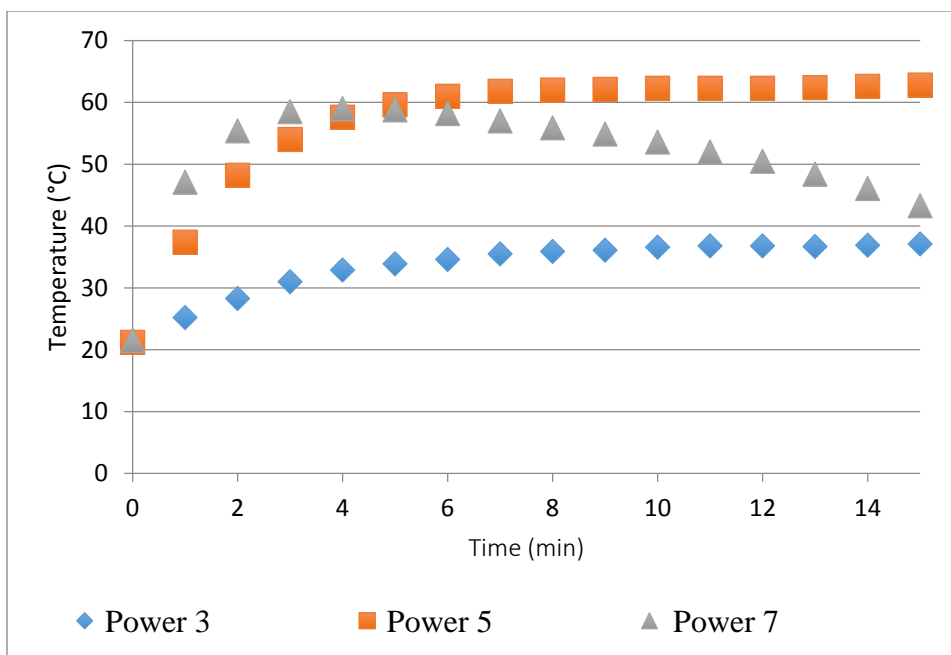


Figure 17. The temperature changes of butanone when sonicated (Kotek and Leedy 5).

decreased to 43.3 °C by minute 15. All butanone samples were predicted to have similar profiles, but a different profile was observed at power 7 potentially due to the low boiling point of butanone. This differentiation from the others could be a result of the butanone beginning to evaporate off, bringing the temperature of the solution down while it attempts to reach an equilibrium point. Butanone boils at 79.6 °C whereas DMF has a much higher boiling point of 153 °C and did not experience this outlying temperature profile.

Figure 18 shows the temperature changes of three IDPU solutions during sonication in DMF. The same general trend is seen in all three samples with only slight variations seen in the sample sonicated at power 7. The temperature profile of the IDPU solutions showed

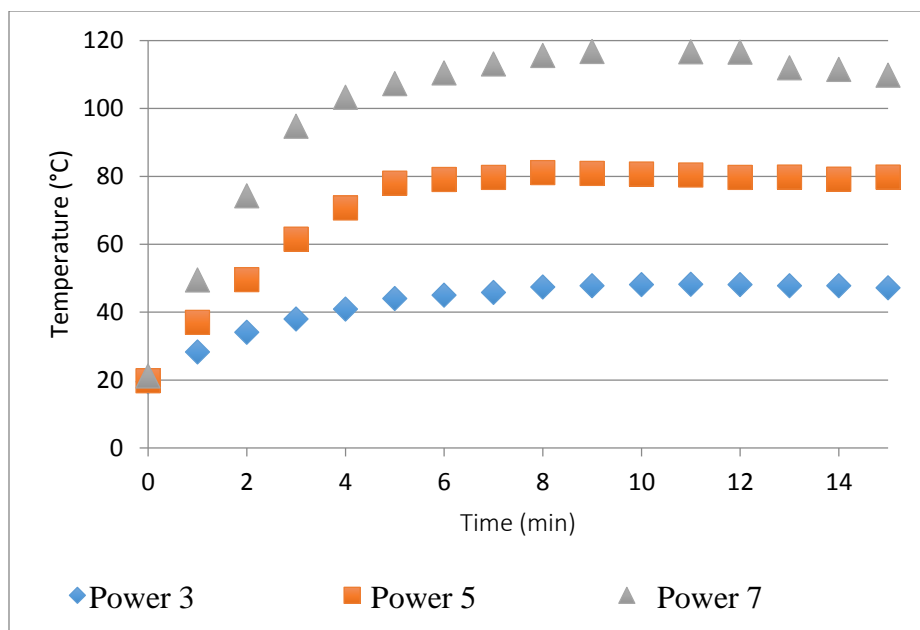


Figure 18. The temperature profiles during IDPU polymerization in DMF at various power settings (Kotek and Leedy 5).

similar trends to figure 16 where DMF was sonicated alone at three different power settings. All three curves were evenly distributed and consistent with one another. All three samples showed a dramatic increase up until minute five when samples sonicated at power 3 and 5 began to level off. The sample sonicated at power 7, however, showed a temperature increase until minute 10 and then a decrease for the remaining five minutes. The maximum temperature of the power 3 sample was 48.2°C at minute 11, the maximum temperature of the power 5 sample was 80.9 °C at minute 9, and the power 7 sample had a maximum temperature of 116.8 °C at minute 9. At the end of sonication (minute 15) samples made at power 3, 5, and 7 had final temperatures of 47.2 °C, 79.8 °C and 109.8 °C respectively. Samples at power 3 and 75 only decreased by 1 °C and 1.1 °C from the maximum to final temperature and the power 7 sample at decreased by 7 °C. A high power setting on the ultrasound probe correlates to a

higher temperature reached during ultrasonic polymerization. When compared to figure 16 IDPU samples sonicated at power 5 and 7 had lower temperatures than when DMF was sonicated at that power alone. However, IDPU at power 3 had a higher final temperature than DMF alone when sonicated at that power. No replicates of these experiments were performed so results are not conclusive to whether this behavior is the norm or the exception.

Figure 19 shows the temperature profiles of IDPU solutions polymerized in butanone at various power settings. Samples sonicated at power 3 and power 5 show similar trends as seen in figure 18 and 17 with variation seen in the sample sonicated at power 7. All samples experienced a steep temperature rate of change for the first few minutes and then samples at power 3 and power 5 began to level out whereas the sample at power 7 continued to increase up to minute 12 reaching a maximum temperature of 94.5 °C. After this maximum point the solution's temperature decreased to a final temperature of 79.3 °C. The continuous decline of the curve after exceeding the boiling point could further support the idea that the butanone solvent begins to evaporate. The maximum temperature reached by samples at power 3 and power 5 was 50.5 °C and 64.2 °C respectively. When compared to the behavior of butanone sonicated alone, the IDPU solutions in butanone showed higher temperature for all three samples. This behavior could be due to the formation of the polymer in solution and its ability to absorb more heat than just the solvent.

The results obtained from the GPC data found in table 2 show that overall, the molecular weight of the IDPU polymers is largely influenced by temperature, procedural variations, and molar ratios. The polymers produced with butanone as the solvent achieved higher molecular weights than those with DMF. The highest molecular weight polymer

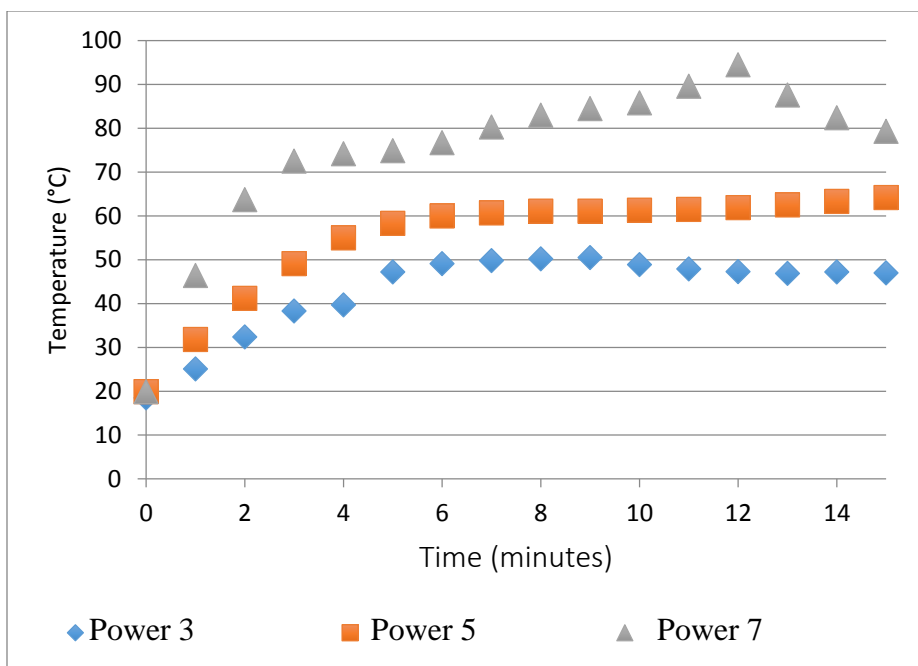


Figure 19. Temperature profiles during IDPU polymerization in butanone at various power settings (Kotek and Leedy 6).

produced was AL-10.3. This reaction included the same mole ratio (1:1.2), the same amount of solvent (butanone), and used the same power setting (7) as AL-4. The only difference between the two reactions is that the procedural method was slightly altered. In sample AL-4 the solvent and monomers were mixed to form a homogeneous mixture prior to sonication. The catalyst was then added immediately before the probe was inserted and turned on. Sample AL-10.3 was sonicated with no prior mixing of the components. All components were added and the probe was inserted and turned on. AL-4 had a measured molecular weight (Mw) of 78,731 D. AL-10.3 had a measured molecular weight of 352,923 D. This was an exceptionally large difference given that the reactions contained the same amount of components, and differed only by the variation to the procedural method. This could be related to the general

idea that as the research continued human errors were limited. However, this proves that overall, properties (i.e. molecular weight) of the polyurethane polymers produced by ultrasonic polymerization can be controlled by factors such as temperature, solvent, mole-to-mole ratios, and procedural methods.

Table 2. The Effect of Solvent Type and Molar Ratio of PEG to ID on Molecular Weight of IDPU Solutions (Kotek and Leedy 6).

Sample Code	Solvent	Molar Ratio of PEG to ID	C _{TOT} (%)	Power Setting	Molecular Weight (D)			
					M _n	M _w	M _p	PDI
AL-1	DMF	1:1.2	46.16	7	15,028	23,407	23,932	1.56
AL-2	DMF	1:1.1	41.40	7	11,596	17,133	19,589	1.48
AL-3	DMF	1:1	41.44	7	9,372	13,170	11,310	1.41
AL-4	Butanone	1:1.2	45.31	7	39,224	78,731	67,445	2.01
AL-5	Butanone	1:1.1	45.34	7	18,934	30,489	28,269	1.61
AL-6	Butanone	1:1	45.38	7	14,991	21,144	20,852	1.41
AL-8.1	DMF	1:1.2	46.16	3	15,292	23,679	23,936	1.55
AL-8.2	DMF	1:1.2	46.16	5	42,895	122,384	69,766	2.85
AL-8.3	DMF	1:1.2	46.16	7	55,070	179,262	84,826	3.26
AL-10.1	Butanone	1:1.2	45.31	3	40,368	93,577	67,787	2.32
AL-10.2	Butanone	1:1.2	45.31	5	61,366	221,590	101,444	3.61
AL-10.3	Butanone	1:1.2	45.31	7	84,775	352,923	137,753	4.16

Note: V_{cat}= 20 μL

GPC results also recorded the M_p and PDI of the samples. The M_p value is the molecular weight of the highest polymer chain in the sample. When comparing samples AL-8.1, 8.2, and 8.3, the PDI increases as the power increases. This shows that with a higher power the polymers have a wider distribution of chain lengths. More homogeneous polymer chains form at lower power settings and higher molecular weight, more dispersed polymers are

formed through the use of higher power settings. These conclusions are also consistent when comparing samples AL-10.1, 10.2 and 10.3. AL-10.3 although having the highest molecular weight (Mw), has the largest PDI. The sample with the smallest Mw corresponding has one of the lowest PDIs and is made at the lowest power setting.

1.13.3 Conclusions

In general figures 16-19 show that the temperature profile was found to have an even distribution and correlated an increase in power and an overall increase in the temperature reached throughout the reaction. This is due to the fact that the reaction temperature did not exceed the boiling point for either DMF or butanone. The 1:1.2 mole ratio used in polymerization for both DMF and butanone yielded the highest viscosity value. The use of DMF as the solvent produced polyurethane polymer samples with higher viscosities. The viscosity measurements of the produced polyurethane polymer samples (AL-10.1 and 10.2) showed a direct correlation to an increase in power setting resulting in an increase in viscosity of the polymer solution.

1.14 Research Motivation and Objectives

1.14.1 Research Motivation

Positive outcomes resulting from the previous research of A. Leedy and R. Kotek as well as the research described in section 1.7 reveal that ultrasonic polymerization can be used to produce IDPU polymer solutions in DMF or butanone. However despite interesting results, more research is needed to fully discover a reproducible and viable ultrasonic polymerization

methodology. A. Leedy and R. Kotek's studies provide useful research leads, but leave several questions unanswered. Using similar techniques and methods to previous research, the reproducibility of both the step-growth ultrasonic polymerization of IDPU and the chain-growth ultrasonic polymerization of PAM will be researched with hopes to answer remaining questions. Experiments will also focus on changes in the IDPU and PAM solutions after sonication and if the use of an ultrasound probe polymerizes the monomer to completion or acts simply a catalyst or a heat source. Delving deeper into the chemistry behind ultrasonic polymerization of IDPU and PAM, additional studies will be conducted to recognize the use of ultrasound in polymerization chemistry.

As traditional uses for ultrasound in chemistry involve the sonicated dispersion of carbon nanotubes, the in situ polymerization of polyacrylamide into carboxylated MWCNTs will also be researched. Applying ultrasound to polymers in this way could create a method of excellent dispersion and integration of CNTs into polymers to create conductive films and lead to more novel uses of nanotechnology.

1.14.2 Objectives

The experiments conducted in this thesis aimed to

1. Refine R. Kotek and A. Leedy's methods to create a procedure to polymerize reproducible IDPU samples through ultrasonication
2. Expand Kotek and Leedy's research to ultrasonically polymerize polyacrylamide which is initiated by a free radical and polymerizes through a chain-growth mechanism

3. Investigate the dispersion of CNTs in situ with the ultrasonic polymerization of polyacrylamide to create a polyacrylamide/CNT film

To achieve the three objectives listed above three separate experiments were conducted with separate experimental design and methods. Further discussion of these separate experiments are described in chapters 2.0, 3.0, and 4.0.

2.0 ULTRASONIC POLYMERIZATION OF ISOPHORONE DIISOCYANATE BASED POLYURETHANE

2.1 Introduction

Refining the ultrasonic polymerization method for polyurethane could reduce polymerization time as compared to traditional polymerization methods. Investigating this process can allow for more polymers to be made through sonication and increase the understanding of this unique technology. In these experiments the effect of nitrogen gas, catalyst amount, probe tuning, power setting, and monomer concentration will be investigated to refine the method for producing IDPU with ultrasound.

2.2 Experimental Methods

2.2.1 Materials

Polyethylene glycol (PEG) with a molecular weight of 600 g/mol from Alfa Aesar was used along with 98% Isophorone diisocyanate (ID) from Aldrich to create the polyurethane made in the experiments described in this chapter. The monomers were in a solvent of 99.8% anhydrous N,N-Dimethylformamide (DMF) from Sigma Aldrich with a catalyst of 95% dibutyltin dilaurate from Aldrich.

ACS reagent grade $\geq 99\%$ Butanone from Sigma-Aldrich and $\geq 98\%$ isopropyl alcohol from Sigma- Aldrich were used for rinsing and cleaning of materials after use.

2.2.2 Equipment

The XL2020 Sonicator from Misonix Incorporated was used for these experiments. The experiments were conducted in a fume hood with an adjacent 49.6 L compressed gas tank

of N_2 from Machine & Welding Supply Company. The temperatures were taken with a Signstek 6802 II Dual Channel Thermometer with a thermocouple sensor probe. Viscosity measurements were taken with a Brookfield DV - E Digital Viscometer.

2.2.3 Polymerization Technique

Reactor preparation

The reactor for the following experiments was made out of a 2 oz, (60mL) Thermo Scientific Narrow-Mouth HDPE Economy Nalgene Bottle from Fisher Scientific. The top of the bottle was screwed off and the mouth of the bottle was cut off with a knife allowing for the ultrasonic probe to fit into the vessel. The incision was made 2.0 - 2.1cm down from the top of the bottle so the new diameter of the mouth was 1.8 - 2.6cm in diameter. Prior to cutting the diameter of the opening was 1.3cm. Two small holes, 2-3mm in diameter, were created near the opening of the bottle with a hammer and nail. These holes allowed for the digital thermocouple and the N_2 gas syringe to enter the vessel and can be seen in figure 20 and 21.



Figure 20. Reactor bottle before preparation.



Figure 21. Reactor bottle after preparation. The top is cut off and two small holes are visible to the left and the right of the enlarged opening for the gas syringe and the thermocouple.

Polymerization Procedure

For the baseline experiment, 12g PEG, 26 mL DMF, 5.1 mL ID, and 20 μ L dibutyltin dilaurate were used and variations to these amounts are noted in the following sections. A molar ratio of 1:1.2 PEG to ID was maintained for all experiments. For solutions IDPU-18a and 18b, the amount of the monomers in the solvent was decreased by half so 6g PEG, 26 mL DMF, 2.55 mL ID, and 12.5 μ L dibutyltin dilaurate were used. For solutions IDPU-19a and 19b, the concentration of the monomers in the solvent was decreased by 75% so 3g polyethylene glycol, 26 mL DMF, 1.3 mL ID, and 6.25 μ L dibutyltin dilaurate were used.

For each experiment, the reactor bottle was tared on a balance and then the PEG was added to the bottle scoop by scoop with a spatula. Then the solvent was measured in a clean and dry graduated cylinder and poured into the bottle. Next the ID was measured with a 10mL glass pipette and pipette pump and dispensed into the bottle as well. The bottle was then placed under the ultrasonic probe, clamped in place, and then the thermocouple was inserted into one

of the two small holes at the top of the bottle. The compressed gas container was opened and a steady stream of N₂ gas was flowed from the cylinder through the attached hose and out through a small needle of an attached 5 mL BD Luer-Lok syringe. The syringe was inserted into the second small hole on the top of the bottle. The setup of materials in the fume hood is displayed in figure 22. Using an Eppendorf pipette, the amount of catalyst was measured and dispensed into the reaction bottle. Then the ultrasonic probe was turned on and set to run on the corresponding power level for 15 minutes. The ultrasonic probe then with the amplitude control knob on 6, 7, or 8 with the probe pulsing 2 seconds on and 1 second off. If applicable, temperature values were taken every minute for the duration of the experiment and for two hours after sonication to profile the cooling of the polymer as well.

After the 15 minute sonication period, the ultrasonic probe was slowly lifted out of the reaction vessel. The polyurethane solution was poured into a clean, dry and labeled 60 mL volumetric graduated glass jar from Wheaton and set to cool on the counter for two hours. Polymer solutions were coded with both a number and a letter. A number correlating to the reaction condition and a letter indicating replication. The reaction bottle was discarded along with the tip of the Eppendorf pipette. The ultrasonic probe was rinsed with isopropyl alcohol and left to dry off in the fume hood. The graduated cylinder for measuring the DMF was washed in the sink with detergent, rinsed thoroughly, and set on the drying rack to dry. To insure it was dry before the next use, air was blown into it. The glass pipette used for dispensing of the ID was rinsed with butanone and then dried with air.



Figure 22. The setup of the ultrasonic probe in the fume hood. The probe is clamped to a stand and held in place adjacent to the body of the sonicator. The syringe for N₂ gas is inserted on the right and the thermocouple enters the bottle on the left.

2.2.4 Characterization Methods

The isophorone diisocyanate polyurethane (IDPU) solutions were characterized by their viscosity values. Measurements were taken at specific time intervals after sonication was complete. Day 1 values were measured two hours after sonication once the samples had cooled to room temperature. DMF was added to the IDPU sample so the total volume of the sample reached 50 mL to maintain a constant concentration of solution. Then the viscosity values were taken with the Brookfield Digital Viscometer with spindle 5 at 100 rpm. Viscosity

measurements were read once the value on the screen stopped fluctuating and reached a plateau.

2.3 Results and Discussion

The results of the IDPU polymer solutions place an emphasis on viscosity. Although not an absolute measure of molecular weight, the viscosity values provide relative molecular weight comparisons as viscosity and molecular weight are directly correlated. A higher viscous solution indicates higher molecular weight polymer. During measurements, the concentration and specifications (spindle, RPM, temperature) must remain constant in order to provide comparable results. Generally indirect methods of taking molecular weight are easier and more convenient to gather than taking molecular weight samples for every sample on every day. A disadvantage relying initially on viscosity is that no absolute molecular weight value is gathered. It is assumed that polymerization is complete when the viscosity value is taken and that concentration is maintained throughout the process through careful transfer of solution. Four samples, two replicates each, were completed to investigate whether the polymerization of IDPU ceases after sonication or continues and to determine the effects of polymerizing the IDPU samples in a nitrogen rich environment. Results are seen in tables 3-5. As seen in table 3 all samples continued to polymerize after sonication. Viscosity measurements were taken every 24 hours over a 3 day period and increases in viscosities were observed in every sample every day. Results shows that nitrogen gas greatly increases the final viscosity of the IDPU solutions as samples IDPU-2a and 2b were more than double the viscosity of the non-nitrogen samples IDPU-1a and 1b. Samples sonicated in the presence of nitrogen gas had the highest

viscosity each day measurements were taken showing that a nitrogen rich environment minimizes the effects of ID reacting with oxygen and other impurities in the open system polymerization process. With nitrogen, more ID is devoted to polymerization of the sample and less to side reactions. IDPU-2a and 2b also experienced a greater rate of change of viscosity over the following three days due to the nitrogen increasing in viscosity by a factor of 22.9 and 1.3. However, the nitrogenized samples are not consistent with each other differing in initial day 1 viscosity values of more than 2700 cP. And consequently, the non-nitrogenized samples do not exhibit reproducibility either.

Table 3. The Effect of Nitrogen Gas on the Viscosity of IDPU Solutions over a 3 Day Period

Sample Code	Presence of Nitrogen Gas	Power Setting	Solution Viscosity (cP)		
			Day 1	Day 2	Day 3
IDPU-1a	No	7	25-26 (25.5)	108-112 (110)	108-112 (110)
IDPU-1b	No	7	1180-1190 (1185)	1650-1660 (1655)	1770-1790 (1780)
IDPU-2a	Yes	7	52-24 (53)	524-528 (526)	1212-1220 (1216)
IDPU-2b	Yes	7	2740-2750 (2745)	3290-3310 (3300)	3640-3660 (3650)

Note: $C_{ID} = 12.76\%$, $C_{PEG} = 28.63\%$, $V_{cat} = 20 \mu\text{L}$, Number in parenthesis is the midpoint

During the sonication of the nitrogenized and non-nitrogenized samples, the temperature of the solutions was taken every minute with a thermocouple. The temperature of 3 additional samples was also taken during sonication with the power setting on 6, 7, and 8.

The temperature changes during sonication of the samples are showed in table 4 and graphed in figure 23. One general trend was observed in all samples and is easily observed in Figure 23: the temperature increased to a point and then reached a plateau around minute 7. All samples reached temperatures of at least 112°C; however the point at which the maximum sample temperature was reached varied. IDPU-1a, 2a, 2b, 3, and 5 reached their maximum temperature at minute 15 whereas IDPU 1b and 4 reached the maximum temperature at minute 10 and 9 respectively. No sample reached a temperature higher than 140.2 °C. Sample IDPU-5 reached the highest temperature showing a correlation between temperature and power setting. A higher power setting on the ultrasonic probe allows the solution to reach a higher temperature during polymerization. This is true for all samples except IDPU-1b, which had the lowest final temperature. However, the maximum temperature (124.3 °C) is consistent with the maximum temperature for other samples sonicated at power 7. Inversely to this conclusion, a lower power setting on the probe, correlates to a lower solution temperature. IDPU-3 had the maximum overall temperature of all the samples due to it being sonicated at the lowest power setting of all the samples. Overall samples IDPU-1a, 1b, 2a, and 2b, showed the same general trend indicating that the presence of nitrogen had no general effect on the temperature of the solution during sonication. Sample IDPU-1b is assumed to be an outlying sample with the typical temperature profile being observed in samples IDPU-1a, 2a, and 2b.

Table 4. The Temperature Changes of IDPU Solutions due to Sonication

Time (min)	Temperature (°C)						
	IDPU-1a	IDPU-1b	IDPU-2a	IDPU-2b	IDPU-3	IDPU-4	IDPU-5
	No N ₂ Power 7	No N ₂ Power 7	N ₂ Power 7	N ₂ Power 7	N ₂ Power 6	N ₂ Power 7	N ₂ Power 8
0	21.0	20.2	23.2	22.9	22.0	22.2	21.6
1	51.5	51.6	53.5	50.0	43.7	51.2	58.0
2	81.3	85.2	83.3	79.9	64.2	80.3	92.5
3	100.3	97.2	97.2	93.6	82.1	94.3	105.0
4	106.6	103.0	103.5	100.1	88.4	100.6	112.7
5	110.3	107.5	108.1	104.1	92.8	105.7	120.9
6	113.0	112.4	113.0	107.4	95.4	110.2	130.6
7	115.4	118.2	115.0	110.5	97.3	116.2	138.4
8	117.7	124.2	122.3	113.3	99.0	123.5	137.0
9	119.4	124.1	125.4	116.8	100.3	127.4	136.5
10	121.3	124.3	127.3	120.5	101.7	123.5	137.5
11	123.7	115.8	129.4	125.2	102.3	122.5	138.1
12	126.0	103.1	130.4	130.1	105.3	123.3	138.8
13	128.8	96.0	132.2	131.7	107.1	122.5	138.7
14	131.4	90.2	131.9	134.2	109.7	123.3	138.3
15	132.7	87.0	132.9	130.2	112.3	119.2	140.2

Note: C_{ID}= 12.76%, C_{PEG}= 28.63%, V_{cat}= 20 μ L

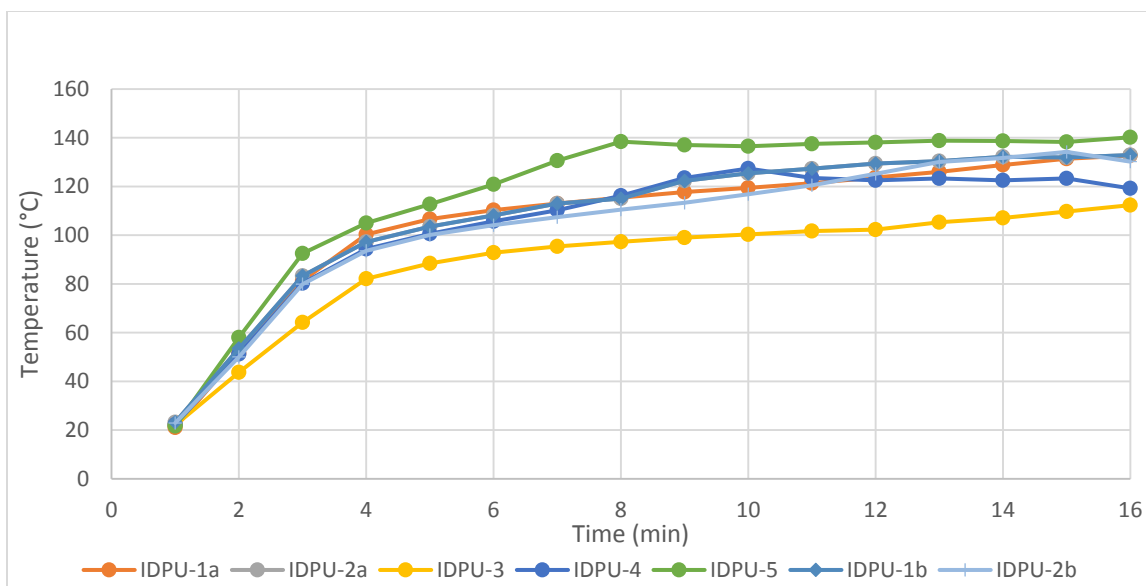


Figure 23. Temperature changes of IDPU solutions due to sonication. $C_{ID} = 12.76\%$, $C_{PEG} = 28.63\%$, $V_{cat} = 20 \mu\text{L}$. IDPU-1a, 2a, and 4 were sonicated at power-7. IDPU-3 was sonicated at power = 6. IDPU-5 was sonicated at power = 8. IDPU-1a and 1b were sonicated with no N_2 gas. IDPU-2a, 2b, 3, 4, and 5 were sonicated with N_2 gas.

The temperature changes after sonication was complete and the probe was removed from the reaction bottles were noted for 5 different samples (IDPU-1a, 2a, 3, 4, and 5). For viscosities to be compared, the solutions needed to be measured at a constant temperature. Cooling temperature changes were observed to gauge when the first viscosity measurement could be taken. The temperature changes are recorded in table 5. All samples regardless of their sonication condition reached room temperature 2 hours after the probe was removed from the reaction bottle. During the first 30 minutes of the sample not being sonicated a dramatic temperature decrease occurred and can be seen in figure 24. After these initial 30 minutes the decrease in temperature leveled out and decreased only by an average of 9.58 additional degrees with the values ranging from 5.9-12.1. Although the temperature increases during sonication differ, the temperature changes after sonication exhibited a more identical trend.

Table 5. The Temperature Changes after the Ultrasonic Probe was removed from the Reaction Bottle

Time (min)	Temperature (°C)				
	IDPU-1a	IDPU-2a	IDPU-3	IDPU-4	IDPU-5
	No N ₂ / Power 7	N ₂ / Power 7	N ₂ / Power 6	N ₂ / Power 7	N ₂ / Power 8
0	132.7	132.9	112.3	119.2	140.2
30	34.2	33.7	33.1	28.2	28.3
60	25.3	25.8	24.8	24.7	23.2
90	22.8	22.7	22.5	22.5	22.2
120	22.2	21.6	21.9	21.5	22.4

Note: C_{ID}= 12.76%, C_{PEG}= 28.63%, V_{cat}= 20 μL

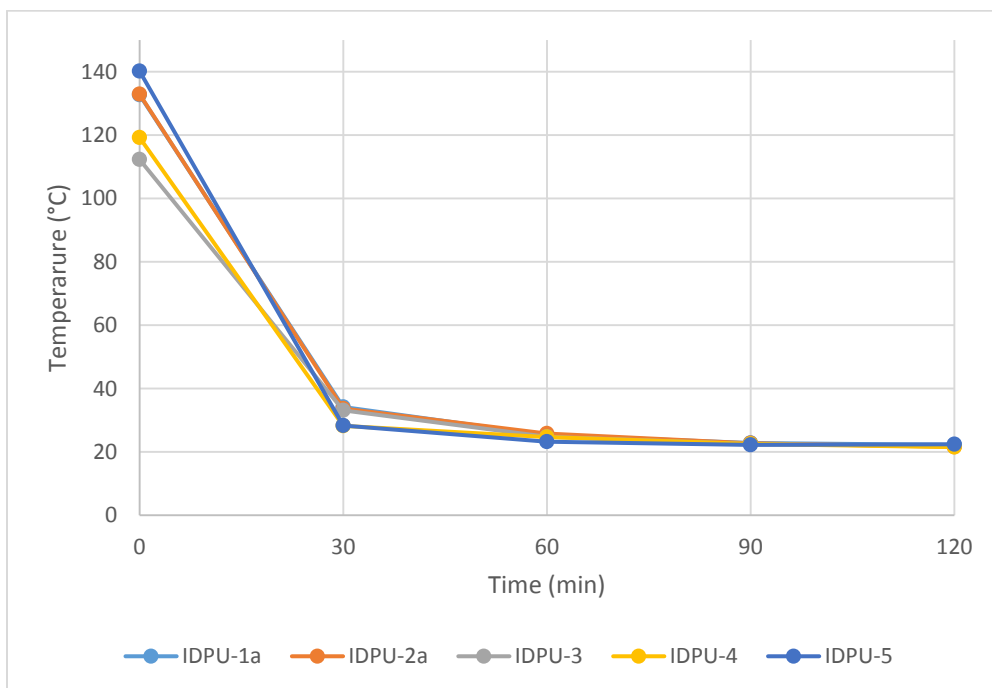


Figure 24. The temperature changes after the ultrasonic probe was removed from the reaction bottle. C_{ID}= 12.76%, C_{PEG}= 28.63%, V_{cat}= 20 μL. IDPU-1a, 2a, and 4 were sonicated at power-7. IDPU-3 was sonicated at power = 6. IDPU-5 was sonicated at power = 8. IDPU-1a was sonicated with no N₂ gas. IDPU-2a, 3, 4, and 5 were sonicated with N₂ gas.

For IDPU-3, 4, and 5 solution viscosities were taken over the course of 5 days to conclude if the polymerization reaction continues after sonication or stops. All samples showed that after sonication, the monomers continue to react and form a polymer. Results are shown in table 6. Sample IDPU-4 that was sonicated at power 7 showed a dramatically higher solution viscosity than IDPU-3 and 5 on all 5 days measurements were taken. Over the five day period IDPU-4 increased by a factor of 5.4. IDPU-3 and 5 increased by a factor of 14.4 and 3.9 respectively over the five days. These results show that a power level of 7 produces the polymer with the highest viscosity. At power 8, the viscosity is lower as a result of the onset of degradation of the IDPU. At power 6, the probe does not have enough energy to create a polymer with a high viscosity. The 5 day trends can be better seen in figure 25. IDPU-4, sonicated at power 7 shows the greatest rate of change over the 5-day period. Sample IDPU-5 shows an increase from day 1 to day 2 and then levels out whereas IDPU-4 shows a steady increase to day 5. IDPU-3 experiences a varying rate of increase and even a decrease between days 4 and 5 perhaps due to the error in viscosity measurements, the possible onset of degradation of the polymer, or the near total conversion of the monomer. Remaining free radicals in the solution could react during this 5 day period to induce degradation of the polyurethane polymer.

Table 6. The Effect of Different Power Settings on the Midpoint Viscosity of IDPU Solutions over a 5 Day Period

Sample Code	Power Setting	Solution Viscosity (cP)				
		Day 1	Day 2	Day 3	Day 4	Day 5
IDPU-3	6	55-56 (55.5)	352-356 (354)	508-512 (510)	508-512 (510)	796-804 (800)
IDPU-4	7	233-236 (234.5)	1028-1032 (1030)	1360-1368 (1364)	1360-1368 (1370)	1252-1260 (1256)
IDPU-5	8	46-48 (47)	176-184 (180)	192-200 (196)	192-200 (200)	180-188 (184)

Note: $C_{ID} = 12.76\%$, $C_{PEG} = 28.63\%$, $V_{cat} = 20 \mu\text{L}$, Number in parenthesis is the midpoint

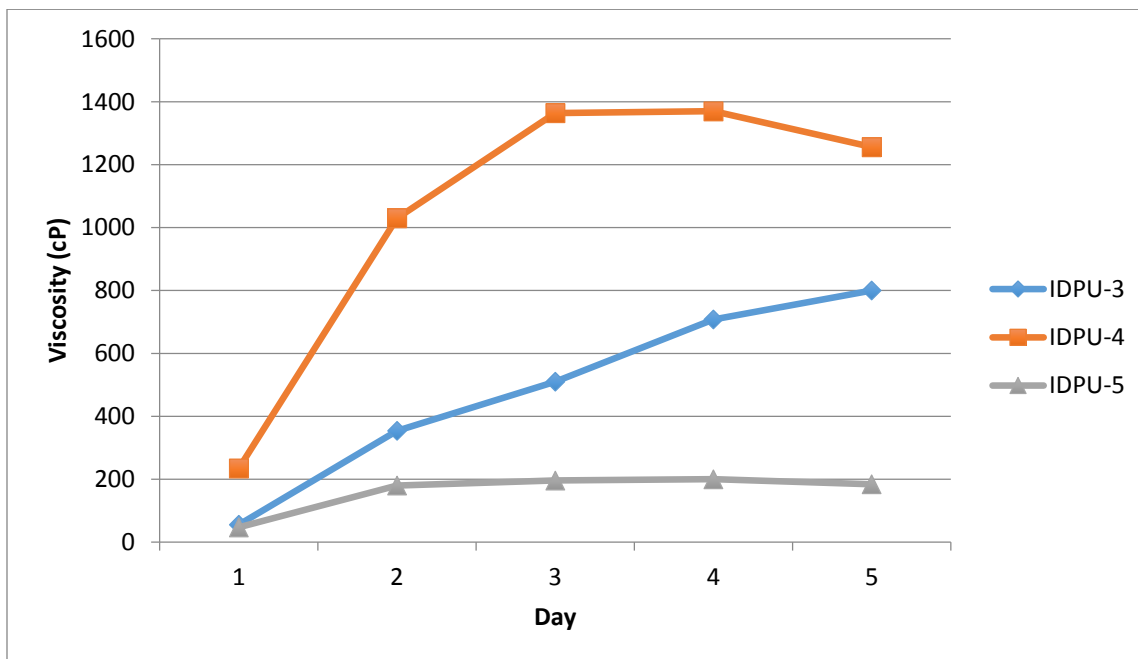


Figure 25. The effect of power on the viscosity of IDPU solutions over 5 days. $C_{ID} = 12.76\%$, $C_{PEG} = 28.63\%$, $V_{cat} = 20 \mu\text{L}$. IDPU-3 was sonicated at power = 6. IDPU-4 was sonicated at power = 7. IDPU-5 was sonicated at power = 8.

As experiments continued, the IDPU samples did not produce reproducible results. To determine the cause of this irreproducibility, the presence of a catalyst was investigated. Three samples were run with the full $20 \mu\text{L}$ of catalyst used as with previous experiments and three

samples were run with 0 μL of catalyst added. Viscosity measurements were recorded on day 1 and shown in table 7. The three samples sonicated with the catalyst showed higher viscosity values than samples IDPU-7a, b, and c. However, IDPU-6a, b and c did not give reproducible results. The day one viscosity values range from 56-480 cP. For the samples sonicated with no catalyst added (IDPU-7a, b, and c) viscosity measurements were not able to be taken under the normal conditions. Typically spindle 5 was used for viscosity measurements, however these solutions had a very low viscosity and did not give a reading with that spindle. Spindle 3 was chosen instead and gave results of 9-12 cP. These results were consistent, but indicate a very, very low molecular weight polymer was made. To polymerize a high molecular weight polymer, a catalyst is needed to expedite the polymerization reaction. Although ultrasonic waves produce high temperature and pressure when traveling through a liquid, these conditions are not all that is needed.

Table 7. The Viscosity Measurements of IDPU Solutions with Varied Amounts of Catalyst

Sample Code	Catalyst (μL)	Viscosity (cP)
		Day 1
IDPU-6a	20	476-480
IDPU-6b	20	56-64
IDPU-6c	20	116-124
IDPU-7a	—	9-12*
IDPU-7b	—	9-12*
IDPU-7c	—	9-12*

Note: $C_{\text{ID}} = 12.76\%$, $C_{\text{PEG}} = 28.63\%$, $V_{\text{cat}} = 20 \mu\text{L}$, Power = 7, *The viscosity measurement was taken with spindle 3, because the solution was not viscous enough to be recorded using spindle 5.

The temperature changes were observed during the polymerization of these 6 samples and shown in table 8. Samples polymerized in the absence of a catalyst were not able to reach high enough temperatures during sonication and therefore not able to produce high viscosity polymers. Samples sonicated with the addition of a catalyst reached an average maximum temperature of 130.37°C whereas samples polymerized without a catalyst reached an average maximum temperature of 108.37°C. The additional 22°C that IDPU-6a, b, and c reached was noteworthy in the polymerization of IDPU. All of these 6 samples reached their maximum temperature at minute 15 of sonication except for sample IDPU-6a and showed the same general trend throughout the duration of the polymerization. These temperature values are graphed in figure 26. All six samples experienced a steep rate of change for the first four minutes. Then the temperature of all samples began to level out with samples IDPU-6a, b, and c reaching higher temperatures than IDPU-7a, b, and c.

More replicates of IDPU-6a, b and c were polymerized to further determine whether the ultrasonic polymerization of IDPU provides reproducible results or not. Viscosity values were taken on day 1 for all solutions and day 14 for IDPU- 8a, b and c. Table 9 shows the data from these experiments. All of IPDU-8 samples were polymerized and sonicated under the same conditions, however a wide range of viscosities was measured on Day 1. Sample IDPU-8a had the highest recorded viscosity value at 560-568 cP whereas samples 8b, e, and f only had viscosities of 20 cP. IDPU-8d had the highest measured viscosity of 968-972 cP. Samples IDPU-8a and c showed an increase in viscosity values after 14 days and the midpoint value of the samples increased by a factor of 1.2. The midpoint value of sample IDPU-8a increased by a factor of 1.1. Although initial viscosities of these three solutions were not consistent,

Table 8. The Effect of Catalyst on the Temperature Changes of IPDU Solutions during Sonication

Time (min)	Temperature (°C)					
	IDPU-6a	IDPU-6b	IDPU-6c	IDPU-7a	IDPU-7b	IDPU-7c
	20 μ L catalyst	20 μ L catalyst	20 μ L catalyst	—	—	—
0	20.7	19.06	20.1	20.7	21.3	20.3
1	51.6	52.5	49.7	47.9	46.4	48.0
2	77.0	81.8	78.1	69.3	66.7	68.3
3	93.4	96.5	95.9	81.1	82.0	81.9
4	99.1	101.9	102.0	87.5	92.1	88.4
5	102.1	106.4	105.8	90.8	98.4	92.0
6	104.4	109.7	109.7	93.5	101.6	95.6
7	106.9	112.7	113.5	95.8	103.2	98.0
8	110.8	116.1	117.4	97.8	103.9	99.6
9	114.1	119.2	120.9	99.7	104.2	101.0
10	118.5	122.2	123.2	102.1	104.6	102.2
11	121.7	124.1	125.5	104.1	105.6	103.3
12	123.7	125.9	127.6	105.9	106.9	104.5
13	129.6	127.4	129.1	107.2	107.0	106.0
14	132.6	128.1	129.2	108.4	107.5	107.3
15	130.1	128.7	130.4	109.1	107.5	108.5

Note: C_{ID}= 12.76%, C_{PEG}= 28.63%, Power = 7

consistency is seen in these samples by the factors of increase of the viscosity samples after sonication. However this factor of increase in viscosity results differs widely then previously discussed samples IDPU-2a, 2b, and 4 that were sonicated under the same conditions. By day 3, samples IDPU-2a, 2b, and 4 had increased in midpoint viscosity values by a factor of 22.9, 1.3, and 5.8 respectively. These results further show that the ultrasonic polymerization of IDPU is not reproducible due to the wide array of various side reactions that can occur during polymerization of a step growth polyurethane made with isophorone diisocyanate in an open system.

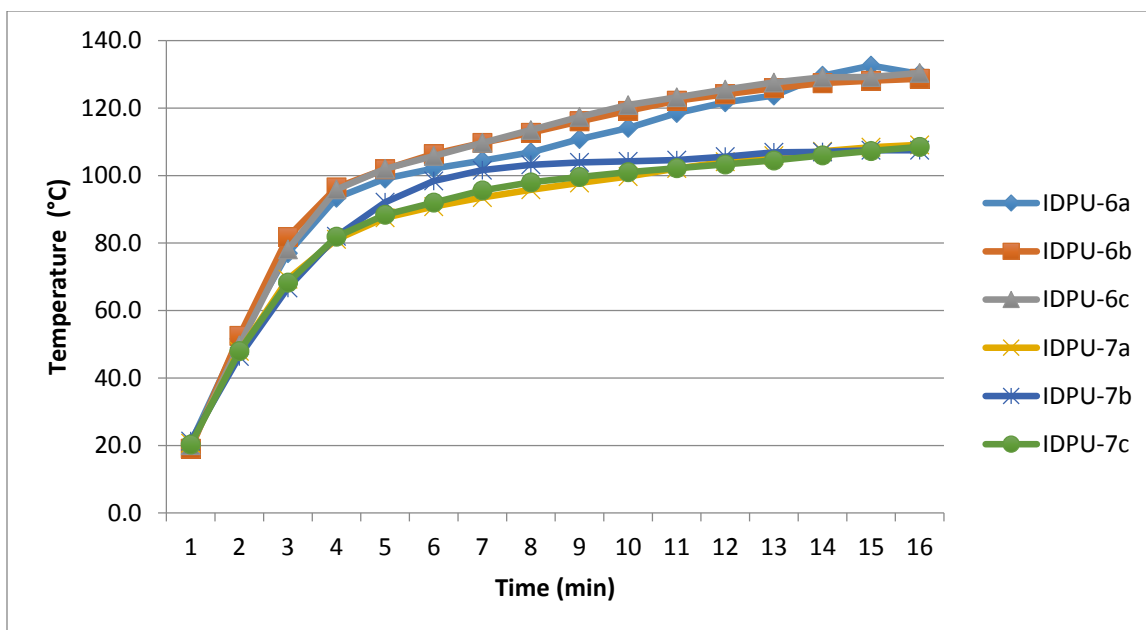


Figure 26. The effect of catalyst on the temperature of IDPU solutions during sonication. 20 μ L catalyst was used for IDPU-6a, b and c. No catalyst was used for IDPU-7a, b and c. CID= 12.76%, CPEG= 28.63%, Power = 7.

Table 9. Viscosity Measurements of IDPU Solutions after 14 Days

Sample Code	Catalyst (μ L)	Power Setting	Solution Viscosity (cP)	
			Day 1	Day 14
IDPU-8a	20	7	560-568 (564)	664-668 (666)
IDPU-8b	20	7	20 (20)	20-24 (22)
IDPU-8c	20	7	192-200 (196)	228-237 (232.5)
IDPU-8d	20	7	968-972 (970)	—
IDPU-8e	20	7	20 (20)	—
IDPU-8f	20	7	20 (20)	—

Note: C_{ID}= 12.76%, C_{PEG}= 28.63%. Number in parenthesis is the midpoint

In hopes to find the exact cause of the irreproducibility of IDPU samples made under the same conditions, attention was turned to the functionality of the probe. According to the manual for the XL2020 Misonix Sonicator (Misonix Incorporated), tuning of the probe is

required when modifying, changing, or removing the probe tip or horn. Two samples were run immediately after tuning of the probe, and one sample was sonicated without immediately prior probe tuning like the other runs previously performed. Data from these two samples are shown in table 10. The two samples that were sonicated immediately after tuning of the ultrasound probe showed a higher viscosity, but only by a few cP. Samples IDPU-9a and b showed variation in both the day 1 and day 2 viscosity measurements. IDPU-9a increased in viscosity by a factor of 6.8. IDPU-9b only increased by a factor of 1.2 which was similar to IDPU-10 that increased by a factor of 1.16. All samples continued to polymerize after sonication and no reproducibility was observed when comparing both sets of samples supporting the idea that probe tuning does not affect IDPU solution viscosity.

Table 10. The Effect of Probe Tuning on the Viscosity of IDPU Solutions over a 2 Day Period

Sample Code	Tuning Before?	Catalyst (μL)	Power Setting	Solution Viscosity (cP)	
				Day 1	Day 2
IDPU-9a	yes	20	7	60-68	408-412
IDPU-9b	yes	20	7	28-30	28-36
IDPU-10	no	20	7	20-24	20-28

Note: $C_{\text{ID}} = 12.76\%$, $C_{\text{PEG}} = 28.63\%$

In further attempts to obtain reproducible results of the ultrasonic polymerization of IDPU, the volume of catalyst in the reaction mixture was increased to 25, 30, and 35 μL . Three replicates were run with each volume of catalyst and viscosity measurements were taken at intervals up to day 22. The solution viscosities are recorded in table 11. Samples IDPU-11a, b and c showed more consistent viscosity measurements, however variation still existed in these

samples. The viscosity measurements of IDPU-12a, b, and c were less than half the values of IDPU-11a, b and c though they contained 5 μL more catalyst. Surprisingly, these three solutions also gave viscosity measurements with the lowest range. Catalyst amount did not directly correlate with solution viscosity. Samples 13a, b, and contained the most μL catalyst and gave the widest range of viscosity measurements. All samples continued to polymerize over the 22 day period and all by different factors. All three IPDU- 11a, 12a, and 13a samples were too viscous to measure by day 22. These samples were made on the same day. Replicates of these three experiments were polymerized on another and those samples did not reach this very viscous state. No overall reproducibility was observed; however it was concluded that samples IDPU-11a, b, and c gave the most consistent measurements. For the remainder of the IDPU samples polymerization 25 μL of catalyst was used.

Additional studies were conducted to investigate the polymerization of IDPU in absence of sonication. Samples IDPU-14a and b were not sonicated, but shaken vigorously for 3 minutes and left closed on the counter for 22 days. The viscosity of both samples increased at different rates as seen in the viscosity measurements taken on day 9 and 12 (see table 12). Both samples reached a very high viscosity that was unable to measure demonstrating that IDPU polymerizes with the absence of an ultrasonic probe. Sample IDPU-11a reached this high, un-measurable viscosity by day 22 and it was sonicated at power 7 for 15 minutes. Sonication does speed up the reaction, but eventually the sonicated and un-sonicated samples will reach similar viscosities with time.

Table 11. Viscosity of IDPU Solutions over a 22 Day Period with Different Amounts of Catalyst

Sample Code	Catalyst (μL)	Power Setting	Solution Viscosity (cP)			
			Day 1	Day 4	Day 18	Day 22
IDPU-11a	25	7	604-676 (640)	2096-2100 (2098)	—	*
IDPU-11b	25	7	912-980 (946)	—	892-972 (932)	984-1004 (994)
IDPU-11c	25	7	736-768 (752)	—	1660-1668 (1664)	1432-1476 (1454)
IDPU-12a	30	7	295-304 (299.5)	1140-1180 (1160)	—	*
IDPU-12b	30	7	280-308 (294)	—	232-248 (240)	380-400 (390)
IDPU-12c	30	7	120-126 (123)	—	738-764 (751)	992-1020 (1006)
IDPU-13a	35	7	876-912 (894)	5273-5300 (5286.5)	—	*
IDPU-13b	35	7	376-384 (380)	—	356-368 (362)	352-364 (358)
IDPU-13c	35	7	76-84 (80)	—	92-100 (96)	624-736 (680)

Note: $C_{\text{ID}}= 12.76\%$, $C_{\text{PEG}}= 28.63\%$ *The solution was too viscous to measure.
Number in parenthesis is the midpoint

Table 12. Viscosity of IDPU Solutions with No Sonication

Sample Code	Catalyst (μL)	Power Setting	Solution Viscosity (cP)			
			Day 1	Day 9	Day 12	Day 22
IDPU-14a	25	none	9-12*	248-256	2416-2432	**
IDPU-14b	25	none	9-12*	148-152	712-716	**

Note: $C_{\text{ID}}= 12.76\%$, $C_{\text{PEG}}= 28.63\%$, *The viscosity measurement was taken with spindle 3, because the solution was not viscous enough to be recorded using spindle 5, **The solution was too viscous to measure

With an increased volume of catalyst, additional studies on the effect of power level on solution viscosity were completed. Results are shown in table 13. Samples were sonicated at

power 6, 7, and 8 similar to IDPU-3, 4, and 5 (see table 6). IDPU-15a and b were sonicated at power 6 and resulted in dramatically different viscosity measurements. On day one IDPU-15a could not be measured whereas IDPU-15b had a day 1 viscosity value of 48-60 cP. Contrary to the day 1 measurements, IDPU-15a had a greater viscosity for the following three measurements. The final recorded viscosity of IDPU-15a was 9.7 times higher than IDPU-15b. IDPU-15a had the highest final viscosity of all samples. Sample IDPU-16 exhibited a viscosity increase from days 1 to 9 then surprisingly had a decrease in viscosity from day 9 to 18. Compared to samples IDPU-11a, 11b and 11c, which were sonicated in the same conditions as IDPU-16, IDPU-16 had a much lower viscosities. The average day 1 solution viscosity of IDPU-11a, 11b, and 11c was 779.3 cP whereas IDPU-16 had a viscosity of 9-12*. No reasoning exists for the difference in these measurements other than the abundant amount of side reactions of isophorone diisocyanate. IDPU-17 had the lowest viscosity of all samples in table 13 due to the beginning of ultrasonic induced polymer degradation. This sample also exhibited the lowest rate of change over the 18 day period. No increase in viscosity indicating a continuation of polymerization was observed until day 18. The results from table 13 support the previous conclusion that power 8 is too high and begins to degrade the polymer, but conflicts with the previous comment that samples sonicated at power 7 continue to react after the initial sonication. Reproducibility was not observed between samples IDPU-15a and b.

Table 13. The Effect of Power Setting on the Viscosity of IDPU Solutions over 18 Days

Sample Code	Catalyst (μL)	Power Setting	Solution Viscosity (cP)			
			Day 1	Day 4	Day 9	Day 18
IDPU-15a	25	6	9-12*	448-476	1480-1520	1760-1792
IDPU-15b	25	6	48-60	48-52	196-212	168-200
IDPU-16	25	7	9-12*	192-204	196-204	176-212
IDPU-17	25	8	9-12*	9-12*	9-12*	112-132

Note: $C_{\text{ID}}= 12.76\%$, $C_{\text{PEG}}= 28.63\%$, *The viscosity measurement was taken with spindle 3 because the solution was not viscous enough to be recorded using spindle 5

Because no reproducibility had yet been noticed in any IDPU samples, final experiments were conducted with varying monomer concentrations to see if this behavior exists at all concentrations or only at the concentrations previously made. Four more samples were run and their values are recorded in table 14. The volume of solvent was kept constant and both samples were sonicated at power 7. The previous concentration of catalyst, ID, and PEG were reduced by 50% for IDPU-18a and b and reduced by 75% for IDPU-19a and b. For samples IDPU-18a and b, both samples showed a continuation of polymerization over 4 days, but the samples did not have the same viscosity values. IDPU-18a had a viscosity 4.38 times less than the viscosity of IDPU-18b. This indicates that regardless of monomer concentration, IDPU polymer solutions cannot be made reproducibly via ultrasonic polymerization. For samples IDPU-19a and b the viscosity was too low to be measured with the traditional means and results are inconclusive for ultrasonic polymerization of IDPU at these monomer concentrations.

Table 14. The Effect of Monomer Concentration on the Viscosity of IDPU Solutions

Sample Code	Catalyst (μL)	C_{ID} (%)	C_{PEG} (%)	Power Setting	Solution Viscosity (cP)	
					Day 1	Day 4
IDPU-18a	12.5	8.05	18.05	7	24-28 (26)	36-60 (38)
IDPU-18b	12.5	8.05	18.05	7	104-124 (114)	116-128 (122)
IDPU-19a	6.25	4.63	10.38	7	9-12*	—
IDPU-19b	6.25	4.63	10.38	7	9-12*	—

Note: *The viscosity measurement was taken with spindle 3 because the solution was not viscous enough to be recorded using spindle 5

2.4 Conclusions

Final conclusions for the ultrasonic polymerization of an IDPU polymer solution in DMF indicate that a high viscosity polymer solution can be produced with this method, but no reproducibility is observed even with altering numerous variables: nitrogen gas, power setting, catalyst amount, probe tuning, and monomer concentration. Due to the high reactivity of the monomer, isophorone diisocyanate, and its ability to easily get involved with side reactions the results were not consistent and ranged widely. Results indicate that the generally, the optimal conditions for producing a high viscosity IDPU solution are a nitrogen rich-environment, 25 μL of dibutyltin dilaurate catalyst, and a power setting of A higher power setting than 7 starts to degrade the IDPU polymer and results in a lower viscosity polymer solution. During sonication, the reaction is not isothermal and the temperature can increase up to 140°C. Overall, sonication has some benefit in inducing polymerization of

IDPU under time constraints, but isophorone diisocyanate and polyethylene glycol will polymerize and reach high viscosities in the absence of any exposure to ultrasound waves. The open system ultrasonic polymerization does yield interesting results sometimes, but it is not reliable for starting the step growth polymerization of an isophorone diisocyanate based polyurethane solution. A closed system would allow for better reproducibility and less side reactions of isophorone diisocyanate in ultrasonic polymerization.

3.0 ULTRASONIC POLYMERIZATION OF ACRYLAMIDE

3.1 Introduction

The ultrasonic polymerization of acrylamide seeks to verify the reproducibility of initiating polymerization via sonication. As concluded from the ultrasonic polymerization of IDPU, the ultrasonic polymerization of a step-growth polyurethane does not produce consistent results due to the reactivity of the diisocyanate isophorone monomer. Acrylamide may provide reproducible results when polymerized with ultrasound because fewer side reactions can occur during this chain growth polymerization process. The only possible reaction than could occur would be the breaking of the double bond that leads to polymerization. Polyurethanes have numerous side reactions that can occur simultaneous with polymerization, but this is not the case when polymerizing acrylamide. The experiments in this chapter seek to investigate the effect of power setting, initiator concentration, and monomer concentration on the viscosity and molecular weight of polyacrylamide solutions to yield consistent results.

3.2 Experimental Methods

3.2.1 Materials

Electrophoresis grade ($\geq 99.9\%$) acrylamide from FisherBiotech was used along with a catalyst of 99% potassium persulfate from Mallinckrodt to create the polyacrylamide (PAM) made in the experiments described in this chapter. The monomer and catalyst were in a solvent of distilled water. For rinsing of the ultrasonic probe, $\geq 98\%$ isopropyl alcohol from Sigma-Aldrich was used.

3.2.2 Equipment

The XL2020 Sonicator from Misonix Incorporated was used for these experiments. The experiments were conducted in a fume hood with an adjacent 49.6 L compressed gas tank of N₂ from Machine & Welding Supply Company. Viscosity measurements were taken with a Brookfield DV - E Digital Viscometer.

3.2.3 Polymerization Technique

Reactor preparation

The reactor for the following experiments was made out of a 2 oz (60mL) Thermo Scientific Narrow-Mouth HDPE Economy Nalgene Bottle from Fisher Scientific. The top of the bottle was screwed off and the mouth of the bottle was cut off with a knife allowing for the ultrasonic probe to fit into the vessel. The incision was made 2.0 - 2.1cm down from the top of the bottle so the new diameter of the mouth was 1.8 - 2.6cm in diameter. Prior to cutting the diameter of the opening was 1.3cm. Two small holes, 2-3mm in diameter, were created near the opening of the bottle with a hammer and nail. These holes allowed for the digital thermocouple and the N₂ gas syringe to enter the vessel and can be seen in figure 20 and 21.

Polymerization Procedure

For the baseline experiment 2.54g acrylamide and 0.0426 g potassium persulfate were used in 35 mL solvent. Variations from these concentrations are described in section 3.3. To prepare the solvent, 50 mL of deionized water was measured in a clean and dry graduated cylinder. The water was then put into a beaker and a steady stream of N₂ gas was bubbled

through the water for 30 minutes using a 5 mL BD Luer-Lok syringe and attached hose. One reactor bottle was tared on an analytical balance and then the acrylamide was added



Figure 27. Reactor bottle before preparation



Figure 28. Reactor bottle after preparation. The top of the plastic reaction bottle is cut off allowing for a larger opening so the ultrasonic probe can be inserted into the vessel. One small hole is visible to the left of the mouth for the N₂ gas syringe. A second small hole is visible to the left for the thermocouple.

to the bottle scoop by scoop with a spatula. Then 35 mL of the solvent was measured in a clean, dry graduated cylinder and poured into the reaction bottle. Next the potassium persulfate was measured on a weigh boat with an analytical balance and added into the bottle as well. The bottle was then placed under the ultrasonic probe and clamped in place. The syringe of N₂ gas was inserted into the small hole on the top of the bottle. The setup of materials in the fume hood is displayed in figure 29. Then the ultrasonic probe was turned on and set to run on the corresponding power level for 15 minutes. The ultrasonic probe then ran in the fume hood with the probe pulsing 2 seconds on and 1 second off.

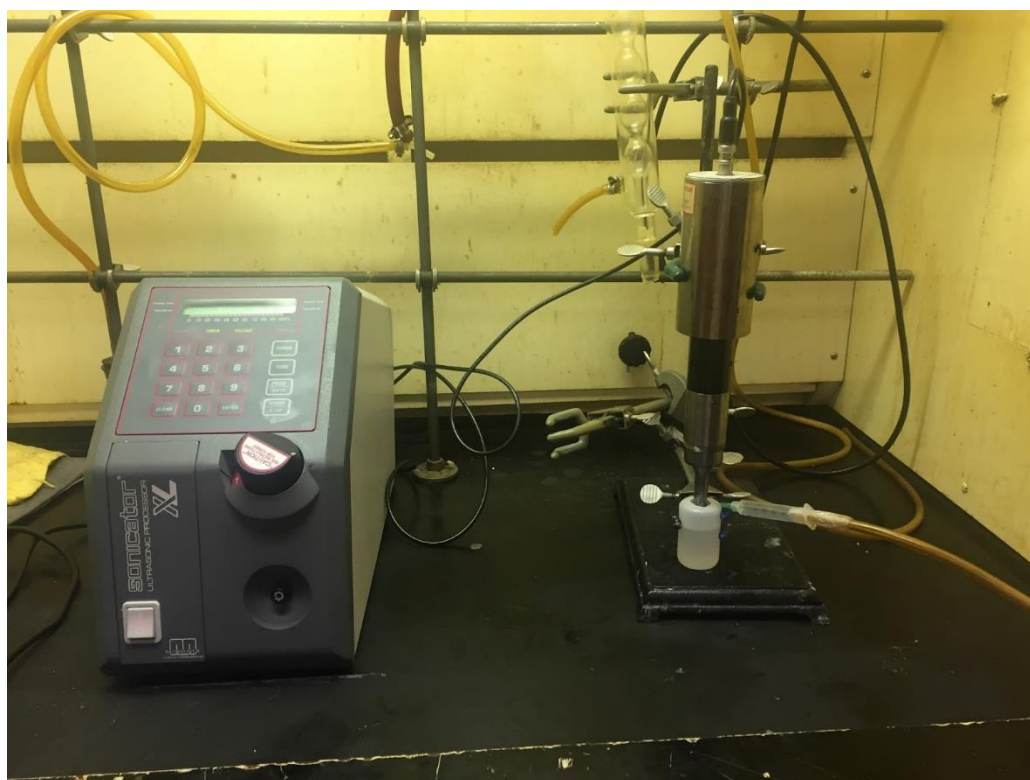


Figure 29. The setup of the ultrasonic probe in the fume hood. The probe is clamped to a stand and held in place adjacent to the body of the sonicator. Additional clamps are available for holding the reaction bottle in place. The syringe of N₂ gas is inserted in the hole to the right of the reaction bottle's mouth.

After the 15 minute sonication, the ultrasonic probe was slowly lifted out of the reaction vessel. The polyacrylamide was poured and scooped into a clean, dry and labeled 60 mL volumetric graduated glass jar from Wheaton and set to cool on the counter for two hours. Polymer solutions were coded with both a number and a letter. A number correlating to the reaction condition and a letter indicating replication.

The reaction bottle was discarded and the graduated cylinder for measuring the distilled water was set on the drying rack to dry. To insure it was dry before the next use, air was blown into it. To clean the ultrasonic probe of any excess residue left on the probe tip, a new reaction bottle containing 35 mL of deionized water was clamped on the stand and the ultrasonic probe was inserted. The probe ran at a power setting of 7 for two minutes pulsing 2 seconds on and 1 second off. Then the probe was rinsed with isopropyl alcohol and set to dry in the fume hood.

3.2.4 Characterization Methods

Viscometry

One method of characterizing the polymer samples was by their viscosity values. Measurements were taken at specific time intervals after the sonication was complete. Day 1 values were measured two hours after sonication once the samples had cooled to room temperature. Distilled water was added to the polyacrylamide sample so the total volume of the sample reached 50 mL. Viscosity values were then measured with a Brookfield Digital Viscometer DV-E with spindle 5 at 100 rpm. Viscosity measurements were read once the value on the screen stopped fluctuating and reached a plateau.

Molecular Weight Determination

Select polymer samples were chosen for molecular weight determination by gel permeation chromatography (GPC). PAM solutions were given to Professor Genzer's research group in the department of Chemical and Biomolecular Engineering at NC State University. Samples were run in a solvent of 0.5M acetone in water.

3.3 Results and Discussion

PAM solutions were first polymerized to determine what monomer and initiator are needed to create a polymer solution that can be measured with the Brookfield viscometer. Table 15 shows the results of the first initial sample runs. PAM-1a and b formed very viscous hydrogel solids with viscosities that could not be measured. Photographs of PAM-1a and b are shown in figure 30. There was some fluidity to the gels, but they behaved more like a solid than a liquid. To produce a polymer with a lower viscosity, the initiator amount was doubled to create more polymer chains of shorter length. PAM-2a and b resulted in polymer solutions with measureable viscosities; however they were dramatically different in values. PAM-2a had a viscosity roughly ten times higher than PAM-2b because the monomer concentration was still too high to produce a PAM solution than could be measured with the Brookfield viscometer. A monomer concentration of 12.45% is still able to form very high chain length polymers that behave like a solid. From the results in table 15, the reproducibility of making a polyacrylamide polymer through ultrasonication was yet to be determined.

Table 15. Viscosity of PAM Solutions with Different Initiator Concentrations

Sample Code	Monomer (%)	Initiator Concentration (%)	Power Setting	Solution Viscosity (cP)
				Day 1
PAM-1a	12.45	0.053	7	*
PAM-1b	12.45	0.053	7	*
PAM-2a	12.44	0.106	7	12720-25240
PAM-2b	12.44	0.106	7	7760-1040

Note: *The solution was too viscous to measure



Figure 30. Samples PAM-1a (left) and b (right) turned upside down. Some movement was seen from the polymer solutions after a several seconds, but the samples were too viscous for viscosity measurements to be taken.

Further studies with manipulated monomer and initiator concentrations were conducted to attempt to gain reproducible samples. Reproducibility in the PAM samples was achieved as the amount of initiator remained constant, but the monomer amount was reduced by half. This

resulted in a change in the concentration of the initiator, but 0.426 grams were used in all PAM-2a, 2b, 3a and 3b. PAM-3a and 3b were sonicated with 6.76% monomer and 0.113% initiator. Viscosity measurements were taken each week over 14 days; these values are presented in table 16. PAM-3a and b had the same, recorded viscosity measurement on day 1 and exhibited similar trends for the duration of testing. After one week both viscosity measurements increased slightly, however they stayed relatively close to their previous measurements with PAM-3a increasing by 42 cP, and PAM-3b increasing only 10 cP. On day 14, both samples experienced a decrease in viscosity with the final, day 14 midpoint viscosities only increasing by 2 and 4 cP for samples PAM-3a and b respectively. This increase and decrease could be due to human error in measurements or a true viscosity increase indicating a minor polymerization post sonication. However, since both samples showed a decrease on day 14, more evidence points to the former reasoning. Regardless, both samples exhibited similar viscosities and similar behavior leading to the belief that chain growth polymers can yield successful and reproducible results via polymerization by ultrasound.

Table 16. Viscosity of PAM Solutions over a 14 Day Period

Sample Code	Monomer Concentration (%)	Initiator Concentration (%)	Power Setting	Solution Viscosity (cP)		
				Day 1	Day 7	Day 14
PAM-3a	6.76	0.113	7	104-108 (106)	144-152 (148)	104-112 (108)
PAM-3b	6.76	0.113	7	104-108 (106)	112-120 (116)	108-112 (110)

Note: Number in parenthesis is the midpoint

Similar to experiments explained in Section 2.3 that were completed using IDPU, two samples of acrylamide (PAM-4a and b) were made in the absence of sonication. Keeping with the same monomer concentrations used for PAM-3a and 3b, samples were run to see how the viscosity of the solution changes with no exposure to ultrasound. All components were added to 26 mL of nitrogenation deionized water in a clean and dry glass jar. The lids were capped and the solutions were shaken vigorously for two minutes until most monomer and initiator dissolved and no particulates were seen by visual observation. Samples were left closed and untouched on the lab bench. Results in table 17 provide evidence that in the absence of sonication polymerization of acrylamide proceeds, but at a slower initial rate. Data from day 1 show that both samples have very low initial viscosities. Due to the low initial viscosity, viscosity measurements could not be taken with the spindle 5 and spindle 3 was used. On day 7 the samples showed signs of polymerization throughout the solution by visual observation. A clump of a transparent hydrogel-like material was formed in the center of the glass jar about 1 inch in diameter. Polymerization of this polymer starts in the middle of solution and spreads outward. Due to the heterogeneous nature of the solution on day 7, accurate viscosity measurements were not obtained. After 14 days the samples both reached very high viscosities showing that a high molecular weight polymer is formed eventually. The day 14 viscosities of PAM-4a and b are higher than the measured viscosity of sonicated samples PAM-3a and 3b, however PAM-4a and 4b gave a larger range of viscosity values showing that when not sonicated the formed polymer is not homogeneous. Sonication produces homogeneous polymer solutions. These results also may indicate that ultrasound waves do induce some

degradation during polymerization or deactivation of free radical species. Sonicated samples (PAM-4a and b) with the same concentrations do not reach the same high viscosities achieved by non-sonicated samples (PAM-3a and 3b) because of this. These results mimic results found in section 2.3 that investigate whether the step growth polymerization of IDPU proceeds in the absence of sonication. Further research needs to be done on the effect of sonication time on solution viscosity and polymer degradation.

Table 17. Viscosity of PAM Solutions over a 14 Day Period with No Sonication

Sample Code	Monomer Concentration (%)	Initiator Concentration (%)	Power Setting	Solution Viscosity (cP)		
				Day 1	Day 7	Day 14
PAM-4a	6.76	0.113	—	18-21*	**	1496-3016
PAM-4b	6.76	0.113	—	18-21*	**	2216-2404

Note: *The viscosity measurement was taken with spindle 3 because the solution was not viscous enough to be recorded using spindle 5. ** The solution was not homogeneous and viscosity measurements were not able to be taken

In previous studies, research showed that during cavitation, free radicals are produced as the bubbles implosively collapse. If a sufficient number of free radicals are produced during this mechanism, polymerization of a chain-growth polymer should proceed in the absence of a free radical initiator. To investigate this theory, two PAM samples were sonicated with no added potassium persulfate (a free radical initiator). Acrylamide was added to the solvent in the reactor bottle and then sonicated. Without initiator, there is no indication that acrylamide polymerization occurred as shown by the values of solution viscosity in table 18. Both samples had the same viscosity values on all days. From this data you can conclude that the amount of

free radicals produced during cavitation is not enough to initiate a polymerization reaction for acrylamide.

Table 18. Viscosity of PAM Solutions over a 14 Day Period with No Initiator

Sample Code	Monomer Concentration (%)	Initiator Concentration (%)	Power Setting	Solution Viscosity (cP)		
				Day 1	Day 7	Day 14
PAM-5a	6.76	0.00	7	18-21*	18-21*	18-21*
PAM-5b	6.76	0.00	7	18-21*	18-21*	18-21*

Note: *The viscosity measurement was taken with spindle 3 because the solution was not viscous enough to be recorded using spindle 5

The next set of PAM samples focused on the effect of the power level of the probe on viscosity measurements of solutions. During the step growth polymerization of IDPU a power setting of 8 yielded lower viscosity solutions than samples polymerized at a power setting of 7. When compared to the results in table 16 of the samples made at power 7, the values of PAM-6a and 6b presented in table 19 show that solutions made at power 8 yield reproducible yet lower viscosity polymer solutions by about half. The same general trend is shown in both samples. On day 1 the viscosities are at their highest and decrease by day 14 while experiencing a slight increase at day 7 whether due to human error or an actual slight increase. Perhaps the polymers are able to polymerize but only slightly before the species produced during degradation take effect.

Table 19. Viscosity of PAM Solutions Sonicated at a Power Setting 8 over a 14 Day Period

Sample Code	Monomer Concentration (%)	Initiator Concentration (%)	Power Setting	Solution Viscosity (cP)		
				Day 1	Day 7	Day 14
PAM-6a	6.76	0.113	8	48-56	44-48	36-40
PAM-6b	6.76	0.113	8	44-52	48-52	40-48

During the sonication of PAM solutions at power 7, one general trend is observed with slight variation. Two samples were run with temperatures recorded every minute for the duration of sonication. The recorded temperatures are listed in table 20 and graphed in figure 31. Both samples experienced a steady temperature increase until minute 3 and then begin to show variation, but in general there was an increase in temperature until they began to plateau. Both samples reach a maximum temperature at minute 11 and then show a decrease of until minute 15. This could be due to the polymer absorbing additional heat, a reduction in cavitation due to the interference of polymer chains or the onset of degradation at this time. PAM-7a decreases by 2 °C while PAM-7b decreases by 6.8 °C during the last 4 minutes of sonication. Neither sample reaches temperatures higher than the boiling point of water (100 °C).

Final experiments conducted on the ultrasonic polymerization of polyacrylamide show the cooling temperature of PAM-7a. Recorded temperatures are in Table 21. Similar to IDPU experiments on this same topic (see section 2.3), two hours after the probe as removed from the reaction bottle the solution reached room temperature. Viscosity measurements were made two hours after sonication to ensure that all samples had cooled back to room temperature.

Table 20. The Temperatures Changes of PAM Solutions during Sonication

Time (min)	Temperature (°C)	
	PAM-7a	PAM-7b
0	17.8	17.7
1	30.8	31.9
2	43.2	44.5
3	52.7	55.0
4	58.9	62.2
5	67.8	72.7
6	80.3	84.3
7	84.9	97.3
8	84.8	96.0
9	88.1	96.0
10	87.8	95.3
11	89.2	97.4
12	88.3	94.5
13	88.3	92.8
14	87.3	91.9
15	87.2	90.6

Note: $C_m = 6.76\%$, $C_i = 0.113\%$, Power = 7

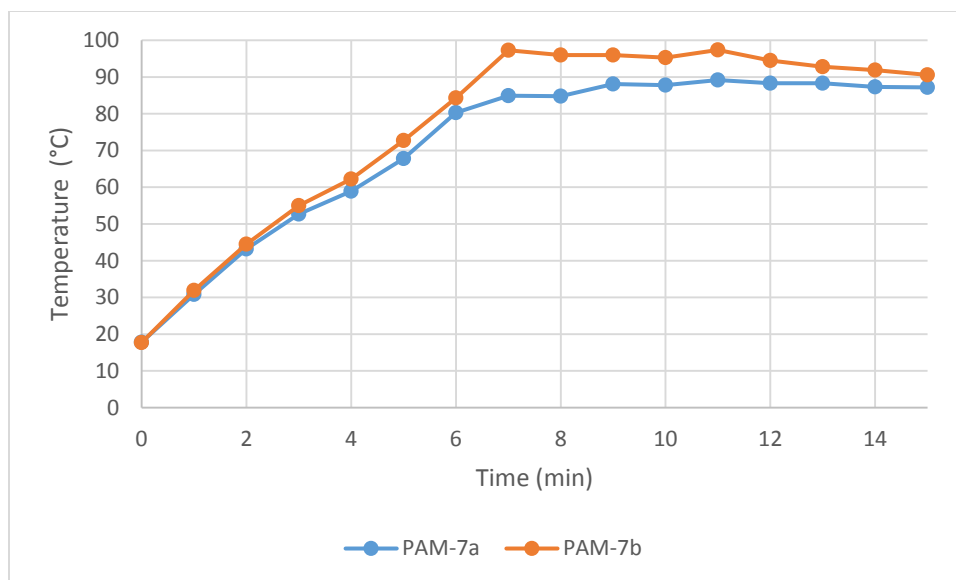


Figure 31. The Temperature Changes of PAM during Sonication. $C_m = 6.76\%$, $C_i = 0.113\%$, Power = 7

Table 21. The Temperature Changes after the Ultrasonic Probe was removed from the Reaction Bottle

Time (min)	Temperature (°C)
	PAM-7a
0	87.2
30	30.4
60	24.7
90	22.7
120	21.5

Note: $C_m = 6.76\%$, $C_i = 0.113\%$, Power = 7

Select PAM samples were chosen for molecular weight analysis by GPC and results are shown in table 22. PAM-4a with no ultrasonication produces the highest molecular weight polymer (M_n and M_w) with the smallest PDI. Sonication for 15 minutes at power 7 may immediately form a polymer, but polymer degradation could be a factor because no sonicated sample was able to reach as high a molecular weight value as the unsonicated sample, PAM-

4a, regardless of the monomer and initiator concentration. PAM-1a and 2a differ in initiator concentration, but this difference is not reflected in the Mw values. The Mw values for PAM-1a and 2a only differ by 21.6 kg/mol. This leads to the conclusion that the viscosity of polyacrylamide is more dependent on the monomer concentration than the initiator concentration. PAM-3a and 3b made at the same concentration as PAM-4a had a Mn roughly one fourth that of PAM-4a and a Mw one third that of PAM-4a due to the onset of degradation. However when referring back to the initial viscosity samples of PAM-4a, low or immeasurable viscosity was observed until day 14 (table 18). This molecular weight data was 44 days after the components of PAM-4a were mixed allowing ample time for polymerization to continue to occur in the absence of sonication. Reproducibility is found in the ultrasonic polymerization of polyacrylamide as the values for PAM-3a and 3b are very close in all values. The Mn values differ by 33, Mw by 3 and PDIs by 0.22. The next highest molecular weight polymer after PAM-4a is PAM-1a followed by PAM-2a because of their high monomer concentrations; however these concentrations were not continued for the duration of the experiment because viscosity measurements could not be easily measured. Samples with the highest PDI value were PAM-3a and 3b indicating that degradation does occur during the 15 minutes of sonication and short polymer chains are produced. After the maximum temperature is reached around minute 11 (see figure 31), possible degradation begins. When comparing all samples produced at power level 7, higher monomer and initiator concentrations correlate with a higher molecular weight polymer with a smaller PDI. When comparing PAM-6a to PAM-3a and b, a power setting of 8 produces a lower molecular weight polymer because polymerization occurs faster and degradation acts on the formed polymer chains.

Table 22. The Effect of C_m , C_i , and Power Setting on the Molecular Weight of PAM Solutions

Sample Code	Monomer Concentration (%)	Initiator Concentration (%)	Power Setting	Rxn Time (Days)	Mn (kg/mol)	Mw (kg/mol)	PDI (Mw/Mn)
PAM-1a	12.45	0.053	7	49	617.24	988.02	1.60
PAM-2a	12.44	0.106	7	49	582.37	966.42	1.66
PAM-3a	6.76	0.113	7	44	296.34	568.86	1.92
PAM-3b	6.76	0.113	7	44	263.79	571.89	2.17
PAM-4a	6.76	0.113	—	44	1116.46	1547.73	1.39
PAM-6a	6.76	0.113	8	33	324.54	542.02	1.67

Note: Rxn stands for reaction

3.4 Conclusions

Final conclusions on the ultrasonic polymerization of polyacrylamide show that reproducible results are obtained from the ultrasonic polymerization of this chain growth polymer with a free radical initiator of potassium persulfate in a solvent of water. Polymers were made varying the initiator concentration, monomer concentration, and power setting of the ultrasound probe. When the sonication time is set to 15 minutes, some degradation is seen in the PAM polymer solution at both power settings of 7 and 8. A power setting of 8 on the probe produces polyacrylamide solutions with a lower viscosity and molecular weight than other polymerized samples made at power 7. In the absence of initiator, no polymerization was observed leading to the conclusion that there were not enough free radicals produced during sonication to initiate the reaction. The polymerization is not isothermal and solution

temperatures reached maximum temperature values up to 90.6°C around minute 11. However, although reproducibility was observed in the sonicated samples, PAM polymerization in the absence of sonication produces an extremely high molecular weight polymer over a much longer time frame. PAM produced with the ultrasonic probe polymerized in 15 minutes, whereas in the absence of ultrasound, the polymer took 14 days to polymerize and continued to polymerize afterwards until molecular weight values were gathered 44 days after the initial mixing of the reactants. After sonication, no continuation of the PAM polymerization reaction was observed. Overall the use of the ultrasound does have advantages for producing reproducible PAM solutions in short time frames.

4.0 SONICATION OF CNTs IN SITU WITH POLYACRYLAMIDE POLYMERIZATION

4.1 Introduction

Carbon nanotubes have been at the forefront of most modern research because of their incredible mechanical properties. However, the major limitation of their large scale, commercial use is their strong tendency to aggregate. They are very hydrophobic and require dispersion through sonication or other means prior to use. Stopping dispersion at any point allows the CNTs to immediately aggregate and form clumps. The one-step, continuous dispersion of MWCNTs during the ultrasonic polymerization of acrylamide could potentially lead to a better dispersion of CNTs in a polymer/acrylamide composite film as opposed to a two-step polymerization and sonication process. The following research focuses on this one-step continuous process in an attempt to investigate the morphology and streamline the formation of a well dispersed CNT/polymer composite film.

4.2 Experimental Methods

4.2.1 Materials

Electrophoresis grade ($\geq 99.9\%$) acrylamide from FisherBiotech was used along with a catalyst of 99% potassium persulfate from Mallinckrodt to create the polyacrylamide (PAM) made in the experiments described in this chapter. The monomer and catalyst were in a solvent of distilled water. For rinsing of the ultrasonic probe, $\geq 98\%$ isopropyl alcohol from Sigma-Aldrich was used. Industrial grade carboxylated Multi-Walled Carbon Nanotubes were purchased from Cheap Tubes (www.cheaptubes.com) out of Grafton, VT. The MWCNTs have

a 20-40 nm diameter and range from 10-30 μm in length. They have a >90% purity and contained 1.43 wt% COOH.

4.2.2 Equipment

The XL2020 Sonicator from Misonix Incorporated was used for these sonication and polymerization.

4.2.3 Polymerization Technique

The reactor bottle was prepared as described in section 3.2.3. To prepare the solvent, 50 mL of deionized water was measured in a clean and dry graduated cylinder. The water was then put into a beaker and a steady stream of N_2 gas was bubbled through the water for 30 minutes using a 5 mL BD Luer-Lok syringe and attached hose. For each experiment, one reactor bottle containing about 1 mL of nitrogenized water was tared on an analytical balance in a particulate hood. In the hood, 0.088g of CNTs were added to the bottle scoop by scoop with a spatula. The rest of the solvent was then added to the reactor bottle. The bottle was then placed under the ultrasonic probe and clamped in place. The ultrasonic probe was lowered into the bottle and set to run for 45 minutes pulsing 2 seconds on and 1 second off. After thirty minutes 2.54g of acrylamide and 0.0426g potassium persulfate was added into the bottle. After the 45 minute sonication period was over, the ultrasonic probe was slowly lifted out of the reaction vessel. A high-walled glass petri dish was tared on a balance and 19.4g of the hot CNT/PAM solution was poured into the petri dish. The dish was then moved to the hood to cast a CNT/PAM film through solvent evaporation. After 24 hours, the CNT film was easily peeled off the dish and put aside for further classification.

The same film casting procedure as above was followed for casting films of PAM. PAM polymerization was carried out as described in section 3.2.3

For the two-step polymerization/sonication process, the polymerization of PAM was followed as previously described with the probe running for 45 minutes pulsing two seconds on, one second off. During the first 15 minutes of sonication, a weigh boat was tared on the analytical balance in a particulate hood and 0.88g MWCNTs were measured scoop by scoop. At minute 15 of sonication, the MWCNTs were added into the reaction bottle containing the PAM solution and sonication continued at power 7 for an additional 30 minutes. At the completion of sonication the ultrasonic probe was carefully lifted out of the reaction bottle. A high-walled glass petri dish was tared on a balance and 19.4g of the hot CNT/PAM solution was poured into the petri dish. The dish was then moved to the hood to cast a CNT/PAM film through solvent evaporation. After 24 hours, the CNT film was easily peeled off the dish and put aside for further classification.

The reaction bottle was then discarded and the graduated cylinder for measuring the distilled water was set on the drying rack to dry. To insure it was dry before the next use, air was blown into it. To clean the ultrasonic probe of any excess residue left on the probe tip, a new reaction bottle containing 35 mL of deionized water was clamped on the stand and the ultrasonic probe was inserted. The probe ran at a power setting of 7 for two minutes pulsing 2 seconds on and one second off. Then the probe was rinsed with isopropyl alcohol and set to dry in the fume hood.

4.2.4 Characterization Methods

All films were characterized by a Phenom G1 SEM and samples were prepared with a Emitech SC7620 Sputter Coater. Select films were further characterized by an FEI Verios 460L field-emission scanning electron microscope with no sputter coating.

4.3 Results and Discussion

Five 10cm in diameter films were made total. The weight of each film before and after solvent evaporation is shown in table 23. All five films are displayed in figures 32-36. Some warping is seen around the edges of film 2 and 4 due to the attempted removal of the film from the glass dish before it was completely dry. Film 1 and 2 were made through the one step continuous sonication/polymerization process. Upon visual observation both films appear to be strong and opaque and exhibit a good dispersion of CNTs. When observed in direct light some areas of less dispersion were observed, but generally a well-dispersed film was cast. The CNTs for films 1 and 2 were sonicated first for 30 minutes in water and then acrylamide and potassium persulfate were added and sonication continued for 15 more minutes. Film 3 and 4 were made by sonicating water, acrylamide, and potassium persulfate for 15 minutes. The solution was then cast into a film through solvent evaporation. Both films 3 and 4 produced a strong, clear, and transparent film. Film 5 was formed from the 2-step polymerization/sonication process (sonicating acrylamide and potassium persulfate for 15 minutes then adding CNTs and sonicating for an additional 30 more minutes) and produced a brittle film with noticeable CNT aggregation upon visual observation by the naked eye (see figure 36).

Table 23. The wt % of MWCNTs in PAM Films casted through Solvent Evaporation

Sample Code	CNT amount (g)	Weight before Solvent Evaporation (g)	Weight after Solvent Evaporation (g)	wt % CNTs
Film 1	0.0088	19.40	2.47	0.355
Film 2	0.0088	19.40	2.56	0.343
Film 3	0	19.40	2.01	0
Film 4	0	19.41	1.66	0
Film 5	0.0088	19.39	2.47	0.355*

Note: *A large clump of CNTs was stuck to the probe and not used for casting of the film. In actuality, this number is lower.



Figure 32. Film 1 - 0.355 wt% CNT/polyacrylamide film. CNTs were sonicated prior to polymerization of acrylamide.



Figure 33. Film 2 - 0.343 wt% CNT/polyacrylamide film. CNTs were sonicated prior to polymerization of acrylamide.

When peeling film 5 out of the glass petri dish, a large crack formed in the center of the film as well as flaking of the film around the edges. Noticeable strength loss was seen when the addition of CNT follows the polymerization of acrylamide. Film 5 appeared not as black or opaque as film 1 and 2 and noticeable specks of CNT clumps are visible on the surface of the film. During preparation of film 5, the CNTs were added to the top of the reaction bottle in the same manner as the addition of the monomer and initiator in films 1 and 2. After sonication had ended, a large amount of CNTs remained in a clump of polyacrylamide polymer surrounding the probe. This area of the probe experienced the localization of sound waves in

this area and this results in the production of a more gelatinous polymer in this area. The CNTs could not be dispersed out of this clump and thus a lighter colored film formed.

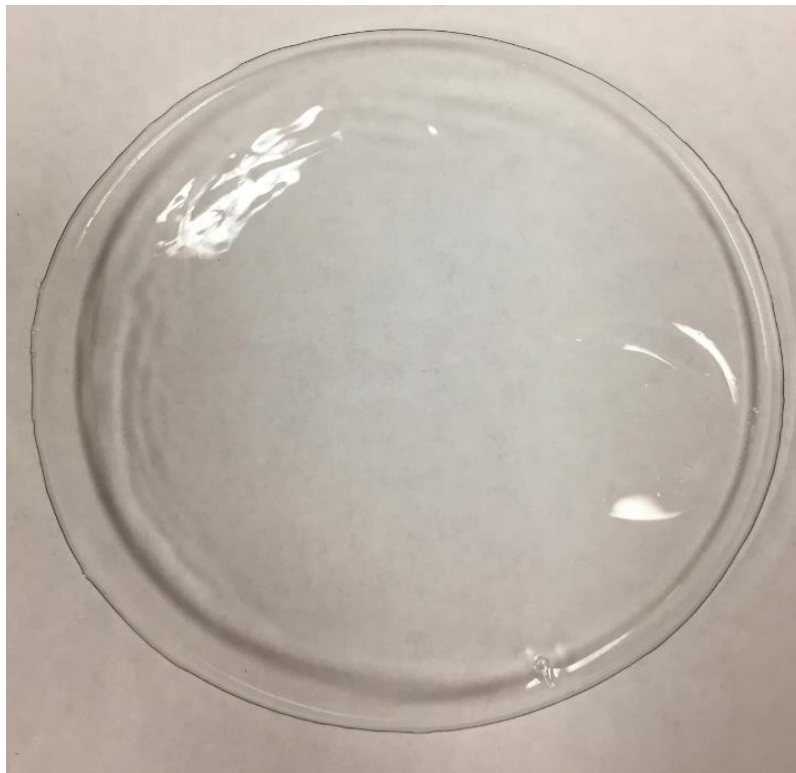


Figure 34. Film 3 - 0.00 wt% CNT/polyacrylamide film.

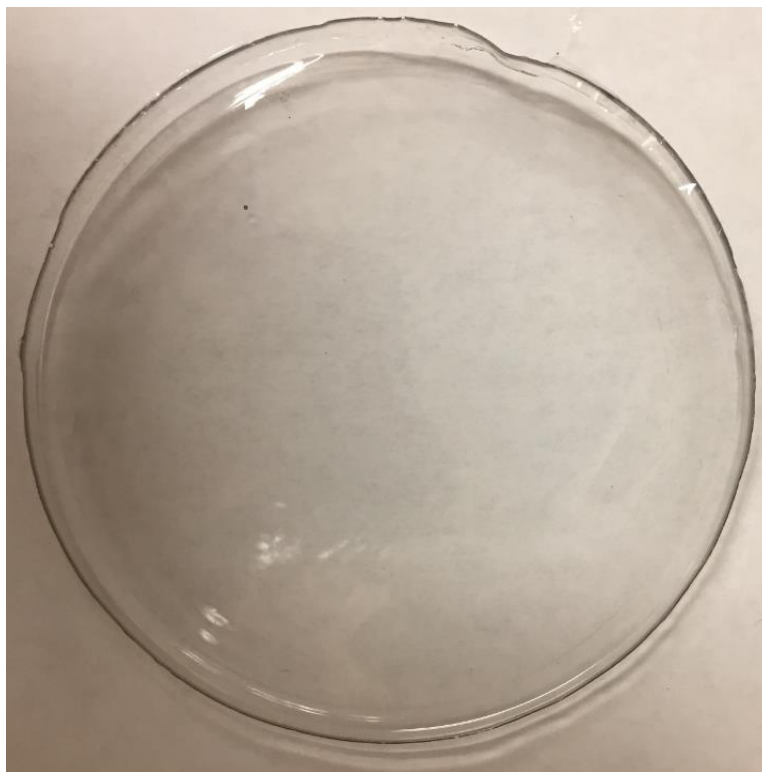


Figure 35. Film 4 - 0.00 wt% CNT/polyacrylamide film.



Figure 36. Film 5 - 0.355 wt% CNT/polyacrylamide film. Polyacrylamide was polymerized with ultrasound prior to sonication of CNTs

For further characterization all films were analyzed first by a Phenom G1 desktop scanning electron microscope. It was not possible to cut the films with a razor blade so the small samples were chipped off and straight edges were obtained by cutting with scissors. The samples were mounted on metal studs with an adhesive tape and sputter coated with a gold/palladium coating. In some SEM photos the adhesive and the metal stud is visible. Samples were analyzed to see the dispersion of CNTs throughout the polymer composite film and to see if any polyacrylamide had grafted onto the nanotubes. Unfortunately, the SEM used for analyzing these samples was not able to see individual carbon nanotube and polymer chains

due to magnification limitations, but other conclusions can be made from looking at these initial images.

Film 1 was the first to be viewed under SEM. Images are shown in figures 37, 38, and 39. Two areas of the film were viewed, area A and area B. Area A was thinner than B as seen when comparing figure 37 and 38. Both areas of the film were viewed initially at 1000x magnification. Figure 39 shows the cross section of film 1, area B, at 3000x magnification. In all figures of film 1, the samples appear to be one solid color and no polymer chains or nanotubes are visible. The cross section has a very rough surface as clumps and an arc like striation pattern are seen in the images. The arc like patterns on the surface may be due to the pouring of the PAM/CNT into the glass petri dish for casting. After the solution was poured into the dish minor shaking of the dish was needed for the solution to spread across the surface of the dish. A different striation pattern is seen in Area B, figures 38 and 39. When small portions of the film were broken off for analysis, polymer chains were broken unevenly. With the applied force of the break, a striated pattern may have arisen from the applied stress during sample preparation. Figures 38 and 39 are pictures of the same area at 1000x and 3000x magnification respectively. SEM images of film 2, also made in the same

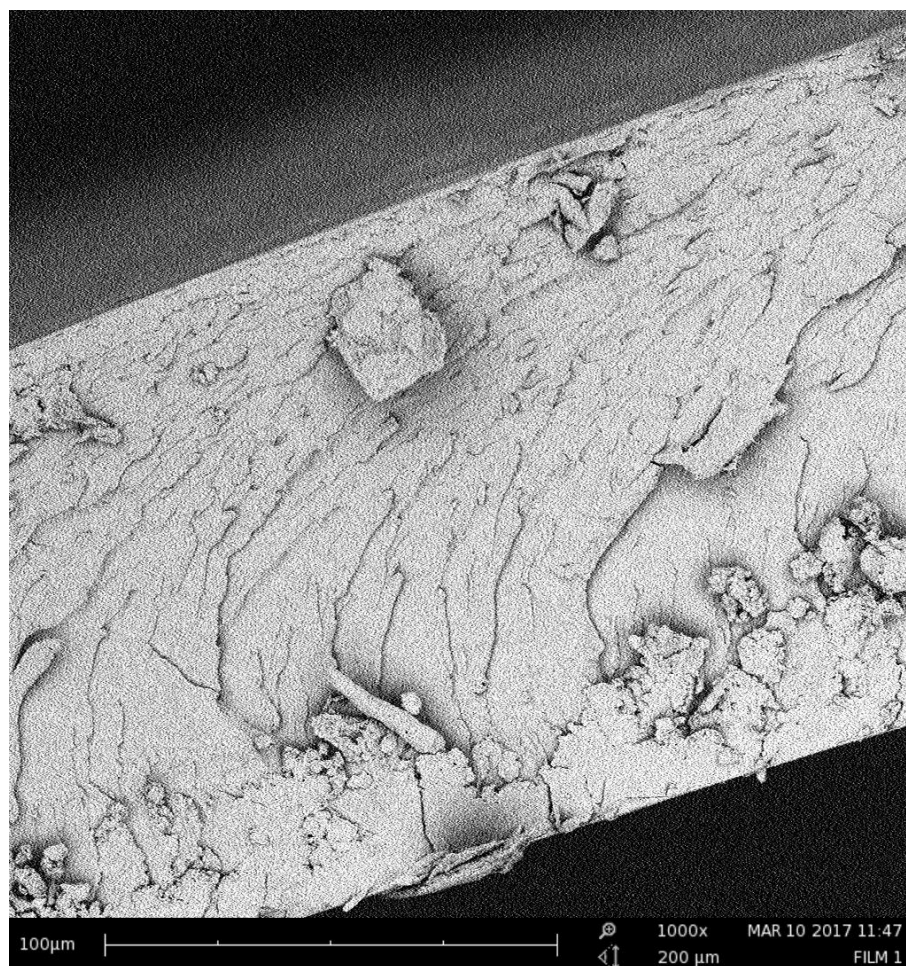


Figure 37. Cross-section of film 1. Area A. 1000x magnification

manner as film 1, are shown in figures 40, 41, and 42. The full thickness of the film can be seen in figure 40. On first glance similar striation patterns exist as in film 1. However at 3000x magnification (see figure 41), the striation patterns and ridges are different. Larger clumps are seen at the top of the image and the space between ridges is larger than the ridges in film 1. Figure 42 shows a larger cross-sectional area of the film and the image shows that the film is not an even thickness throughout. During casting the improper spreading of the CNT/PAM solution on the dish led to an uneven film thickness. Polyacrylamide could have been unevenly

distributed on the dish from the initial casting or the entanglement of polymer chains could have led to a differing thickness of the film.

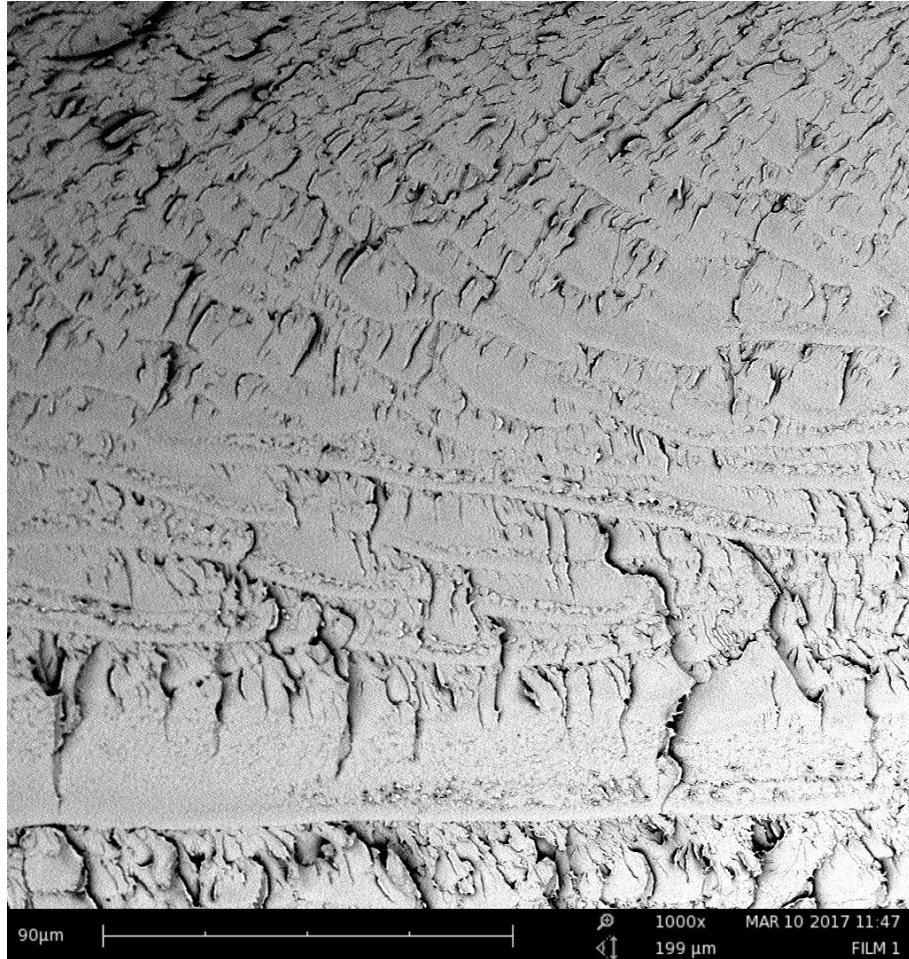


Figure 38. Cross-section of film 1. Area B. 1000x magnification

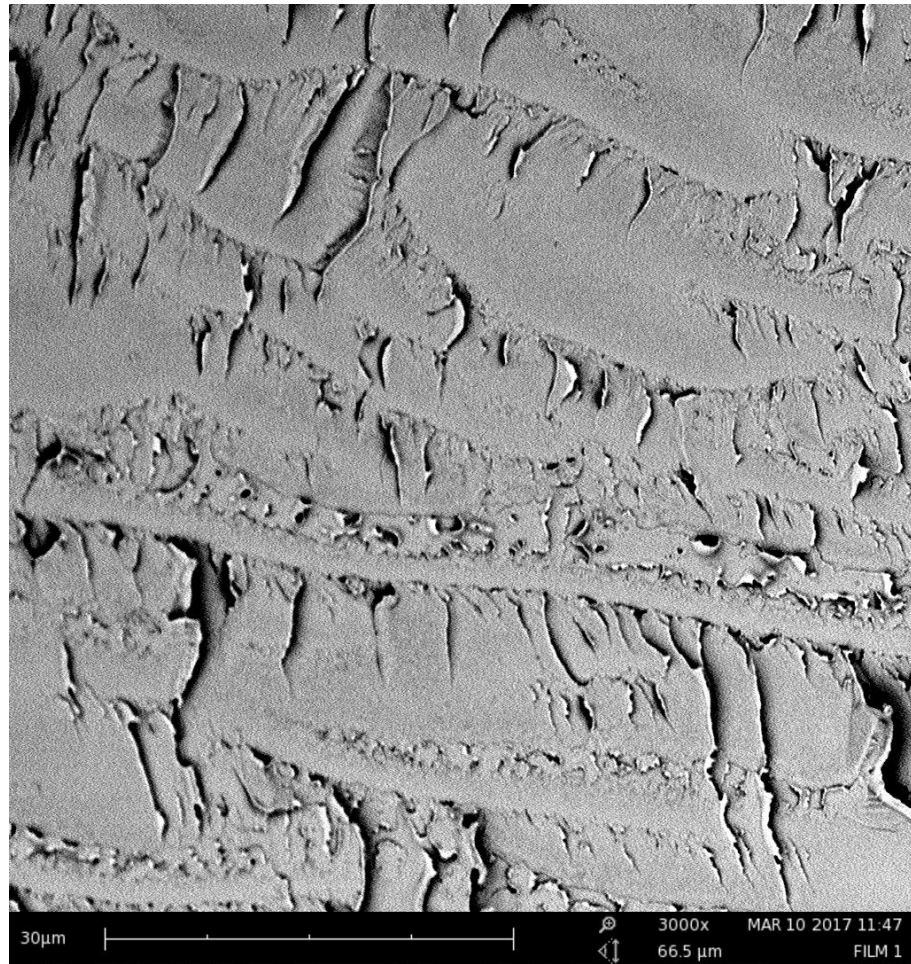


Figure 39. Cross-section of film 1. Area B. 3000x magnification

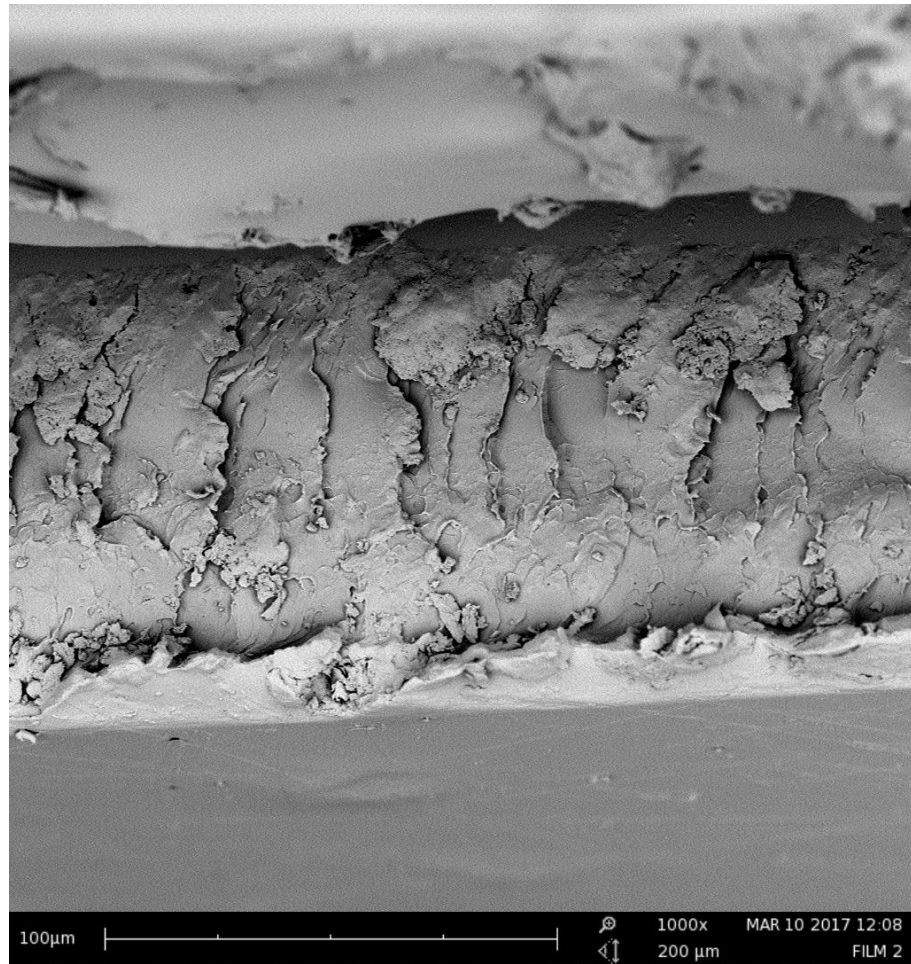


Figure 40. Cross-section of film 2. Area A. 1000x magnification

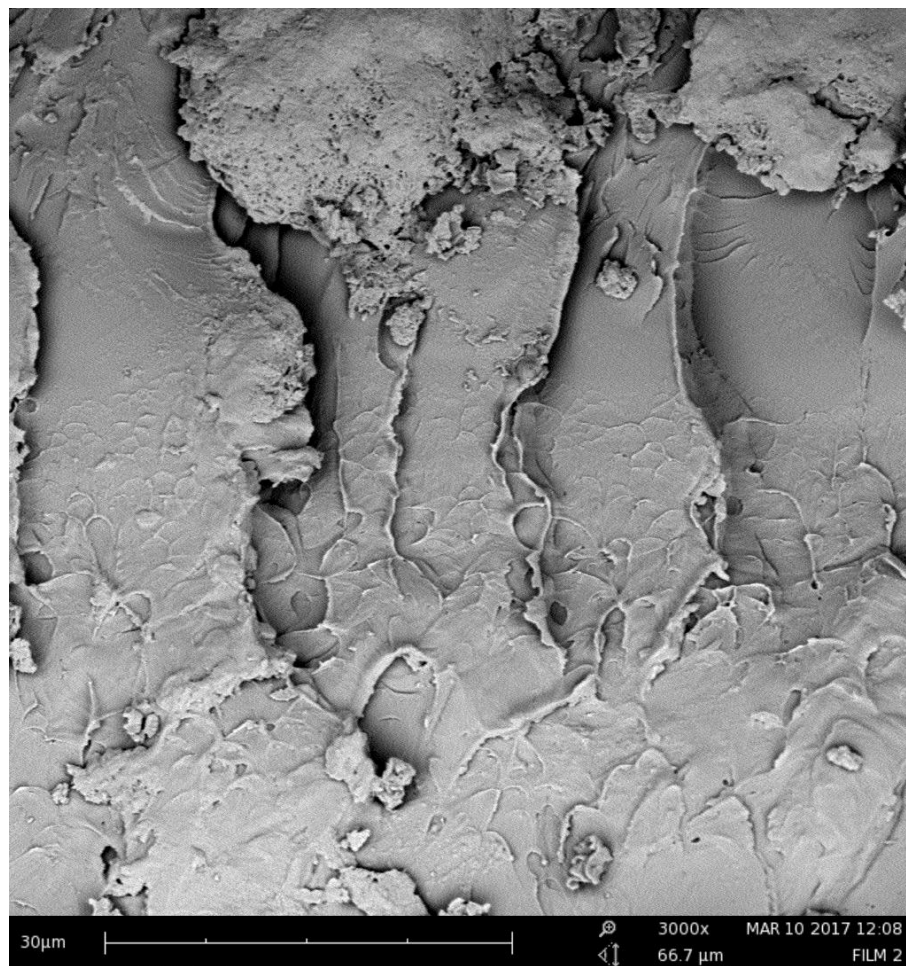


Figure 41. Cross-section of film 2. Area A. 3000x magnification

In Figure 42, the metal stud is seen by the bright white line and the adhesive is seen below this white line but above the film. The film is the third layer from the top. The surface of the film is also visible below the cross-section of the film and appears to be rather smooth when compared to the cross-section. Figure 43 shows the cross sectional area of film 3 and can easily be compared to figure 42 as both images were taken at 330x magnification. Figure 43 shows the metal stud and adhesive at the top of the image and the film is the layer adjacent to the black space at the bottom of the image. When compared to film 2 in figure 42, film 3

appears to have a more even thickness. Film 3 is comprised of only PAM and no nanotubes were incorporated. In the film, two different layers have formed— an overall smooth area on top with a more rough edge on the bottom. Perhaps during the solvent evaporation film casting method, the solvent evaporated out of the film differently at different depths creating different textures throughout the film. These areas can be better seen in figure 44, which was taken of the same area but at 3000x magnification.

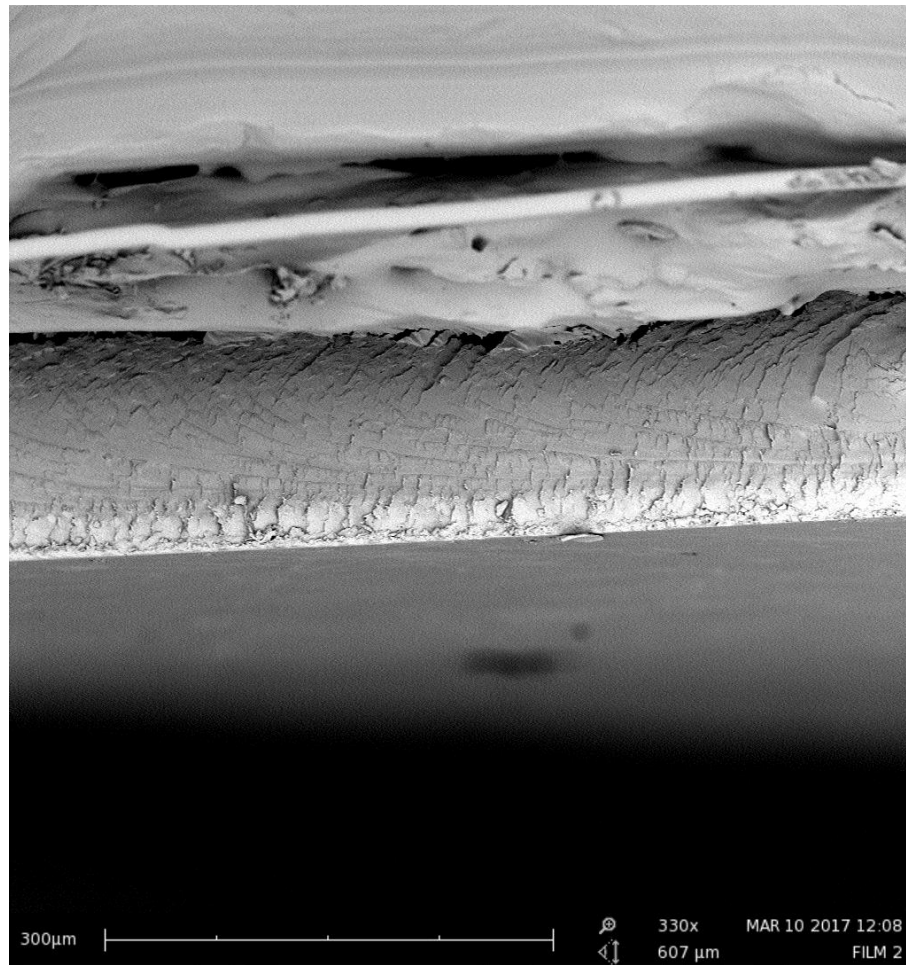


Figure 42. Cross-section of film 2. Area B. 330x magnification

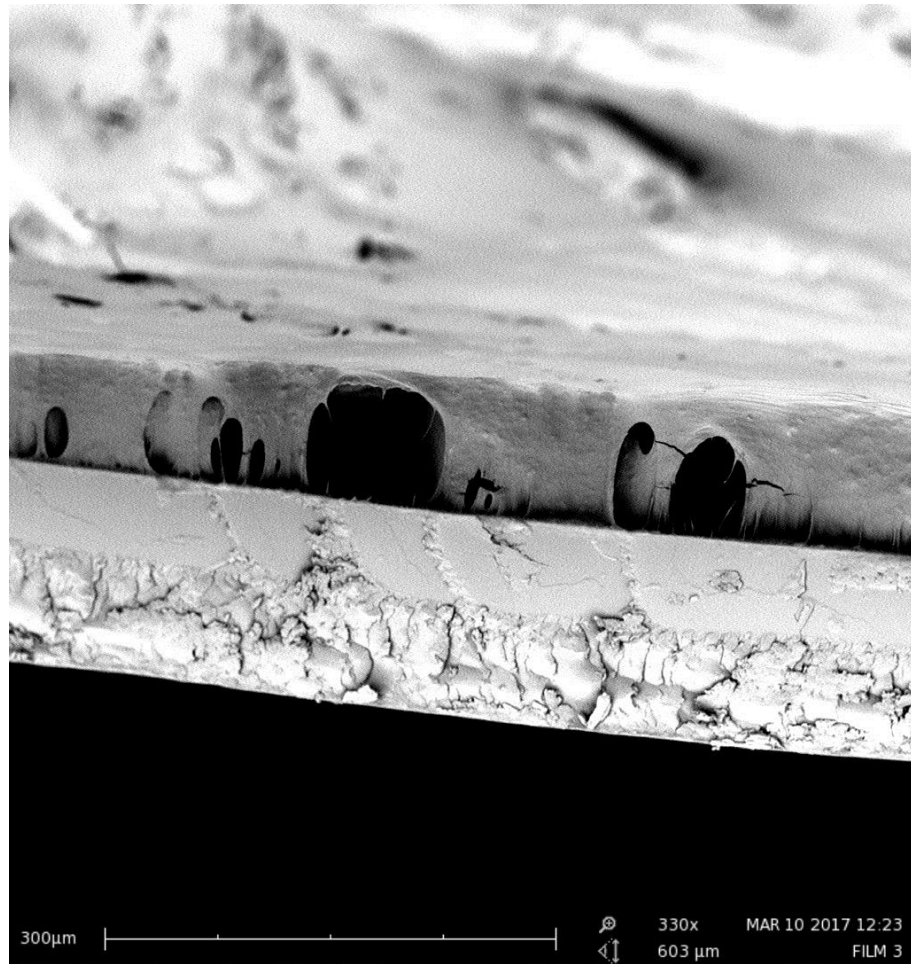


Figure 43. Cross-section of film 3. Area A. 330x magnification

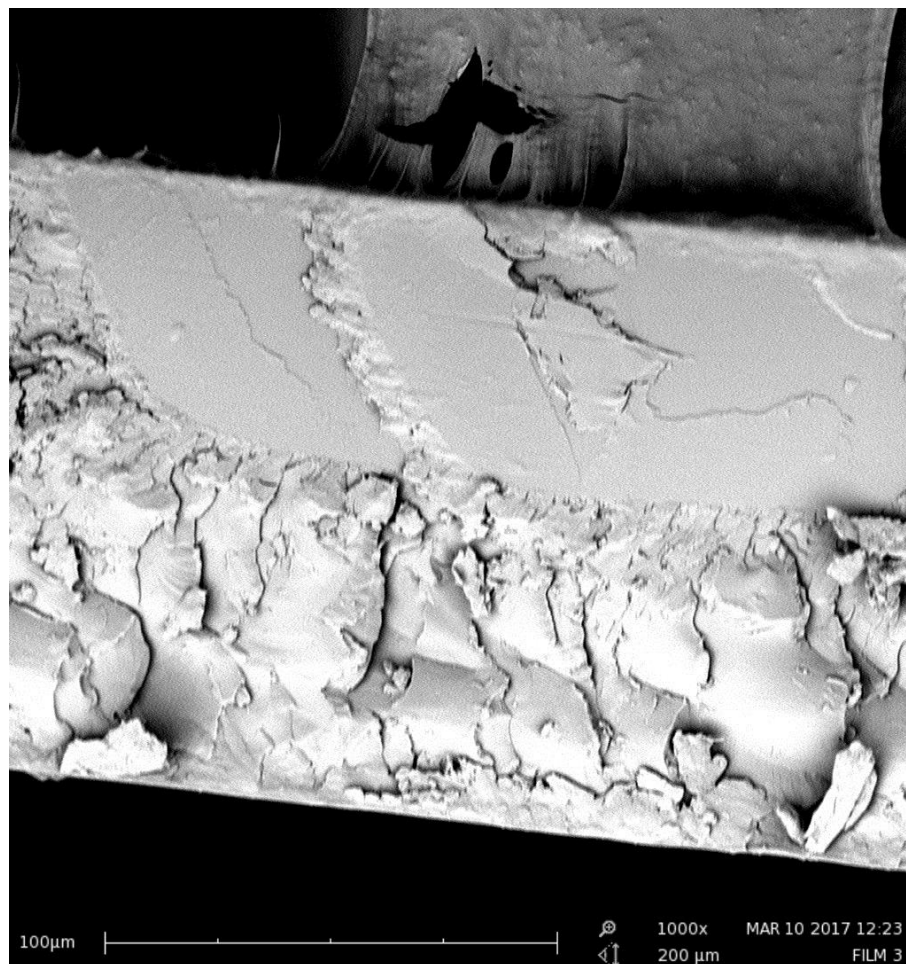


Figure 44. Cross-section of film 3. Area A. 1000x magnification

Figures 45 and 46 display film 3 also, but a different area – area B. In area B, thick textured ridges are seen and the two layers shown in area A of the same film are seen here. The smooth and rough layers previously seen throughout the cross-section of the film are not consistent throughout. In figure 46, the sample seems to have chipped off less cleanly and formed a rougher edge. These ridges shown in figure 46 could be oriented differently than the ridges shown in figure 44 due to different areas of the PAM film fracturing differently when a stress is applied. The films, originally thought to be strong, turned out to be brittle. During

preparation of all film samples for SEM imaging, all films cracked with little resistance. Films 3 and 4 were replicates of the same process, but displayed different characteristics after SEM imaging. Film 4 as seen in figures 47 and 48 showed a similar cross-sectional area as film 1 (Figure 38) even though film 1 contained MWCNTs and film 4 was only comprised of PAM. The striations in the films were not due to the addition of the carbon nanotubes in the film and due to the orientation of the polymer. Generally, there are some similarities in films 1-4, but film 5 exhibits a different behavior all together.



Figure 45. Cross-section of film 3. Area B. 1000x magnification

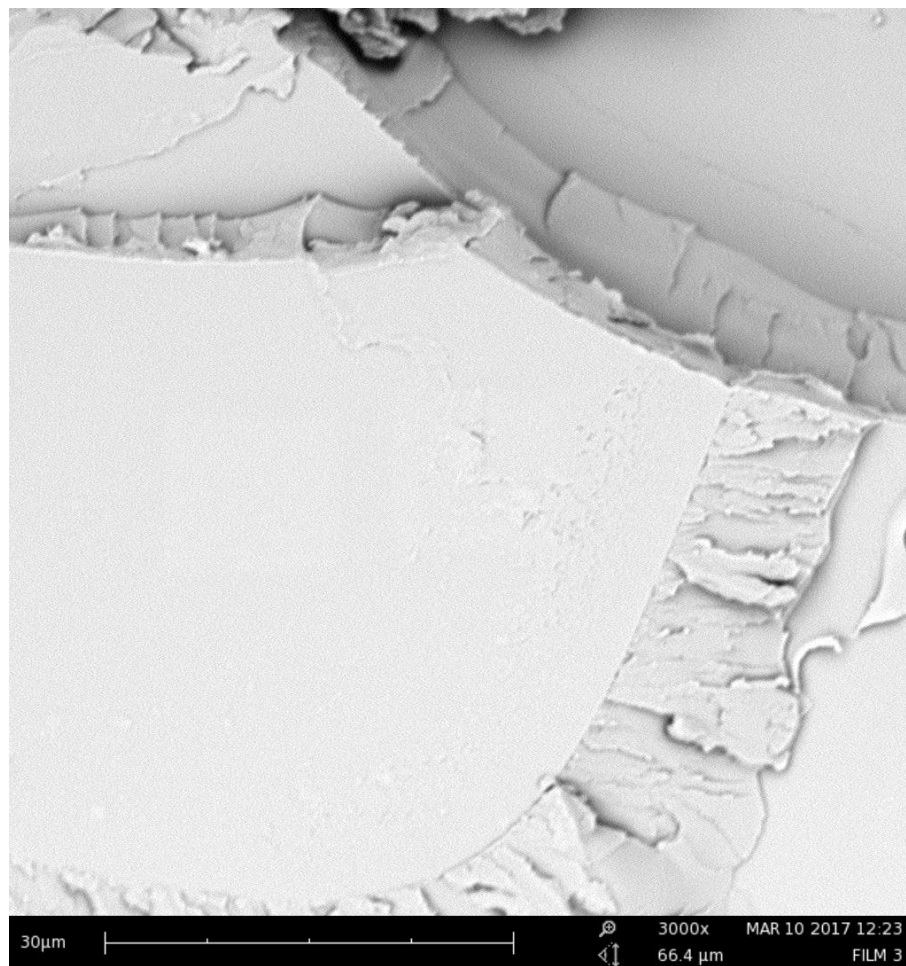


Figure 46. Cross-section of film 3. Area B. 3000x magnification

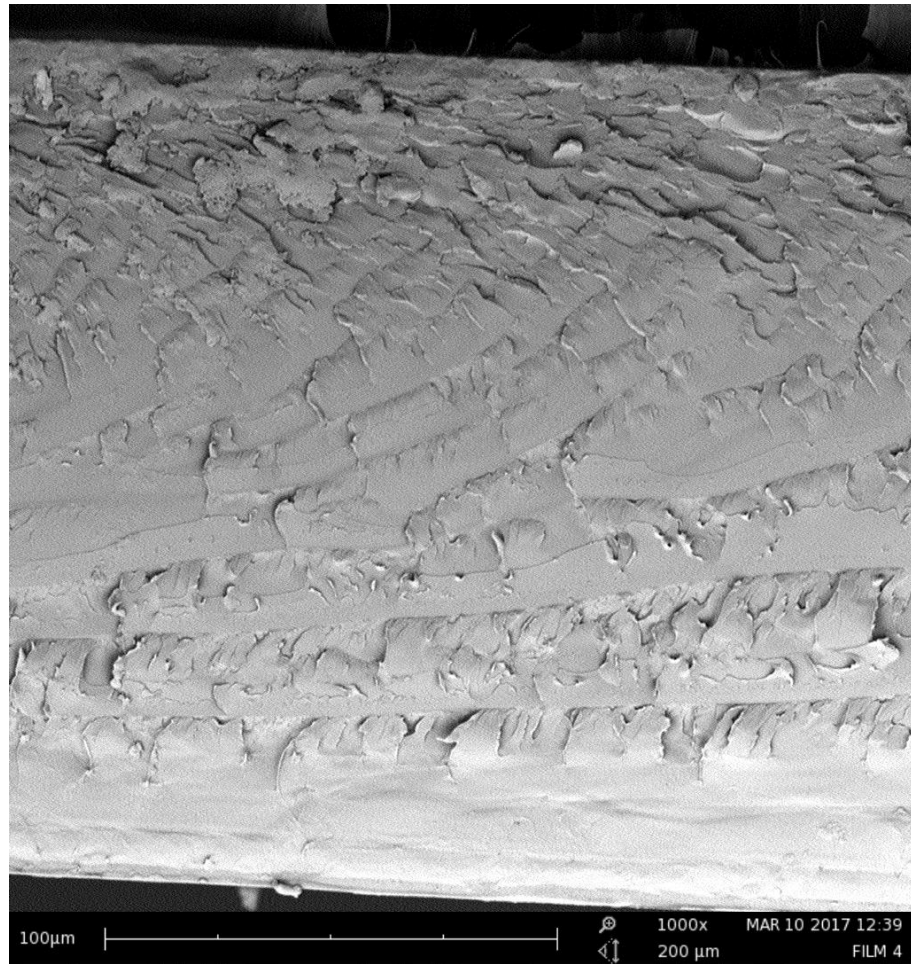


Figure 47. Cross-section of film 4. 1000x magnification

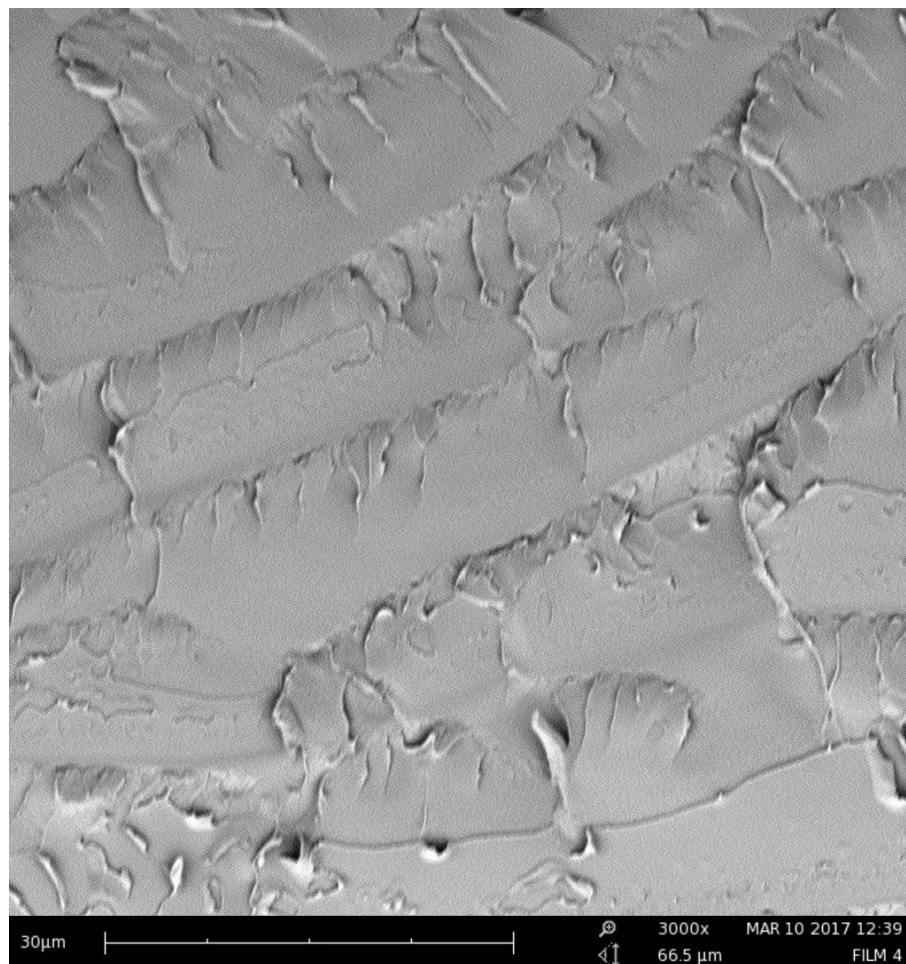


Figure 48. Cross-section of film 4. 3000x magnification

Figures 49-52 show cross-sections of film 5. A row of adhesive is seen at the top of the image attaching the very rough edge of the film to the stud. This edge of the film is very rough and bumpy, unlike the other films made prior. Films 1-4 have a smoother surface than film 5. The cross-sectional area of film 5 shows an extensively texturized surface with large hollow cavities. Figures 49 and 50 both show this at 1000x magnification although the images were taken in different areas of the film. In figure 50 there are black dots at the bottom of the figure leading to the conclusion that carbon nanotubes have aggregated on the surface. This is the first film in which clumps of nanotubes are visible. Films 1 and 2 contain CNTs, but there is

no visible indication of this in the SEM images. Figure 51 also shows a large round area of black material at the bottom left corner of the image indicating the presence of a large carbon nanotube clump in this region. On the right side of figure 51, a large crater is seen. Whereas the other films exhibited a rigid cross-sectional area with no cavitation or air bubble pockets, film 5 contains lots of air bubbles. These air bubbles may have enhanced the brittleness of the film and led to the cracking during removal of the film from the dish. Figure 52 shows an enlarged area of a CNT clump that can also be seen in the bottom of figure 50. From the large clumps of CNTs shown in figures 50, 51, and 52 the in situ sonication of CNTs with the polymerization of polyacrylamide results in a better dispersion of CNTs in a polymer composite. SEM images of film 1 and 2 do not show the same clumps of CNTs and based on the SEM images at this magnification level less CNT aggregation is seen in these films. During the sample preparation of film 5, the PAM polymer was exposed to ultrasound waves for an additional 30 minutes because dispersion of the CNTs occurred in a polymer solution. The additional exposure to sonication time could have induced degradation in the polymer and led to shorter polymer chains giving the film a different morphology and cross-sectional area. Films 3 and 4 were made as a control to see the morphology of a cross-section of a PAM film, however, based on the images it appears as if the PAM in film 5 was a different length or molecular weight than films 1 and 2 since the images do not display similar cross-sections.

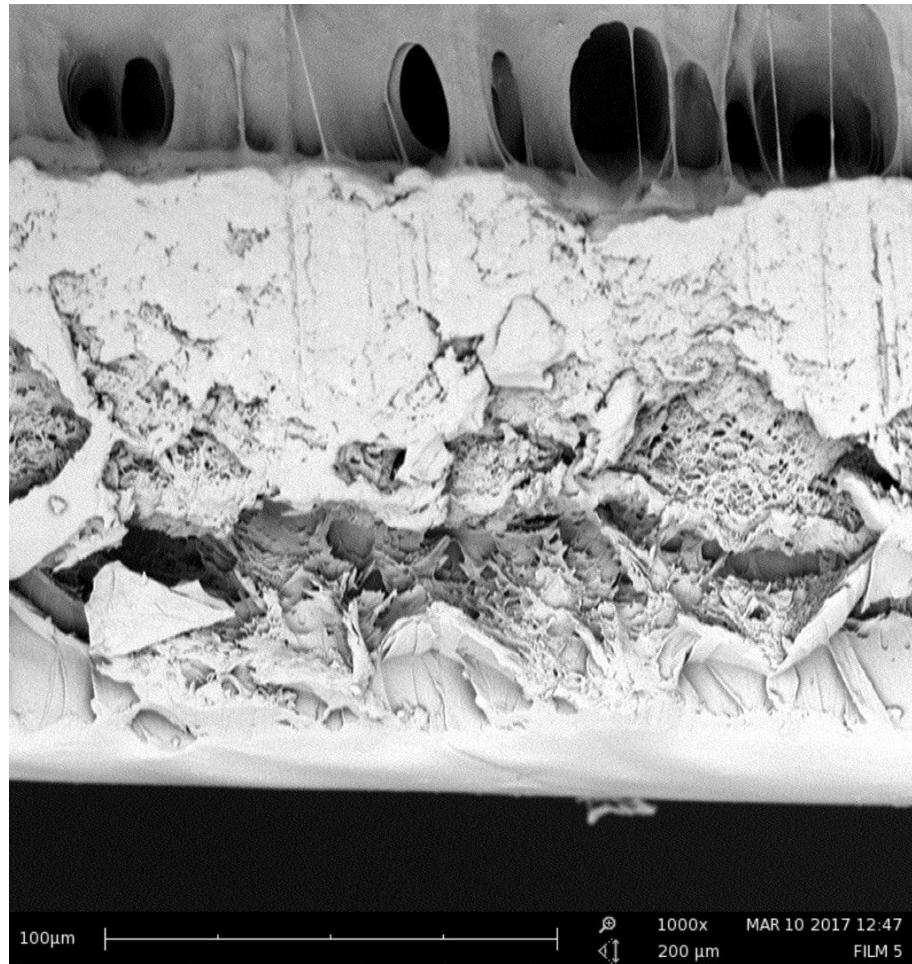


Figure 49. Cross-section of film 5. Area A. 1000x magnification.

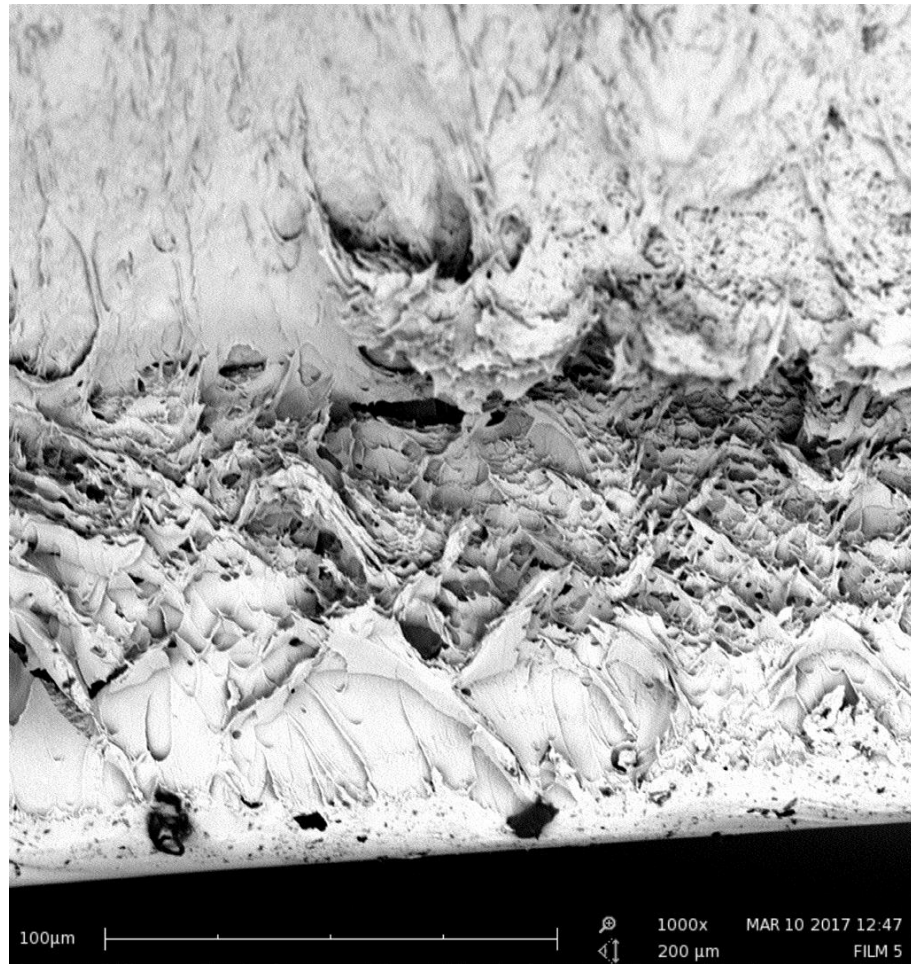


Figure 50. Cross-section of film 5. Area B. 1000x magnification

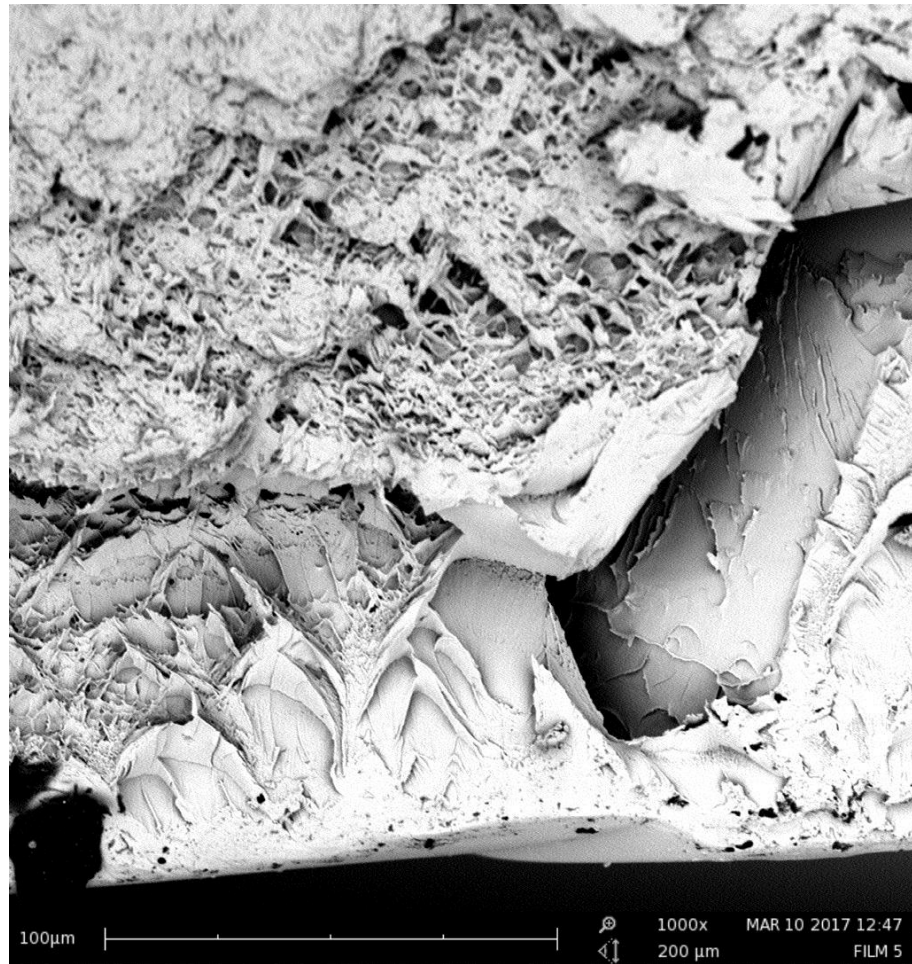


Figure 51. Cross-section of film 5. Area C. 1000x magnification



Figure 52. Cross-section of film 5. Area B. 3000x magnification

For further characterization, films 1 and 5 were viewed with an FEI Verios 460L field-emission scanning electron microscope. This microscope allows for high resolution imaging on insulating, non-conductive samples. The samples for viewing were broken off and no addition scissors or tampering was done to the films. The samples were taped and mounted in between a metal stud so they were held perfectly upright during analysis. Figures 53-56 are the images taken with this higher power microscope. Figures 53 and 54 show film 1 at 2 different locations. In figure 53 three areas of CNTs are seen in the film. One are contains only 2 or 3 individual tubes, one area in the middle contains a cluster of tubes or a

combination of the tubes grown inside a polymer and the small area to the left contains one nanotube. All suspected nanotubes were measured when the images were being taken and the tube diameter corresponds to the tubes used during this research. All diameters when in the 20-40nm range. Figure 54 shows two CNTs in the film. This image is taken of a different area than figure 53 and at increased magnification. The nanotubes seen here are not grouped and exist more isolated than those seen in figure 53. Not many CNTs are visible in this film overall due to the low wt% of CNTs in the film. And although by naked eye observation, this film looks as if the CNTs have been well dispersed they still exhibit some grouping. As the CNTs in both figure 53 and 54 are in the same general area.

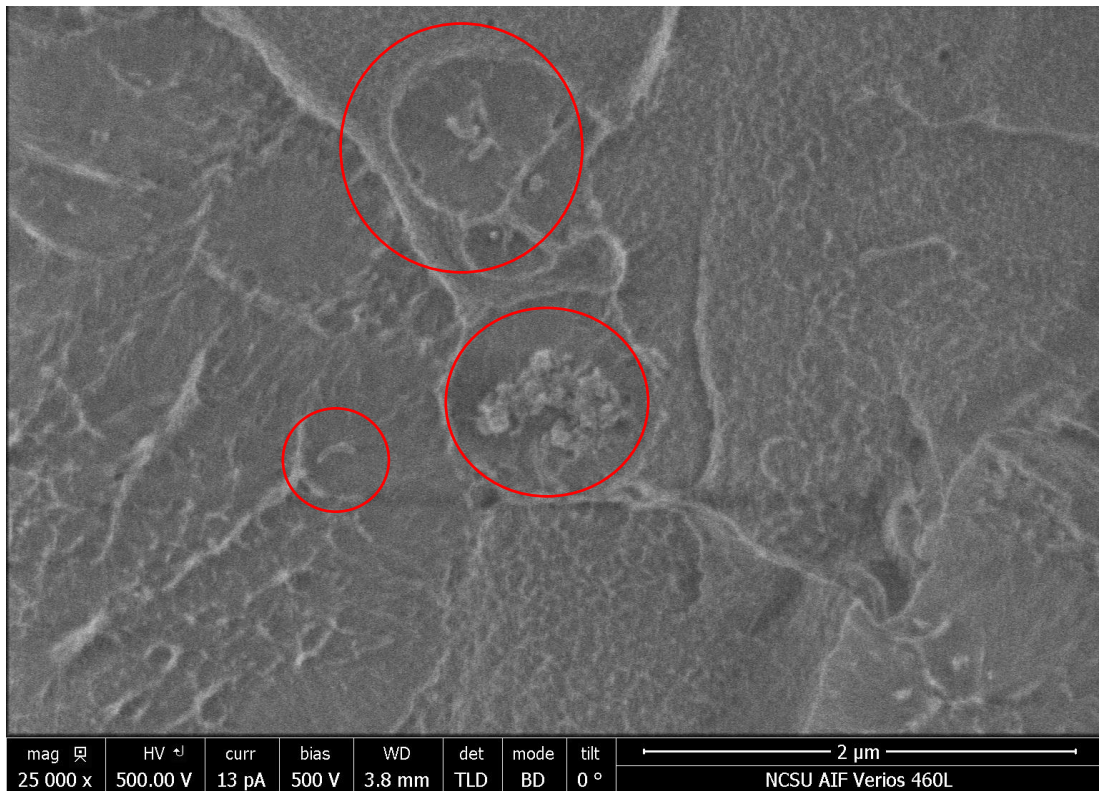


Figure 53. Cross-section of Film 1. 25000x magnification.



Figure 54. Cross-section of Film 1. 50000x magnification

Film 5 was also chosen for high magnification viewing. A large area indicating CNT presence is shown in figure 55. This image was taken at 10,000x magnification so this clump is much larger than that seen in film 1 (figure 53). The small black dots towards the top of the circled area are the diameter of the MWCNTs used in this research. Upon breaking the tubes could have been pulled out of this area and left indentations of where they were. There are many holes here indicating many CNTs aggregated here with PAM polymer in between. Near the other side of the circled area a branch like tube is seen coming up out of the area. This looks a group of 3-4 nanotubes is entwined together in PAM. One tube is more visible in the front and matches in size to the dimension of the MWCNTs sonicated. Figure 56 also shows

the presence of CNTs, but only one nanotube is seen in this image. No other nanotubes can be seen in this image. Although by this image, dispersion looks better than in film 1, this film had a lower wt% of CNT in solution because many of the CNTs did not make it into the film and was stuck to the probe. Overall it appears as if the one step sonication/polymerization produced a better dispersed film, but a higher concentration of CNTs should be sonicated in solution to confirm these initial findings.

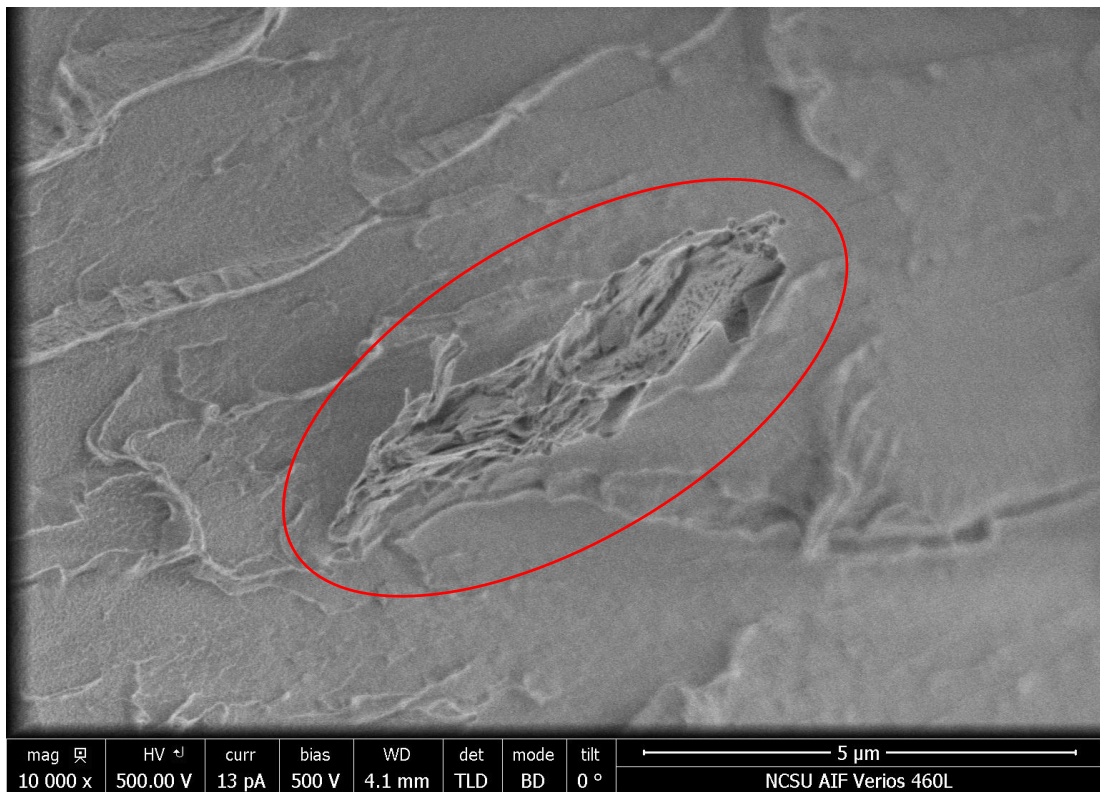


Figure 55. Cross-section of Film 5. 10000x magnification

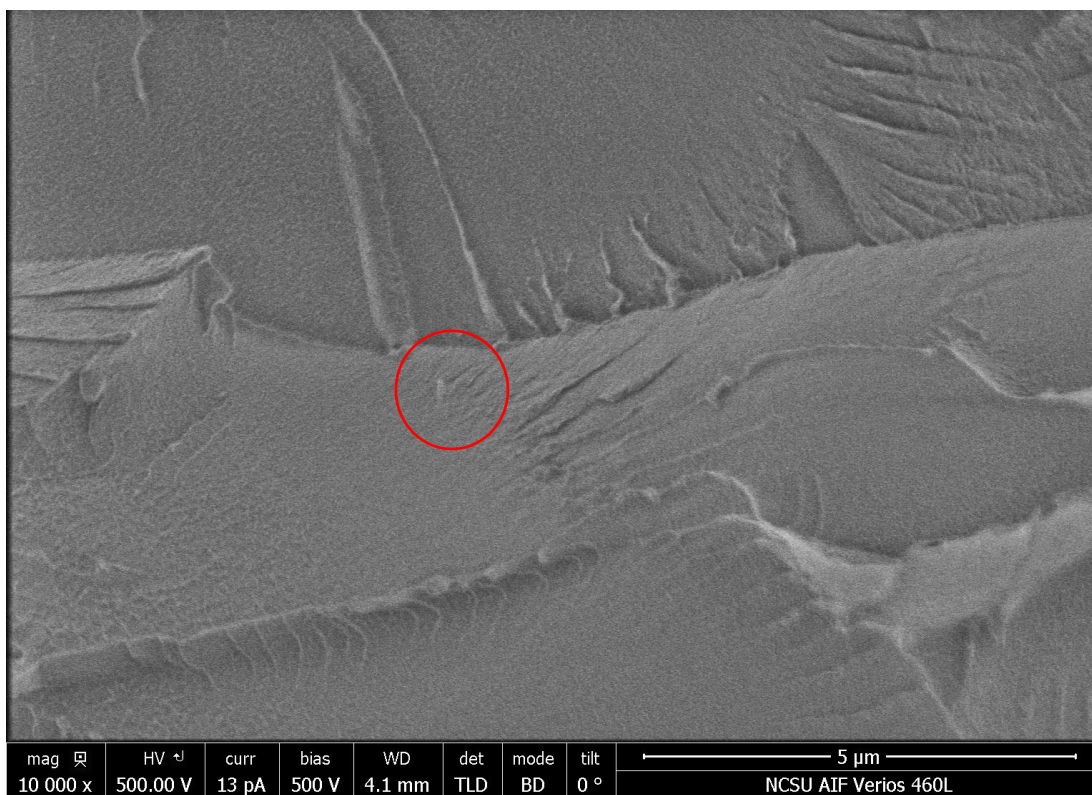


Figure 56. Cross-section of Film 5. 10000x magnification.

4.4 Conclusions

The in situ continuous sonication and polymerization produces a stronger and better-dispersed CNT/polyacrylamide composite. Based on observations by the naked eye, no visible CNT aggregations were seen in films 1 and 2 when CNTs were sonicated prior to and during the ultrasonic polymerization of acrylamide. When the films were viewed at high magnification individual tubes were seen, but a comparison of dispersion could not be made due to the low concentration of CNTs in the film. When the CNTs were sonicated in a previously made PAM solution, large and small clumps of CNTs were seen on the surface of the film. Film 5 exhibited a different morphology of the cross-sectional area further indicating

that CNTs are better dispersed before a polymer is formed and sonication of the polymer film at increased time leads to the creation of cavities in solution. Film 5 has a rough surface with abundant CNT lumps, contrasting the smooth surface of films 1-4. Although grafting of polyacrylamide onto MWCNTs cannot be seen through these SEM images and no large scale dispersion conclusions can be gathered on the molecular level, this preliminary research provides insight that the one-step continuous sonication and polymer synthesis method does produce better-dispersed composites. All film cross-sections had rough edges due to the brittleness of the polymer and the stress fractures induced during samples preparation. The striation patterns on the cross-section of the film were not consistent and all had some variation with film 5 being quite different from the others due to the different film preparation method.

5.0 CONCLUSIONS

5.1 Final Conclusions

Final conclusions on the exploration of ultrasonic polymerization prove that ultrasound waves can make polymers but is most effective for polymers with limited side reactions. Polyurethanes solutions made from isophorone diisocyanate and polyethylene glycol in DMF cannot be reproducibly polymerized with an ultrasound probe due to the amount of side reactions that can take place with the isophorone diisocyanate monomer. Polyacrylamide can be reproducibly polymerized through ultrasonic polymerization with a 15 minute reaction time, but molecular weights are not as high as polyacrylamide made in the absence of ultrasound. However polyacrylamide made without sonication, does not polymerize as quickly. Very high molecular weight polymer can be made after 44 days of the reaction. When acrylamide is polymerized during the sonication of carbon nanotubes, a good dispersion of CNTs throughout a composite polymer matrix is achieved as opposed to the sonication of CNTs in a premade PAM polymer solution.

5.2 Future Work

Future work from this study would be focused on several objectives: investigating the effects of ultrasonic induced molecular weight of other polymers or copolymer blends, increasing the wt% of CNTs in a CNT/PAM composite film to reach conductivity, and exploring the ultrasonic polymerization of other chain-growth monomers to see if initiator is truly needed or not. Some estimates have been made during this study as to when degradation occurs, but to effectively polymerize a high molecular weight polymer adjustments need to be

made to the current methodology. To combat the derivative effects of ultrasound waves and further determine what temperatures induce ultrasonic degradation, lower power settings at increased reaction times could be used or shortening the time but maintaining at power setting of 7. For a conductive CNT/polymer composite film, the wt% of CNTs in a polymer film needs to be increased to at least 2%. To achieve this percentage, the amount of CNTs could be increased or smaller amounts of monomer would need to be added after the initial sonication time. Of importance during this is that sonication time may need to be lengthened in order to get a well-dispersed CNT/polymer film. Expanding the ultrasonic polymerization of chain-growth monomers to polymerize other polymers would allow for ultrasonic polymerization technology to be further understood while allowing for more application of this one-step, continuous sonication and polymerization process.

Literature Cited

- Abdel-Rahem, Rami A et al. "Novel Dispersion of MWCNTs in Polystyrene Polymer Induced by the Addition of 3-Hydroxy-2-Napthoic Acid." *Journal of Dispersion Science and Technology* 36.March (2015): 747–754. Web.
- Aqel, Ahmad et al. "Carbon Nanotubes, Science and Technology Part (I) Structure, Synthesis and Characterisation." *Arabian Journal of Chemistry* 5.1 (2012): 1–23. Web.
- Bahattab, Mohammed A. "Preparation of Poly(vinyl Acetate) Latex with Ultrasonic and Redox Initiation." *Journal of Applied Polymer Science* 98.2 (2005): 812–817. Web.
- Balasubramanian, Kannan, and Marko Burghard. "Chemically Functionalized Carbon Nanotubes." *Small* 1.2 (2005): 180–192. Web.
- Carraher, Charles E., Jr. *Seymour/Carraher's Polymer Chemistry*. 7th ed. Boca Raton: CRC, 2008. Print.
- Chen, Dong, et al, ed. *Handbook on Applications of Ultrasound: Sonochemistry for Sustainability*. Boca Raton, Fla: CRC, 2012. Web.
- El'piner, I. E. "The Chemical Action Of Ultrasonic Waves On Macromolecules." *Russian Chemical Reviews* 29.1 (1960): 1-11. *IOP Science*. Web. 26 Jan. 2017.
- Fevola, Michael et al. "Molecular Weight Control of Polyacrylamide with Sodium Formate as a Chain-Transfer Agent: Characterization via Size Exclusion Chromatography/multi-Angle Laser Light Scattering and Determination of Chain-Transfer Constant." *Journal of Polymer Science, Part A: Polymer Chemistry* 41.4 (2003): 560–568. Web.
- Haghi, A. K., and V. Mottaghtalab. "Carbon Nanotube/Chitosan Nanocomposites." *Carbon Nanotubes*. Ed. A. K. Haghi. New York: Nova Science, 2012. 1-28. Print.
- Kharissova, Oxana V., Boris I. Kharisov, and Edgar Gerardo de Casas Ortiz. "Dispersion of Carbon Nanotubes in Water and Non-Aqueous Solvents." *RSC Advances* 3 (2013): 24812. Web.
- Kotek, Richard, and Allison Leedy. *Ultrasonic Polymerization of Polyurethanes*. Raleigh: N.p., 2015. Print.
- Kruus, P. "Polymerization Resulting from Ultrasonic Cavitation." *Ultrasonics* 21.5 (1983): 201–204. Web.

- Kruus, P., et al. "Polymerization and Depolymerization by Ultrasound." *Ultrasonics* 26.6 (1988): 352-55. *ScienceDirect*. Web. 26 Jan. 2017.
- Li, Junjun et al. "Preparation of Biocompatible Multi-Walled Carbon Nanotubes as Potential Tracers for Sentinel Lymph Nodes." *Polymer International* 59.2 (2010): 169–174. Web.
- Lin, Jianming, Qunwei Tang, and Jihuai Wu. "The Synthesis and Electrical Conductivity of a Polyacrylamide/Cu Conducting Hydrogel." *Reactive and Functional Polymers* 67.6 (2007): 489–494. Web.
- Mason, T. J., and J. Phillip. Lorimer. *Sonochemistry*. West Sussex: Ellis Horwood Limited, 1988. Print.
- Misonix Incorporated. "Sonicator Operation Manual." Farmingdale, 2011. Print.
- Ntim, Susana Addo et al. "Effects of Polymer Wrapping and Covalent Functionalization on the Stability of MWCNT in Aqueous Dispersions." *Journal of Colloid and Interface Science* 355.2 (2011): 383–388. Web.
- Odian, George G. *Principles of Polymerization*. 4th ed. Hoboken: John Wiley & Sons, Inc, 2004. Print.
- Omidian, Hossein, Jose G. Rocca, and Kinam Park. "Advances in Superporous Hydrogels." *Journal of Controlled Release* 102.1 (2005): 3–12. Web.
- Park, Myounggu et al. "Excellent Dispersion of MWCNTs in PEO Polymer Achieved through a Simple and Potentially Cost-Effective Evaporation Casting." *Nanotechnology* 22.41 (2011): 415703. Web.
- Paulusse, Jos M J, and Rint P. Sijbesma. "Ultrasound in Polymer Chemistry: Revival of an Established Technique." *Journal of Polymer Science, Part A: Polymer Chemistry* 44 (2006): 5445–5453. Web.
- Price, Gareth J., Emma J. Lenz, and Christopher W G Ansell. "The Effect of High Intensity Ultrasound on the Synthesis of Some Polyurethanes." *European Polymer Journal* 38.8 (2002): 1531–1536. Web.
- Price, Gareth J, Diane J Norris, and Peter J West. "Polymerization of Methyl Methacrylate Initiated by Ultrasound." *Macromolecules* 25 (1992): 6447–6454. Print.
- Rao, C N et al. "Nanotubes." *Chemphyschem : a European journal of chemical physics and physical chemistry* 2.2 (2001): 78–105. Web.

- Saunders, K. J. *Organic Polymer Chemistry: An Introduction to the Organic Chemistry of Adhesives, Fibres, Paints, Plastics and Rubbers*. 2nd ed. New York: Chapman and Hall, 1988. Print
- Sesis, Achilleas et al. "Influence of Acoustic Cavitation on the Controlled Ultrasonic Dispersion of Carbon Nanotubes." *Journal of Physical Chemistry B* 117.48 (2013): 15141–15150. Web.
- Suslick, Kenneth S. "ULTRASOUND IN SYNTHESIS." *Modern Synthetic Methods* 4 (1986): 1–60. Web.
- Suslick, Kenneth S, and Lawrence A Crum. "Sonochemistry and Sonoluminescence." *Encyclopedia of Acoustics*. Ed. Malcolm J. Crocker. New York: John Wiley & Sons, Inc, 1997. 271–281. Web.
- Suslick, Kenneth S, and Gareth J Price. "Applications of Ultrasound to Materials Chemistry." *Annual Review of Materials Science* 29 (1999): 295–326. Web.
- Tang, Qunwei et al. "Polyaniline/Polyacrylamide Conducting Composite Hydrogel with a Porous Structure." *Carbohydrate Polymers* 74.2 (2008): 215–219. Web.
- Tasis, Dimitrios et al. "Chemistry of Carbon Nanotubes." *Chemical Reviews* 106.3 (2006): 1105–1136. Web.
- Zhang, Qing. *Carbon Nanotubes and Their Applications*. Vol. 1. Singapore: Pan Stanford, 2012. *ProQuest Ebrary*. Web. 8 Feb. 2017.
- Zhou, Chengjun, and Qinglin Wu. "A Novel Polyacrylamide Nanocomposite Hydrogel Reinforced with Natural Chitosan Nanofibers." *Colloids and Surfaces B: Biointerfaces* 84.1 (2011): 155–162. Web.
- Zhou, Chengjun et al. "Application of Rod-Shaped Cellulose Nanocrystals in Polyacrylamide Hydrogels." *Journal of Colloid and Interface Science* 353.1 (2011): 116–123. Web.